MSC

An evaluation of novel Cyanoacrylamides for use as covalent Kinase inhibitors in fragment-based drug discovery

Yang, Philip

Award date:
2019

Awarding institution:
University of Nottingham

School of Chemistry

4th Year Research Project (F14RPC)

Title: An evaluation of novel Cyanoacrylamides for use as covalent Kinase inhibitors in fragment-based drug discovery

Student's name: Philip Bernard Yang
Student ID Number: 4249656

Supervisor: Chris Hayes

Second Supervisor(s), if applicable:

Assessor: Hon Lam

Personal Tutor: Ross Denton

I hereby certify that this project report is my own work:

Student's signature:

Acknowledgments

During the course of this project I have been aided by some individuals and would like to thank them accordingly. Firstly, I would like to thank my supervisor Professor Christopher Hayes for the experience of working in his research group and for his advice during this project.

As for the help on a day-to-day basis, I would like to thank Matt for his help and training over the past year with many of the techniques used in this project. The other members of the research group (Michael, Katie, Mustafa, Daniel, Aamina, Yijia, Frank) were very friendly and helpful and made the experience a memorable one. I would also like to thank KeyOrganics for supplying us with the majority of the amines used in this project, and for the opportunity to work with them.

List of Figures

List of Tables

List of Abbreviations

HATU = 1-[Bis(dimethylamino)methylene]-1H-1,2,3-triazolo[4,5-b]pyridinium 3-oxide hexafluorophosphate

NMR = Nuclear Magnetic Resonance

DMSO = Dimethyl Sulfoxide

HTS = High Throughput Screening

FBDD = Fragment-based Drug Discovery

ATP = Adenosine Triphosphate

CML = Chronic Myelogenous Leukaemia

FDA = Food and Drug Administration (US)

CSKI = Covalent Small-molecule Kinase Inhibitor

βME = β-mercaptoethanol

DMSO-d_6 = Deuterated DMSO

PBS-d = Phosphate Buffered Saline

LC-UV-MS = Liquid Chromatography – Ultraviolet – Mass Spectrometry

EDC = 1-Ethyl-3-(3-dimethylaminopropyl)carbodiimide

MS = Mass spectrometry

DCC = N, N'-Dicyclohexylcarbodiimide

HOBt.H_2O = 1-Hydroxybenzotriazole hydrate

DIPEA = N, N-Diisopropylethylamine

DCM = Dichloromethane

DMF = Dimethylformamide

HBTU = N,N,N′,N′-Tetramethyl-O-(1H-benzotriazol-1-yl)uronium hexafluorophosphate

HOAt= 1-Hydroxy-7-azabenzotriazole

CHCA = alpha-Cyano-4-hydroxycinnamic acid

Abstract

Kinase enzymes play an important role in many biological processes and their malfunction in the body can lead to diseases, such as cancer and muscular dystrophy. Covalent kinase inhibitors are a relatively new and exciting field of research in drug discovery due to advantages in selectivity, provided toxicity from off-targeting effects can be controlled. Our industrial partner (KeyOrganics) required a small but diverse fragment library of such molecules for fragment-based drug discovery (FBDD) applications. In this report, we present a versatile route to a wide variety of cyanoacrylamides for this purpose that is largely underrepresented in the literature; cyanoacrylamides have been shown to be reversible inhibitors and were of particular interest as a result.

To achieve this, cyano-acrylic acids were synthesised as precursors to the amide coupling step, and the ability to vary both the acids and the amines of this reaction sequence created a flexible method. 17 Fragments were made from 3 precursor acids using this approach, and the process was adapted and optimised over time using different coupling reagents and methods.

Due to the application of these fragments, testing was conducted by reacting the molecules with glutathione (in place of the reactive thiol residue present in kinase enzymes) to get relative comparisons of their binding affinities. This was monitored via ^{1}H NMR, where the variation in size of the relevant integral on the inhibitor could be linked to reaction with glutathione. Most of the fragments tested binded to the thiol residue but in different extents, and the behaviour of the integral sizes over time was indicative of reversible inhibitors.

The binding affinities were compared by fitting the data to first order kinetics to yield a rate constant for the interaction. While the quality of fit was not good enough to give any quantitative data, it did allow for relative comparisons of inhibitors, and a trend could be seen in their performance based on estimated steric/inductive effects. However, the solvent used for this test likely interfered with the equilibrium (as seen in one case) by providing an oxidative environment, causing the glutathione to dimerise.

Table of Contents

1 Introduction

Fragment based drug discovery relies on a diverse library of molecules to screen[1], and the major objective of this work was to produce and evaluate a range of new fragment molecules in the rising field of covalent kinase inhibitors. This new class of kinase inhibitors have seen an increased interest in recent years and can present notable advantages to their non-covalent counterparts. It is thus important to have an appropriate fragment library of these molecules to provide a large array of species to test.

1.1 The rise of fragment-based drug discovery

High throughput screening (HTS) has long-established problems with high attrition rates[1], meaning the majority of hits found (i.e. potent compounds against a target) are discarded soon in the development process. In an attempt to address this, FBDD identifies low-molecular-weight ligands (in the region of 300 Da or less) that bind to the biologically important macromolecules related to the disease in question. The key difference between FBDD and HTS is that FBDD focuses more on the quality of fit of a fragment to a binding site on the protein target, whereas in HTS potency is the main driving force for selection of a hit compound[2].

The three-dimensional experimental binding interaction can be investigated via NMR or X-ray Crystallography, and this extra information is used to better optimise fragments into lead compounds[3]. Although initial fragments have poor potency as a result of their small size, they typically form high quality interactions and can be readily converted into leads using this method. In addition, Proficient fragments can also be combined to yield a more potent combination. An illustration of the conversion of a fragment to lead compound is shown on the next page (see Figure 1)

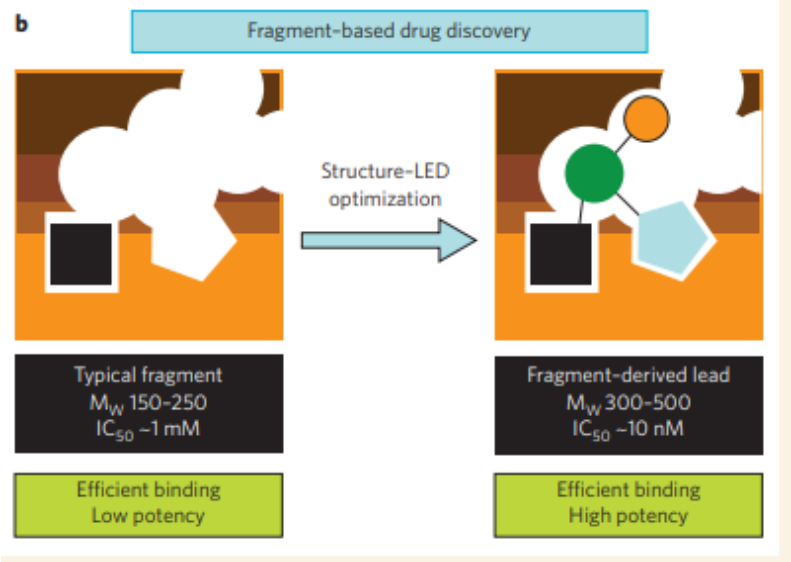

Figure 1: Illustration of how fragments can be optimised for a specific target[1]

Figure 1 illustrates how a fragment can be moulded into a lead compound, and how information about the binding mode is used to understand how best to fit an inhibitor to the target (i.e. the blank spaces in the diagram give an indication of how to alter the fragment). Optimising in this way improves potency, giving a stronger lead compound. While the more traditional HTS approach will tend to find a lead compound faster, fragment-based approaches are becoming more popular due to their more scientific nature and lower attrition rates. Both methods are considered viable as a result but FBDD allows progress to be made with only a small library of compounds, making it more accessible in that regard.

Since the first report of the fragment-based method in 1996, two clinically approved drugs have been developed and at least 30 FBDD-derived compounds are in various stages of clinical development[4]. Notable challenges for FBDD include the need for specialised techniques for screening as the fragments will have weaker binding affinities than the molecules tested in HTS.

FBDD is now frequently adopted in the pharma industry but (due to its method) requires varied fragment libraries for each drug discovery case in order to be effective. Hence the need for this project and its collaboration with an industrial partner.

1.2 Kinase and an overview of current covalent inhibitors

To understand this particular class of fragments, it is important to first understand Kinase enzymes and the details of their inhibitors. Kinase inhibitors block the action of Kinase enzymes, which moderate the process of phosphorylation[5] whereby a phosphate group is added to a substrate (specifically a protein in this case) using Adenosine triphosphate (ATP) as a phosphate donor (see Figure 2). The process can also be reversed via the action of phosphatases.

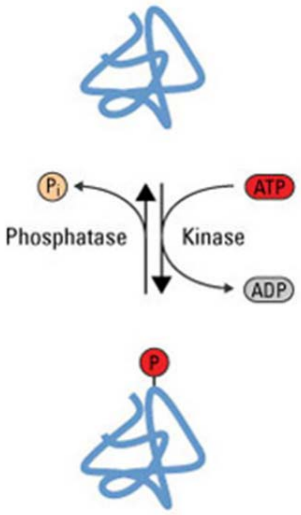

Figure 2: Protein Kinase phosphorylation process[5]

Phosphorylation changes the activity of a protein in various ways, and leads to the activation of signal-transduction pathways which are crucial in many biological processes[6]. Protein Kinases thus play an important role in intracellular signalling pathways, and these regulate cell growth, differentiation, development, functions and death.

As a result, any disruption of the phosphorylation process will alter cell function and can result in disease. There are about 550 human protein kinases[7], so the need for specificity in any inhibitor is paramount. Inhibition (and thus regulation) of a deregulated protein kinase can be desirable in combatting ailments such as Cancer, Alzheimer's disease and Muscular Dystrophy.

For example, Chronic Myelogenous Leukaemia (CML), is caused by excess activity of the Abelson tyrosine kinase[8]. Imatinib (see Figure 3) is a molecule designed to bind to the active site of this particular kinase and inhibit its ability to phosphorylate targets, thus regulating it.

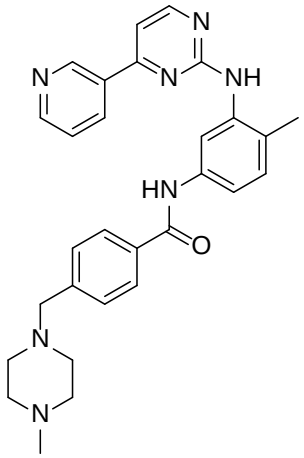

Imatinib

Figure 3: Imatinib molecule

Kinase inhibitors are classified into types depending on where/how they bind to their targets[9]: Type 1 inhibitors bind to the active kinase conformation while the inactive form is targeted by the type 2 class. Both type 1 and 2 inhibitors occupy the adenine binding pocket of the kinase, interacting using hydrogen bonds.

Type 3 inhibitors bind next to the ATP-binding pocket, and type 4 variants do not bind to either of the ATP or peptide binding sites; these two are both allosteric in nature, meaning they bind to an effector molecule at a site other than the enzyme's active site. Type 5 inhibitors are bivalent, meaning they bind to two different regions of the protein kinase domain, and type 6 inhibitors bind through covalent means.

The majority of kinase inhibitors have been non-covalent in their binding up until now, and this is largely due to toxicity concerns of off-targeting effects[10] (i.e. a covalent bond is far more permanent than, for example, a hydrogen bond). However, recent research has shown that with a carefully designed inhibitor for the target site, covalent drugs can be viable. They can also gain added selectivity[11] from the covalent binding mode as the inhibitor can be assembled with a specific covalent interaction in mind; This measured approach goes hand-in-hand with the nature of FBDD.

Over the past few years, the FDA have approved 4 covalent kinase inhibitors, and this has resulted in a renewed interest in their research. One of these (see Figure 4), Afatinib[12], is to be used in the treatment of metastatic non-small cell lung cancer.

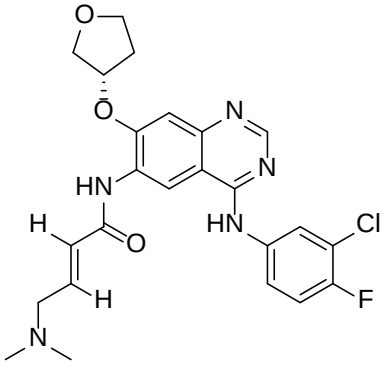

Afatinib

Figure 4: Afatinib molecule

Like Imatinib, it is a type of tyrosine kinase inhibitor, and blocks the proteins sending signals to the cancer to grow. Blocking the signals causes the cells to die, which may help stop or slow down the cancer; selectivity for the growth of the cancer cell only is imperative.

To act as a covalent kinase inhibitor, drug molecules require a reaction moiety known as a warhead[10], which is key to finding the balance between toxicity and efficacy. It is the warhead which helps to improve the binding affinity and selectivity of the covalent interaction with the reactive residue of the kinase. Covalent interaction-related residues in kinases can be cysteines, lysines and aspartic acids among others, although most often they are non-catalytic cysteines near the ATP-binding site.

A paper on the recent progress of the field[10] investigated covalent small-molecule kinase inhibitors (CSKI's) from recent papers and databases, ranking the most common warheads being utilised (see Figure 5 on next page). The most popular choice by far were the acrylamides and their related derivatives, which interact via a 1,4-addition of the cysteine thiol to the conjugated carbonyl (Afatinib has this warhead for instance). Many of the other warheads form covalent interactions in a similar way, such as enones (ranked 3rd in Figure 5) and cyanoacrylamides (4th).

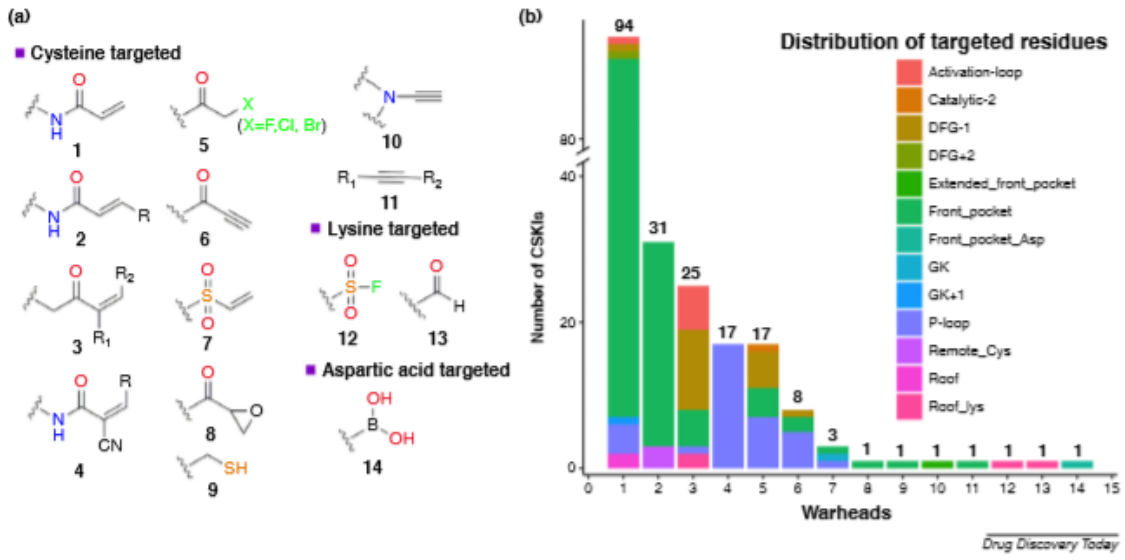

Figure 5: Figure ranking the popularity of different warhead types for all covalent small-molecule kinase inhibitors from recently published review papers and databases[10]

Figure 5 shows a large variety of functional groups being explored for covalent kinase inhibition and the distribution on the right-hand side of Figure 5 shows the variety of sections of kinase that have been targeted with these warheads. Unlike the other warheads, the cyanoacrylamides were noted to have been used as reversible inhibitors of Kinase, making them particularly interesting to this project.

Reversibility allows for more control over the reactivity with the target[10], which may help in treating different ailments that require less permanent modifications to enzymes. Also, all cyanoacrylamides covered in the study target cysteines in the P-loop region, in contrast to the behaviour of the other popular inhibitors which target a range of cysteine residues.

1.3 Cyanoacrylamides as reversible covalent inhibitors

Further investigation into this reversible nature found a study in which[13] simple thiols (akin to the cysteine residues on a protein kinase) were seen to be reacting immediately with 2-cyanoacrylates, but products of the interaction could not be isolated. It was shown that this only occurred when both the ester and nitrile groups were together on the molecule, as the interaction with the lone esters and nitriles did not result in this observation.

By using ^{1}H NMR and dilution experiments (see Figure 6), it was confirmed that the adduct thioether did form, and that the reaction was rapidly reversible with a tuneable equilibrium. The first spectrum in Figure 6 shows the lone cyanoacrylate, the middle spectrum shows it treated with β-mercaptoethanol (βME) in DMSO-d_6:PBS-d (3:1) giving a mixture which favoured the adduct 15:85, and the bottom spectrum shows a ten-fold dilution which shifts the equilibrium towards the left (45:55). The red and blue asterisks indicate peaks that were used to determine the ratios of cyanoacrylate: adduct.

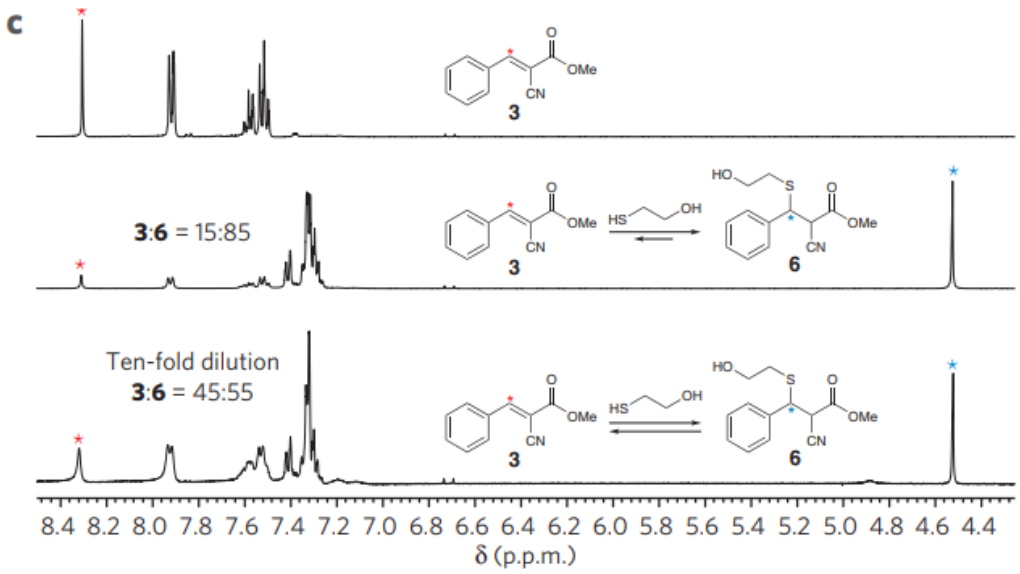

Figure 6: Thiol reacivity of a 2-cyanoacrylate explored using NMR and dilution experiments

It was this uncommon property and the lack of exposure for these molecules compared to regular acrylamides that resulted in cyanoacrylamides becoming the focal point of this project. More specifically, the aim was set to make at least 15 fragments with at least 20 mg of each to allow for appropriate testing in pharmaceutical applications.

A previous paper on cyanoacrylamide synthesis[14] for use as kinase inhibitors involved an array of aldehyde fragments which were combined with cyanoacetamide in a condensation reaction (see Figure 7). These fragments were screened against three human kinases, giving notable differences in potency. The method yields a decent variety of fragments, but the majority of these are based off of similar aromatic rings and the amine portion of the fragment was not altered (i.e. it was always NH_2).

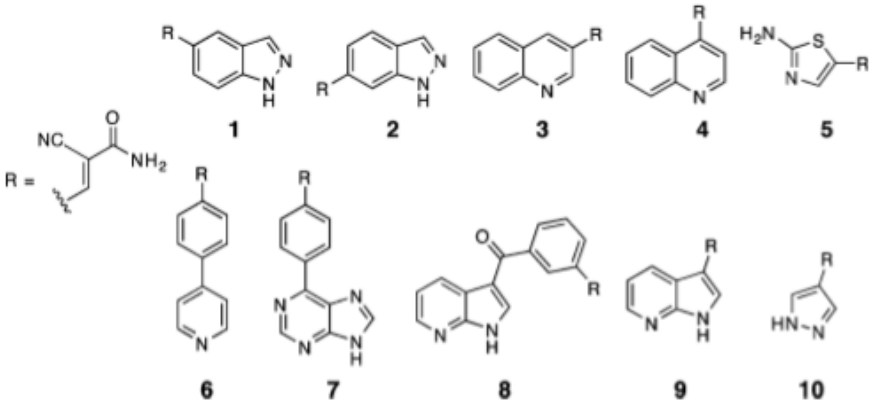

Figure 7: Set of cyanoacrylamide fragments made in a previous study[14]

Thus, creation of a set of fragments using a similarly formulaic approach, but with a larger variation in the molecules was seen as an effective route for the project aims. This would allow room for further understanding of what makes a fragment particularly effective in binding to kinase, while deviating from the papers approach of a condensation reaction and variation of the aldehyde. The chosen method was an amide coupling, which was quite underrepresented in literature for cyanoacrylamide synthesis.

Similar to the acrylamides, the cyano-equivalents are electrophilic and would likely interact with the reactive thiol group of cysteine residues on the kinase in a type of Michael addition (see Figure 8). The position of the nitrile group increases the susceptibility of the β-carbon to nucleophilic attack as it is now more electron deficient, improving binding affinity[13]. Its presence also gives the fragments the ability to form both polar and hydrophobic interactions with proteins[15].

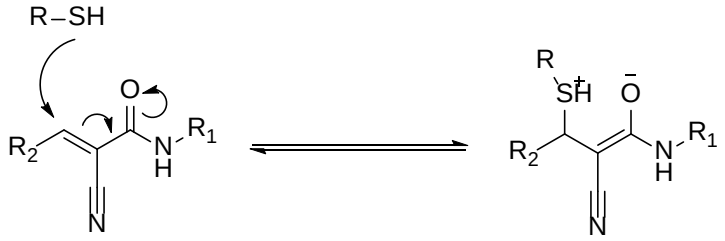

Figure 8: Mechanism of thiol residue interaction with a cyanoacrylamide

In order to compare cyanoacrylamides made in this project, this interaction would need to be mimicked and any changes observed/measured. A similar test was used in a recent paper[16] whereby covalent inhibitors were reacted with an excess of Glutathione (Figure 9), which is made up of cysteine, glutamic acid and glycine units.

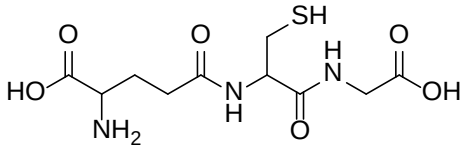

glutathione

Figure 9: Glutathione molecule

The interaction was monitored via LC-UV-MS, allowing the researchers to produce a pseudo-first order rate constant and compare their molecules quantitatively. Due to the applications of the molecules that would be produced in this project, it became a secondary aim to test some of the fragments made in a similar fashion.

The performance of similar inhibitors tested in another recent paper was found to be closely related to the electron-withdrawing nature of substituent groups and steric effects. We would thus expect a similar impact on the molecules produced in this project. Later on, a more crude method was implemented using ^{1}H NMR which gave good relative data, and was also able to highlight the reversible behaviour of the inhibitors.

2 Results and Discussion

Initial work centred on finding methods of making cyanoacrylamides that could be repeated in a formulaic fashion, such as the one mentioned in the introduction. This led to the discovery of an amide coupling method[17] (below):

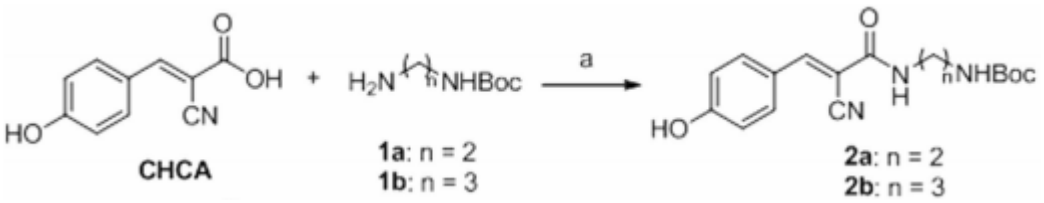

Figure 10: Potential method for varied cyanoacrylamide synthesis[17]

The process, using 1-Ethyl-3-(3-dimethylaminopropyl)carbodiimide (EDC) in a standard amide coupling procedure, was seen as a potential route to an array of cyanoacrylamides through variation of both starting reagents. The cyano-acrylic acid (and variants of it) would also make valuable precursors (to the industry) for these types of molecules if the versatility of the route could be proven. The process used in the referenced paper was part of a larger scheme to synthesise a different molecule, so its capabilities with producing different cyanoacrylamides was not explored. Amide couplings in this way to form cyanoacrylamides have not been covered very much overall, and thus it was thought to be valuable to investigate this approach further.

2.1 Precursor molecule synthesis

Synthesis of a selection of cyano-acrylic acid molecules to explore this route in depth became of interest because of these findings (see Figure 11):

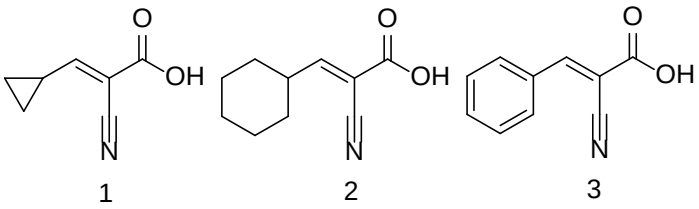

Figure 11: Precursor molecules for cyanoacrlyamide synthesis

The molecules were chosen to provide varying degrees of steric influence and inductive effects. Other options could have been the isopropyl or substituted benzyl precursors, but these 3 were chosen on account of simplicity and ease of availability of the starting materials to make them from. Preparation of the cyclopropyl precursor (1) is documented in literature as well as some aromatic versions, but the cyclohexyl variant (2) had not been seen in the literature. The synthetic methods found typically used piperidine as a catalyst, and the chosen route is shown below[18]:

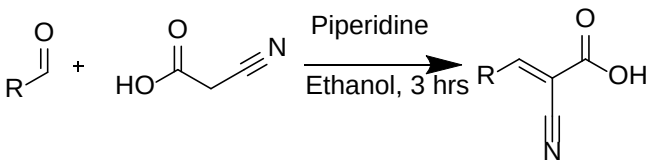

Figure 12: Synthetic route for the compounds in Figure 11

This was attempted for the compounds in Figure 11 with mixed results. Synthesis of the cyclohexyl and cyclopropyl variants worked well and gave the best yields; they were also easiest to purify. However, the benzyl precursor was more difficult to make as purely, and the reaction gave poorer yields. This could have been due to added steric bulk of the aromatic group which may hinder the reaction progressing. The yields of each reaction can be seen below:

R group (in Figure 12)	**Yield**
Phenyl	25%
Cyclohexyl	43%
Cyclopropyl	47%

Table 1: Yields of cyanoacrylamide precursor syntheses

Synthesis of a tert-butyl precursor (see Figure 13) was also attempted, but the reaction appeared to have trouble going to completion. The ^{1}H NMR showed a peak that did not belong to the desired product (see Figure 14 on next page), and it was thought that this was one of the starting materials. As there were some difficulties with the benzyl precursor as well, it makes sense that the even bulkier tert-butyl form would pose problems.

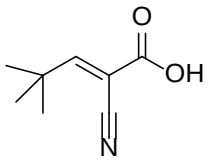

Figure 13: Tert-butyl precursor molecule

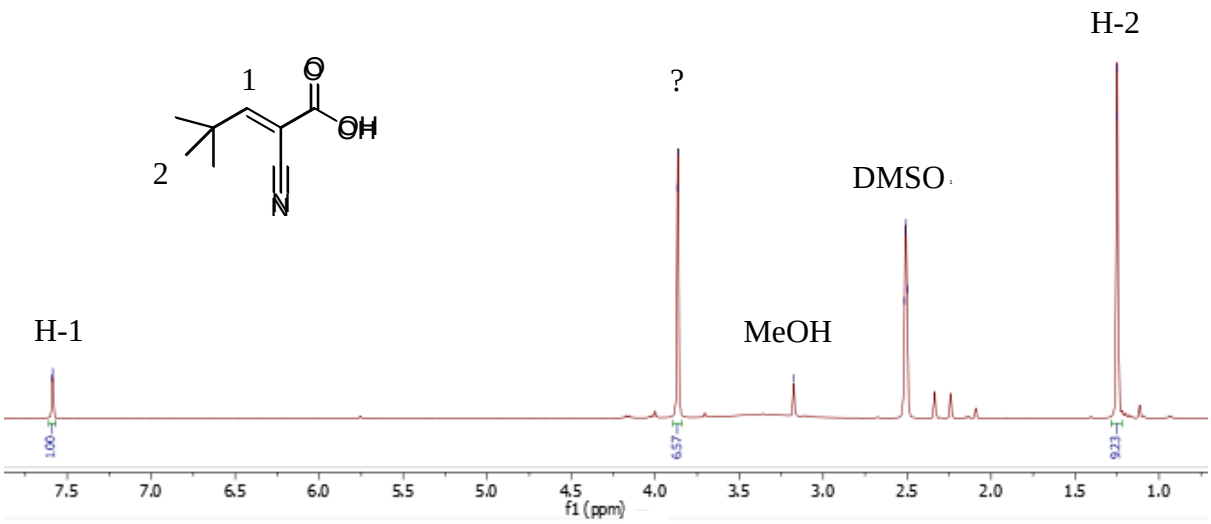

Figure 14: NMR of tert-butyl precursor, showing desired peaks as well as a substantial unexplained peak, likely to be the cyanoacetic acid

The Figure above shows the ^{1}H NMR of the sample for the tert-butyl reaction, annotated with the identity of each peak. The peak in question at 3.86 is not supposed to be in the final structure. Mass spectrometry (MS) of the sample confirmed that some of the product had been made, but it also confirmed the presence of the starting 2-cyanoacetic acid and the theory that the reaction had not gone to completion. Attempts were made to do the reaction with an excess of the aldehyde (as opposed to a 1:1 ratio) and for a longer period of time, but these gave the same outcome.

Finally, the procedure followed stated that the crude product precipitates out of the reaction mixture when cooled to zero degrees and was removed by filtration. This was not observed in any of the syntheses in this project and the solvent was removed via rotary evaporator to get the crude product instead.

2.2 Cyanoacrylamide synthesis and evolution of the method

The three successful precursor molecules were then used in amide couplings (using the conditions in the paper of Figure 10[17]) with a variety of amines (mostly supplied by KeyOrganics). One such reaction was successfully attempted with the benzyl precursor:

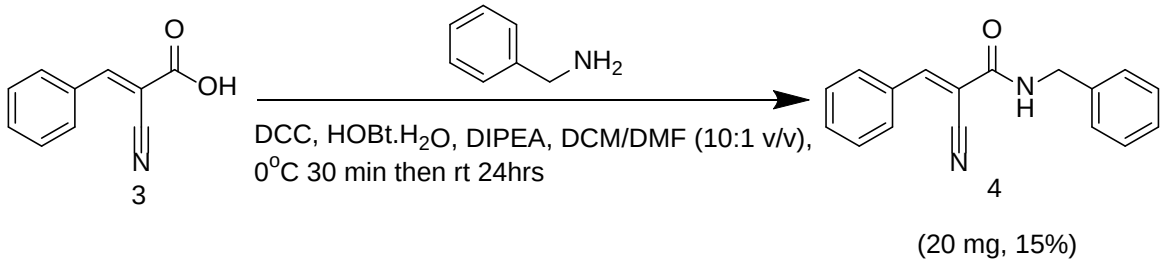

Figure 15: Initial coupling reaction done with benzyl precursor molecule.

Synthesis of cyanoacrylamides 4 and 5 were done with N,N'-Dicyclohexylcarbodiimide (DCC) instead of EDC due to availability issues, but the two work very similarly. DCC was later replaced by EDC due it being easier to remove from the reaction mixture. The reaction of the benzyl precursor and benzylamine (Figure 15) was successful, giving an adequate amount of material for the original aims of the project. More reactions were attempted with the other precursors due to their better yields and purities, and those reactions carried out with the cyclopropyl variant are shown below:

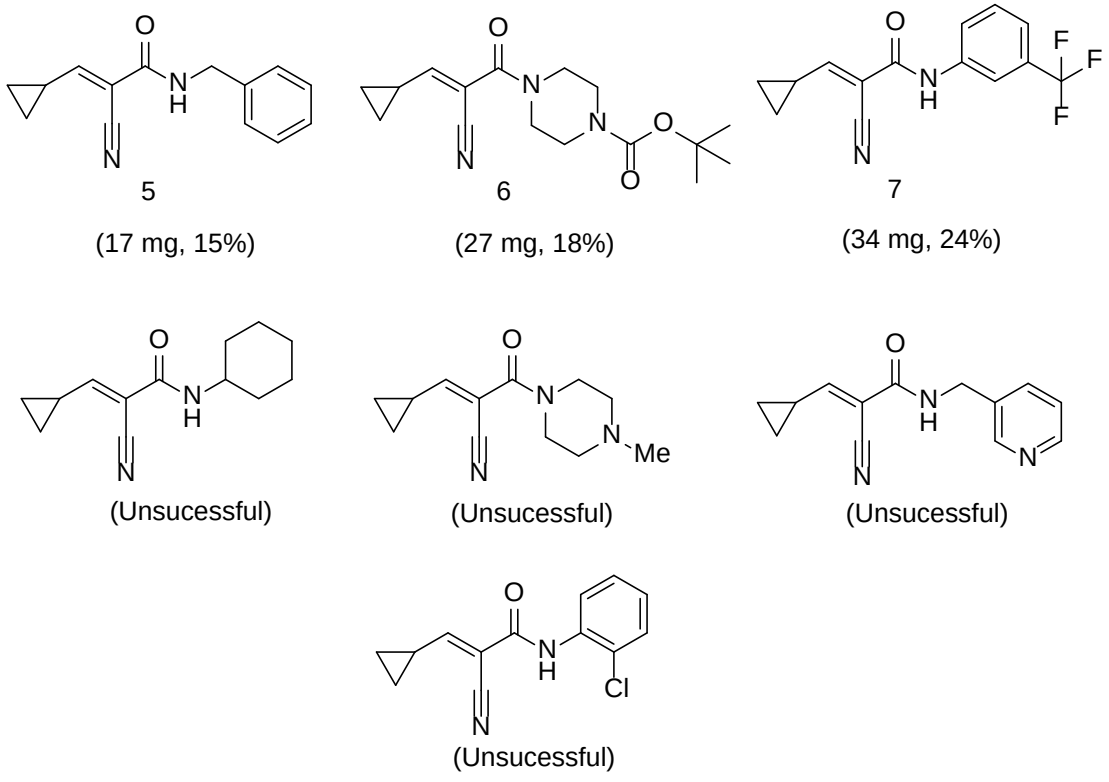

Figure 16:Attempted cyanoacrylamide syntheses from the cyclopropyl precursor and their results

A wider selection of amines was used here, giving mixed results. The benzylamine coupling (5) worked as well as it did for the benzyl precursor, giving the same yield and a similar amount of material. The other two successful reactions (6 and 7) gave better yields, but the majority of couplings in Figure 16 failed to yield useable products.

Couplings with cyclohexylamine, 1-methylpiperazine and pyridine-3-ylmethanamine (2nd row) seemed to work from the NMR data but purification (by flash chromatography) was an issue. Final products were either very impure or failed to leave the column. The last reaction with 2-chloroaniline had problems with conversion, with just the starting aniline coming out after an attempt at purification. This was likely due to the reduced nucleophilicity of the amine (which needs to attack the carbonyl on the acid to react), on account of the electronegative chlorine and mesomeric electron-withdrawing effect of the aromatic ring. The reaction was left for longer to try and accommodate for this, but it was still unsuccessful.

Finally, the cyclohexyl precursor was tried in two amide couplings, the results of which are shown below:

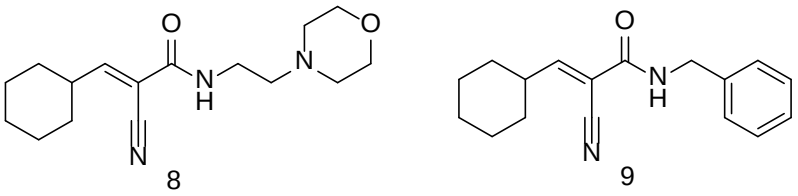

8 (20 mg, 16%)

9 (45 mg, 34%)

Figure 17: Attempted cyanoacrylamide syntheses from the cyclohexyl precursor and their results

Again, these are in similar yields and amounts to the reactions with the other precursors. Overall, the process worked for 6 of the 10 coupling reactions tried, giving a decent array of initial fragments. Problems arose in poor yields (although they gave adequate amounts for our initial aims) and difficulties with weakly nucleophilic amines, but the main issue with the method was the need to use 1-hydroxybenzotriazole (HOBt, see Figure 18) in the reaction. This reagent is explosive when dry, and the restricted material became unavailable halfway through the project.

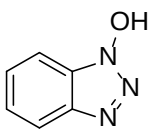

Figure 18: HOBt molecule

The need for this reagent stems from the need to suppress racemization in carbodiimide-mediated coupling reactions[19]. This is key in this project particularly as different enantiomers can have different binding affinities and activity levels in the body[20]. The lack of availability for this reagent and the problems found with the method led to the use of a new coupling agent.

In future, HOBt should probably be substituted directly for a less problematic option such as OxymaPure, but for this project it was chosen to use HATU (below), which combines a coupling agent (HBTU) and a variant of HOBt (HOAt) in one molecule[19].

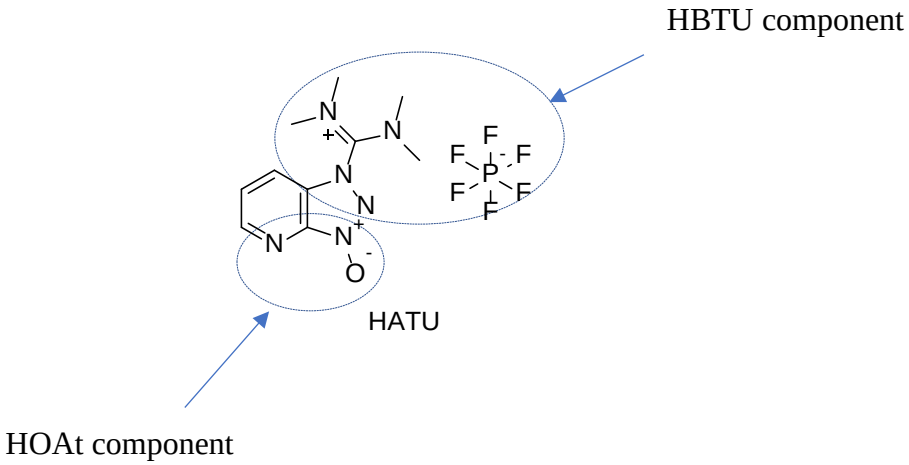

Figure 19: HATU molecule, showing HOAt and HBTU components

The same conditions were used for the HATU couplings as before, with the lack of HOBt being the only other difference to the previous method. The results of these reactions for the benzyl precursor are listed below:

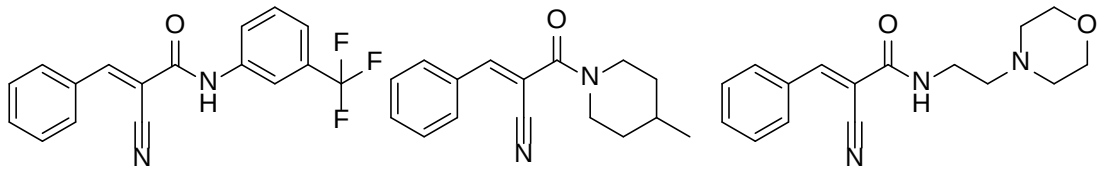

Figure 20:Attempted cyanoacrylamide syntheses from the benzyl precursor using HATU and their results

The two unsuccessful reactions failed in the purification stage, and a different column solvent was likely needed to get them out successfully. It is worth noting that the morpholino-amine (right side of Figure 20) worked with the cyclohexyl precursor but not with the benzyl equivalent. However, the cyclohexyl reaction was likely aided by its reduced steric bulk and had a different Rf value. The one reaction that was successful (compound 10) gave the best yield so far of any coupling, and the cyclopropyl precursor also provided good yields:

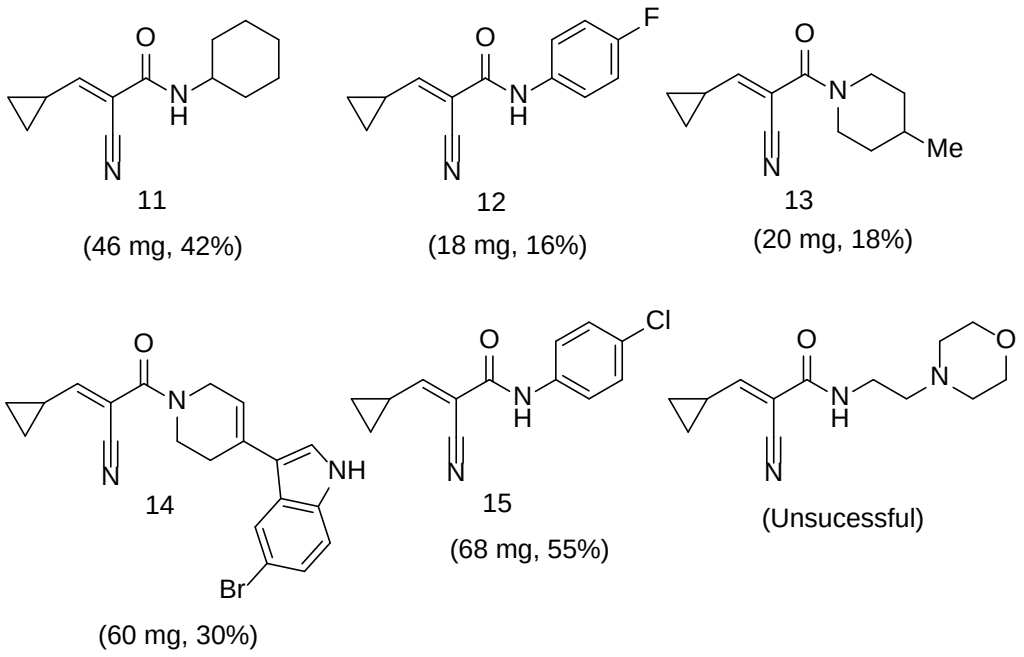

Figure 21:Attempted cyanoacrylamide syntheses from the cyclopropyl precursor using HATU and their results

The results with HATU were generally strong, with good yields overall and mostly successful reactions. Notably, the reaction with cyclohexylamine (11) worked far better than the failed EDC attempt (in Figure 16), although it was still not entirely pure. This was the only EDC reaction that was repeated with HATU, so a full direct comparison between the two methods was not possible.

It was also interesting that the 4-chloroaniline reaction was successful considering that the 2-chloro counterpart was not. This may be due to the use of HATU, or the amine may have been more nucleophilic as the electron withdrawing chlorine atom is positioned further from the amine; this could have helped the reaction progress further. Finally, reactions attempted with the cyclohexyl precursor are shown on the next page (see Figure 22).

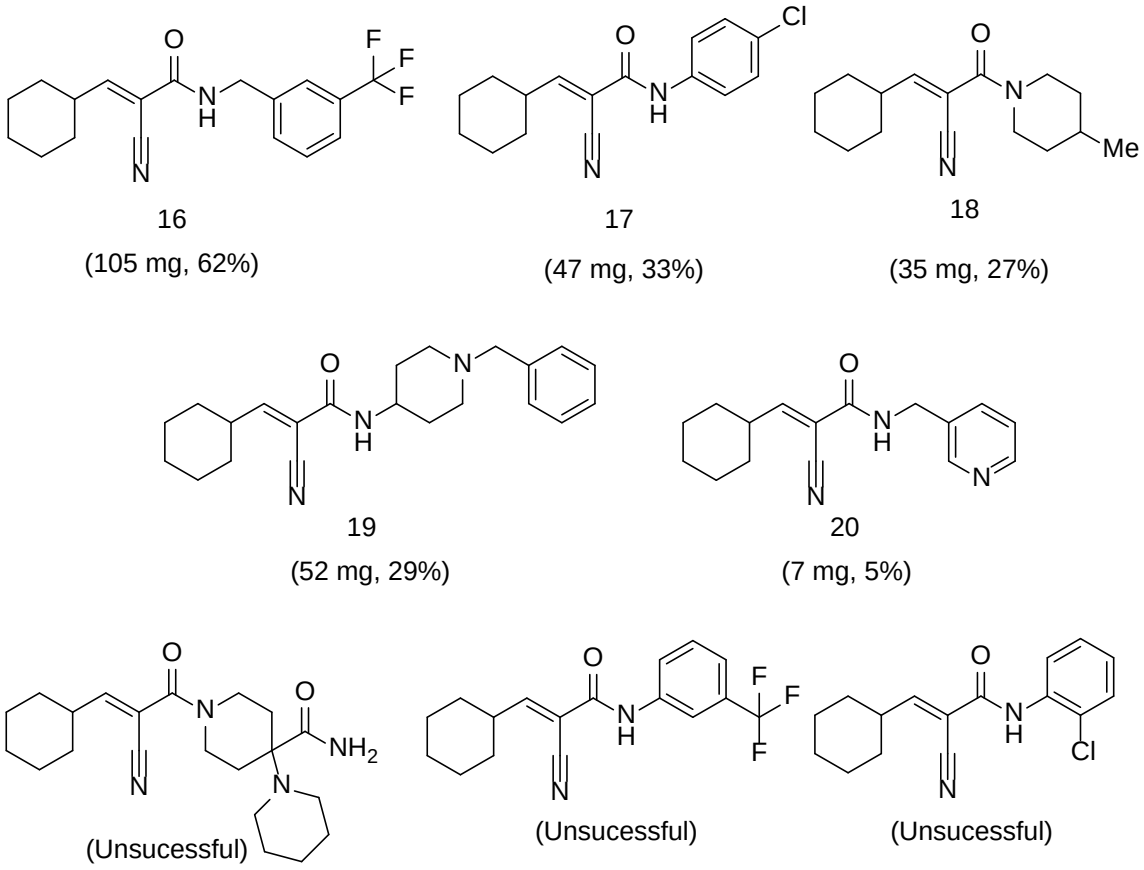

Figure 22: Attempted cyanoacrylamide syntheses from the cyclohexyl precursor using HATU and their results

Similarly to the other HATU results, these reactions were largely successful, with most giving better yields on average compared to the EDC method. The unsuccessful 2-chloroaniline (Bottom right) reaction from the cyclopropyl set was tried here but failed to give any usable product again. Mass spectrometry of these samples did show that some of the cyanoacrylamide had formed, but the lack of conversion was clear to see on the NMR spectra. It is also interesting to note that, while the trifluoro methyl aniline (16) worked in this coupling and gave a strong yield, the same amine without the methyl group was unsuccessful (bottom row, middle in Figure 22). The crude NMR's indicated the reaction had not gone to completion very well and the mixture was swamped with what appeared to be HATU.

The amine is not very nucleophilic for similar reasons as the 2-chloroaniline, and it may be that the effect of the methyl group in molecule 16 was able to push the reaction far enough to completion, although the product of that reaction itself was not entirely pure.

And the final unsuccessful reaction (bottom left) failed in the purification stage, likely needing another column solvent such as DCM:Methanol. Further improvements to the method include the introduction of a workup which was not present in the original literature procedure. This came largely as a result of poor product purity, with large amounts of HATU also being found in some final products. Finding the coupling agent in the final product was a much more notable issue with HATU compared to the carbodiimide reactions.

2.3 Investigation into Stereochemistry

The stereochemistry of the molecules produced in this project was debatable, as the nitrile group in each could be cis or trans with respect to the alkene bond (see Figure 23):

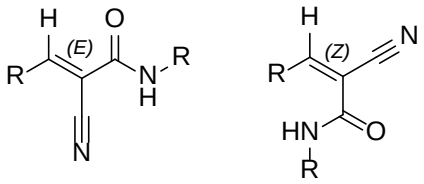

Figure 23: The two possible stereochemical arrangements of the cyanoacrylamides

Typically, the NMR coupling constants between the two protons on the alkene bond would provide an answer, as they differ depending on the conformation of the double bond[21]. However in this case, there was no such pair of protons where this could be seen due to the presence of the nitrile group on the alkene.

Structural probing methods such as X-ray crystallography would have been able to distinguish between the two, but these were not available so instead an attempt was made through NOESY (Nuclear Overhauser Effect Spectroscopy)[22]. This is a 2-D NMR method which highlights through-space interactions between protons in close vicinity. When a proton is saturated or inverted, nearby protons may exhibit an intensity increase, dubbed the Nuclear Overhauser Effect (NOE). This effect is unique among other NMR techniques in that it depends solely on the spatial proximity between protons, not via through-bond J couplings.

To show a signal on the NOESY spectrum, a molecule needs to be able to align the relevant protons in close vicinity. The Figure on the next page shows how the two possible conformations can orientate themselves to give a NOE (using the cyclopropyl group as an example). It shows that an amide (or hydroxy)-alkene NOE correlation could only be seen if the nitrile group was cis to the double bond (left-hand side of Figure 24).

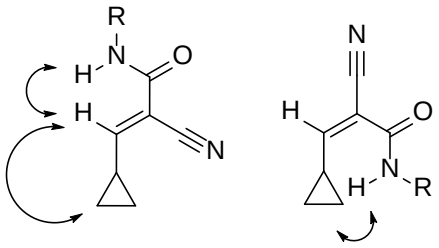

Figure 24:Possible NOESY interactions for cis nitrile (left) and trans (right) conformations

In the other configuration (right side), the amide proton cannot angle itself to be in close vicinity with the alkene proton and would not show NOE correlation. NOESY spectra were ran on the 3 precursor acids and 3 of the cyanoacrylamides which showed clear alkene/amide ^{1}H NMR peaks. If the spectra showed a 2-D cross peak, the molecule would have to be in the cis-nitrile format. The data from these spectra was not great overall, as 5 of the 6 samples did not show clear correlation between the protons in question, and the samples were not completely clean which may have interfered with the data.

However, one of the cyanoacrylamides (fragment 15) did show such a correlation (see below), albeit a weak one, and the lack of correlation in the other samples does not necessarily mean their protons are not in close vicinity, due to the dynamic nature of the NOE[23]. As a result, it can be confirmed that this molecule, and likely the other fragments from the cyclopropyl precursor, are of the conformation shown in this report.

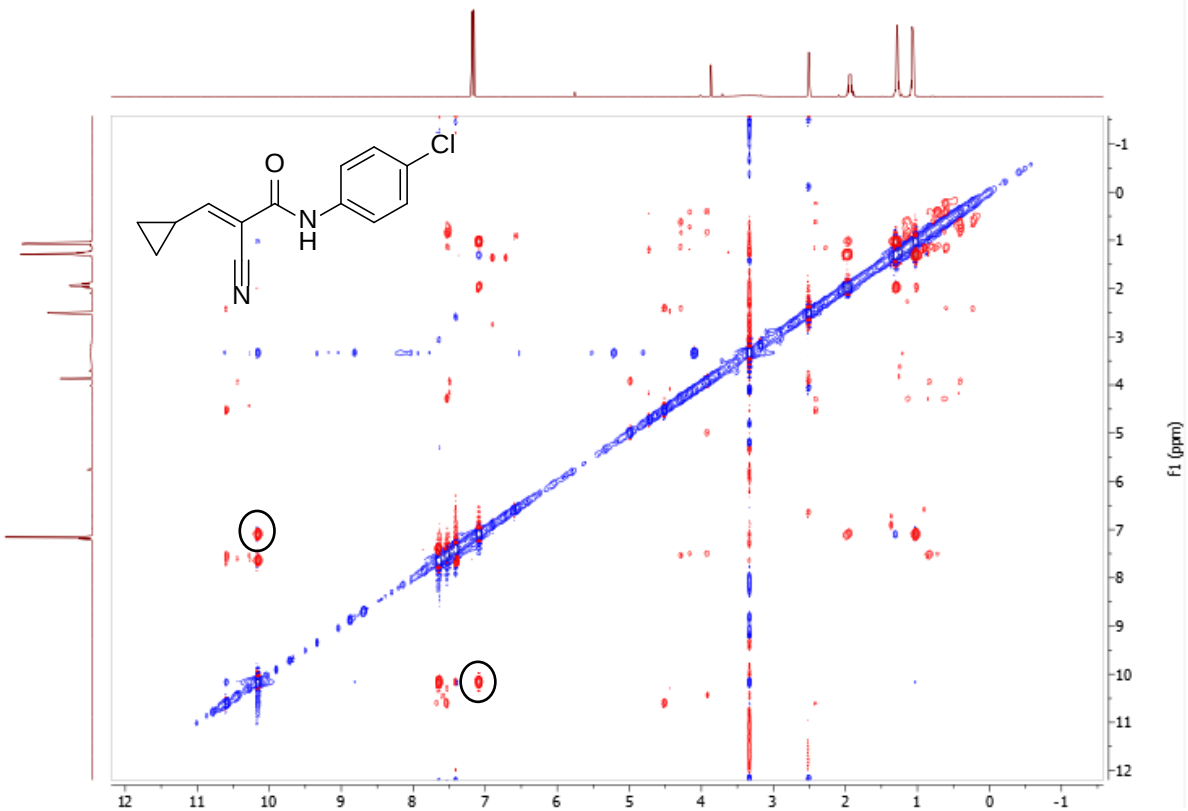

Figure 25: NOESY spectrum for fragment 15, showing a weak NOE signal (circled) between the alkene proton at 7.1 ppm and N-H proton at 10.2 ppm. N-H proton not shown on spectrum here but can be seen in regular ^{1}H NMR

The other molecules tested using this method cannot be assigned stereochemistry in such a conclusive way, but this result does allow for the assumption that they would adopt the same conformation. The surrounding literature also supports these results.

The molecules in this report are all pictured with the nitrile group cis to the olefin as this is how they were shown in surrounding literature reviewed. Further investigation into these sources yielded more information on the stereochemistry of these types of molecules. Firstly, a source covering the synthesis of compound 1[24] also studied a version of the molecule without the nitrile group (see below). The alkene bond in this molecule was confirmed to be trans with respect to the carboxylic acid group via ^{1}H NMR coupling constant of the two protons on the alkene.

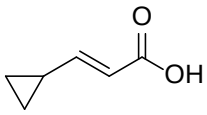

Figure 26: Version of compound 1 without nitrile group, proven to be in the trans configuration[24]

This supports the claim from the NOESY experimental data. Furthermore, the source from which Figure 10 (the amide coupling method) was acquired uses alpha-Cyano-4-hydroxycinnamic acid (CHCA), a well-known molecule which has been studied far more than those made and used in this project. The results from X-ray crystallography analysis[25] on CHCA show the carboxylic acid group again adopting a trans configuration (see Figure 27) with respect to the double bond.

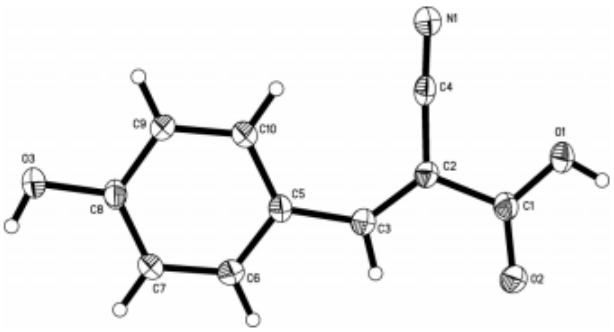

Figure 27: Molecular structure of CHCA, as derived from X-ray analysis methods[25]

CHCA is very (structurally) similar to the benzyl precursor used in this project, so the molecules based on this precursor can likely be assumed to adopt the same conformation. This source also supports the NOESY data, and as a result the molecules in this project have all been drawn with this conformation.

2.4 Glutathione testing

In total, 17 successful cyanoacrylamides were produced, out of 28 total coupling reactions during this project. As FBDD focusses on a strong fit to its target as opposed to biological potency, it was considered important to test a subset of this small fragment library in terms of binding affinity in a pseudo-real case. A test was devised using ^{1}H NMR as mentioned before to follow the interaction of some of the inhibitors with Glutathione and get preliminary data, as well as to deduce the contributing factors to a strong binding mode in this case. The paper that inspired this test used LC-MS, but this was not selected for this test due to unavailability of this instrument and the simplicity/ease of peak identification of NMR.

In a similar way to the interaction of 2-cyanoacrylates with β-ME (see Figure 6), if the reactive thiol in glutathione interacted with an inhibitor, the environment around β-hydrogen would change (from alkene to alkane). As a result, there would be a measurable drop in the alkene proton peak which would be proportional to a reduction in inhibitor concentration upon it inhibiting the glutathione (see Figure 28)

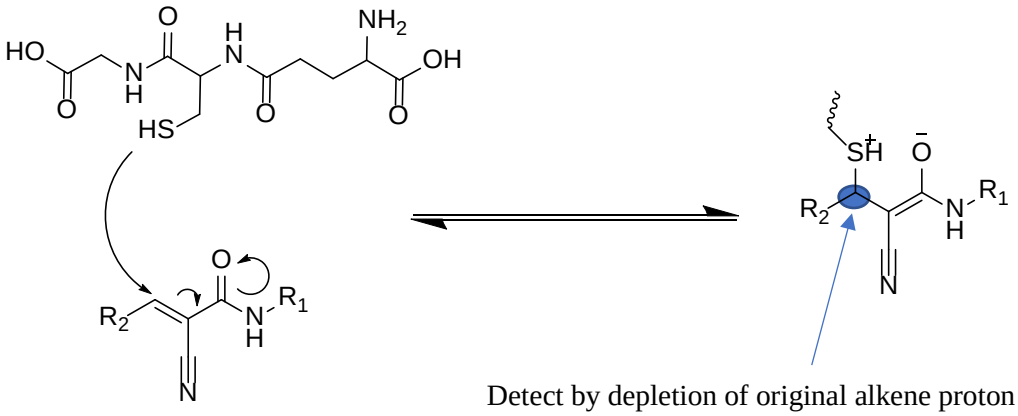

Figure 28: Illustration of Glutathione-Inhibitor interaction, showing how it might be detected by hydrogen NMR

If the process reaches an equilibrium, it should be possible to see this happening in NMR as the integral height would begin to plateau or fluctuate. This would be a good indication of the reversible behaviour of cyanoacrylamides and, depending on the depletion of the integral, would also allow for relative comparison of the inhibitors for their binding affinities in the form of rate constants for these interactions.

Difficulties arose with this method initially in terms of solubility however. The paper being followed described an excess of Glutathione reacted with inhibitors in water, but the fragments in this project are not soluble in water. The reactions therefore had to be ran in deuterated DMSO which glutathione is only sparingly soluble in. As an initial test, a subset of 3 fragment molecules were reacted in excess with glutathione to see if there was any effect in the NMR data. This ratio of reactants meant that there would be less glutathione to dissolve to get the interaction started.

As mentioned in the introduction, the interaction should depend largely on the electrophilicity of the inhibitor (i.e. its susceptibility to nucleophilic attack from the thiol residue), so the electron withdrawing nature of the amine portion should have a major impact on binding affinity. A trio of samples were tested, with notably different structures (see Figure 29).

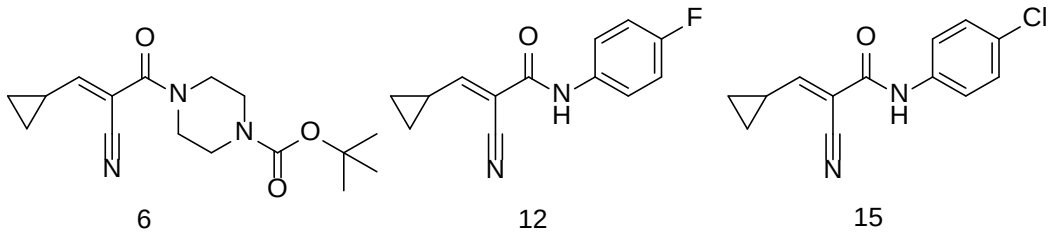

Figure 29: Initial subset of fragments tested with Glutathione

Note that only fragments from one precursor molecule (cyclopropyl) were selected in order to compare the effect of the amine only. Of these 3, only fragment 12 was noticeably affected by the interaction, and is shown in Figure 30 on the next page. This result is in line with previous expectations as the amine portion is both more electron-withdrawing than its chloro-variant (15) and far less bulky compared to fragment 6.

The graph shows how the size of the alkene proton on fragment 12 varied over hourly intervals after being mixed with Glutathione. The alkene proton was set to 1 in the pure inhibitor NMR and was then measured compared to a known NMR peak in the inhibitor that would not vary upon interacting with Glutathione.

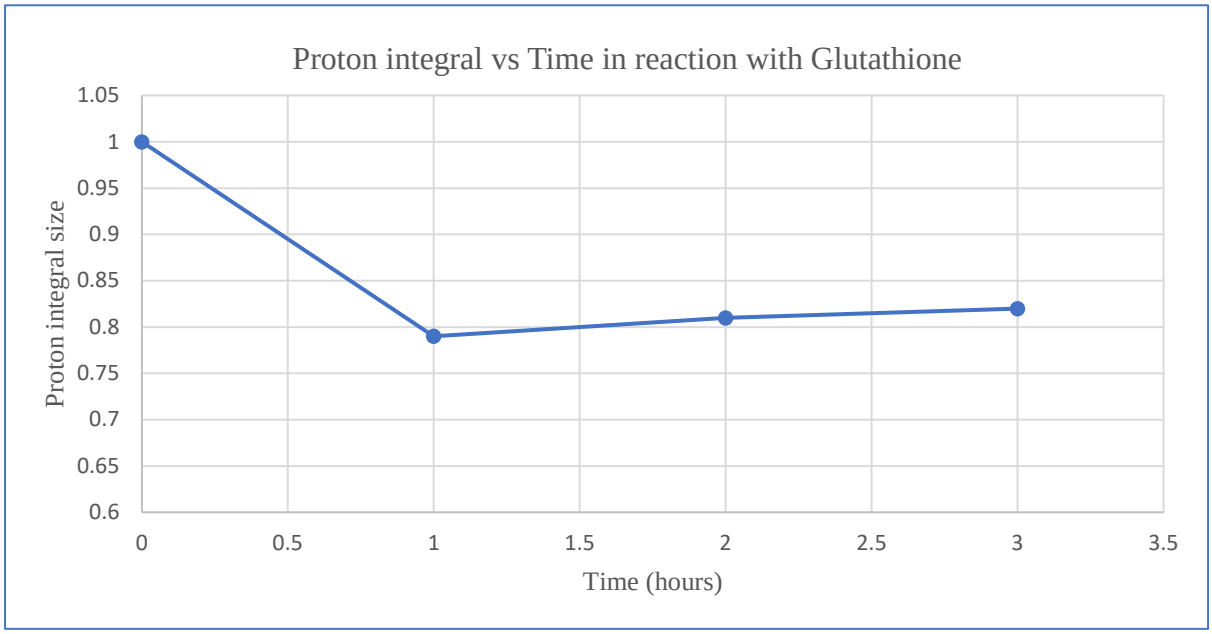

Figure 30: Graph showing variation of inhibitor proton integral upon reaction with Glutathione over time

The proton integral dropped noticeably from its initial level, peaking at 21% loss. The behaviour of the graph over time is also important; it plateaued almost immediately, which is a sign of an equilibrium being found. This may however be due to the glutathione being the limiting reagent in this test, and the inhibitor may have simply reacted with all the glutathione present in the sample. An NMR taken 24 hours after the interaction began gave a proton integral of 0.79, so the effect was sustained.

Fragments 6 and 15 were monitored in the same way for a similar amount of time (as were future tests) and showed no noticeable difference. The reason for monitoring the interaction for such a short length of time is because this was purely preliminary data used to probe the interaction (if any) taking place.

The data can (largely for ease of comparison as opposed to accuracy) be best fitted to first order kinetics (like in the paper this method is based upon) via a natural log vs time graph. The negative gradient of the trendline gave a rate constant for the interaction, 0.057 hr^{-1}, left in units of hours for convenience sake. This value is solely for relative comparison, and the R^2 value (0.4597) indicates the level of correlation between the data and the trendline it has been fitted to. With a value of 1 representing perfect correlation and 0 representing no relation between the data points, this data does not correlate well and thus cannot be considered quantitative. Although, in most of the later experiments, the correlation was much better.

From this initial data, it was concluded that it is viable to garner relative data using this method and that further preliminary testing on more fragments would be of use to the project. To better probe the interaction, a 1:1 ratio of inhibitor:glutathione was used in future tests. If the inhibitor was reacting with all glutathione present, the NMR would show complete depletion of the proton integral to zero and this could be confirmed. 6 fragments were tested using the 1:1 conditions, giving mixed results. The table on the next page (Figure 31) details the rate constants for these experiments (k_{GSH}), along with the R^2 value for the natural log vs time graph to give an indication of the quality of fit to first order kinetics.

Sample	k_{GSH} (hr^{-1})	R^2
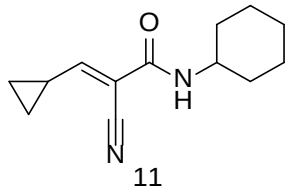 11	0.0542	0.4452
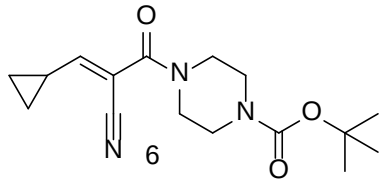 6	0	0
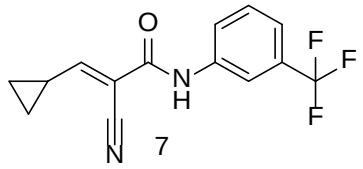 7	0	0
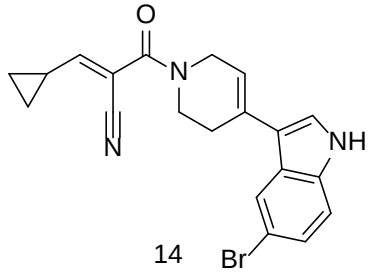 14	0.1337	0.6828
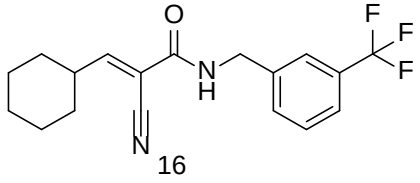 16	0.0312	0.6657
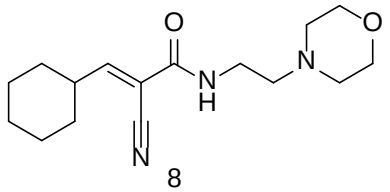 8	0.1887	0.7733

Figure 31: Table showing rate constants and R squared values for the 1:1 interaction between various fragments and Glutathione

The higher the rate constant, the more favourable the interaction and thus the better relative binding affinity of the fragment to the glutathione. Two of the fragments didn't have an interaction, one of these being a repeat fragment from Figure 29 (fragment 6) and the other being fragment 7.

The trifluoro group in fragment 7 is very strongly electron withdrawing but was not favoured in this interaction, presumably due to the steric hinderance of such a nearby aromatic ring, and a somewhat bulky trifluoro group. This is further evidenced by fragment 16, where the added methyl group seemed to give the space needed to accommodate an interaction.

Fragment 11 was structurally less imposing compared to the other fragments tested, and this seemed allow it to inhibit the glutathione, albeit to a small extent. More favourable interactions came from the other two entries in the table, with fragment 8 having a morpholino group with two electronegative atoms which were separated from the amide by two methyl groups. This combination provided steric and inductive favourability towards an interaction, so it made sense that this yielded the highest rate constant. Fragment 14 has a similar make-up with electronegative atoms and bulky groups at a good distance from the amide, although to a lesser extent, giving it the second-highest rate constant. Overall, the best-performing fragments having some separation between their bulkiest groups and the amide was a noticeable trend here. Note also that the final 3 entries in this table showed much improved R^2 values. The data shows an interesting variety of rate constants, and importantly the plateau behaviour exhibited in the first test was mostly maintained here, which implies partial, reversible inhibition of the glutathione and an equilibrium being reached.

The data for the first entry in Figure 31 was particularly interesting, as it seemed to show a back-and-forth between the binded and unbinded forms of the glutathione adduct. The integral size vs time graph (Figure 32) is shown below:

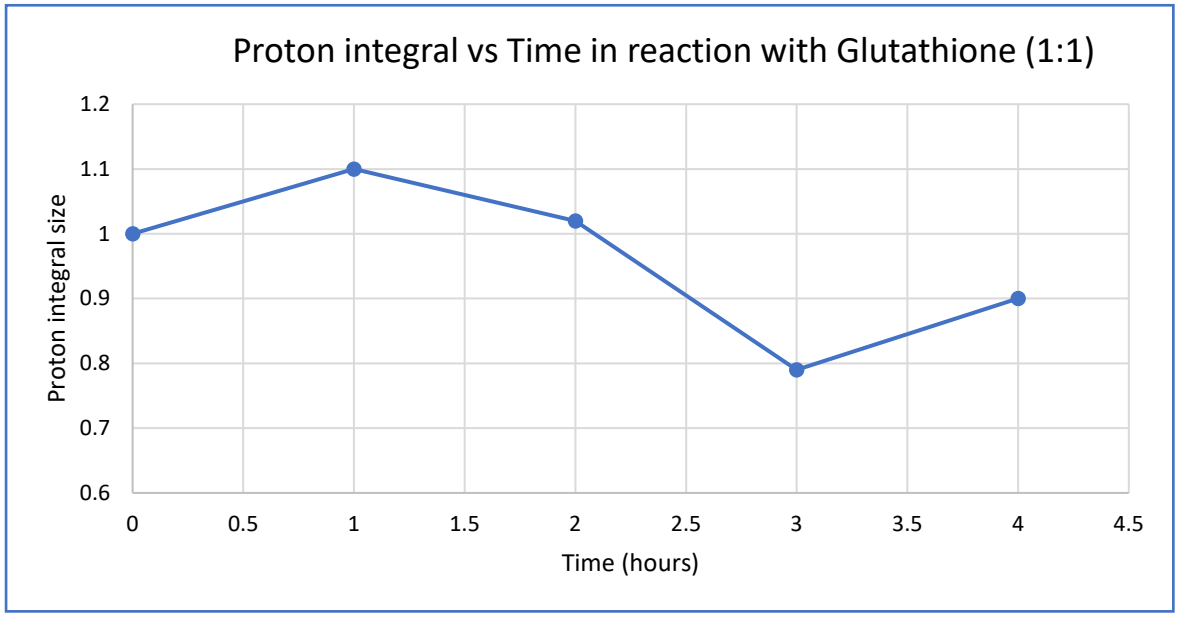

Figure 32: Graph showing size of proton integral vs time for Fragment 11 in Figure 30

This behaviour was very different from the other fragment interactions in which the integral merely dropped and levelled off immediately. Each hour, the size of the integral changed noticeably, initially rising (it is unknown as to why) and then dropping to its minimum value of 0.79 (a 21% reduction on the starting value) before rising again to 0.90. An NMR taken 24 hours after the interaction showed the integral had effectively returned to its original size (1.03).

Naturally, the effects of Le Chatelier's principle on equilibria were considered when trying to explain this behaviour. As conditions around the sample remained largely the same (i.e. temperature pressure etc), the loss of one of the reactants was thought to be the culprit, as this would cause the equilibrium to favour the reactants to account for this loss. It is unlikely that the inhibitor compound would degrade under these conditions or take part in any side reaction, but the thiol source (glutathione) could have been lost in another reaction due to its role in the body.

Glutathione is an antioxidant present in cells in the body which helps to remove reactive oxidising species by undergoing a redox reaction in which it is oxidised[26]. The product is the dimer, glutathione disulfide (see Figure 33), and the process in turn causes reduction of these reactive species, protecting the cells from any damage they might cause. To give an example, sufferers of Cystic Fibrosis have a lower concentration of glutathione compared to others[27].

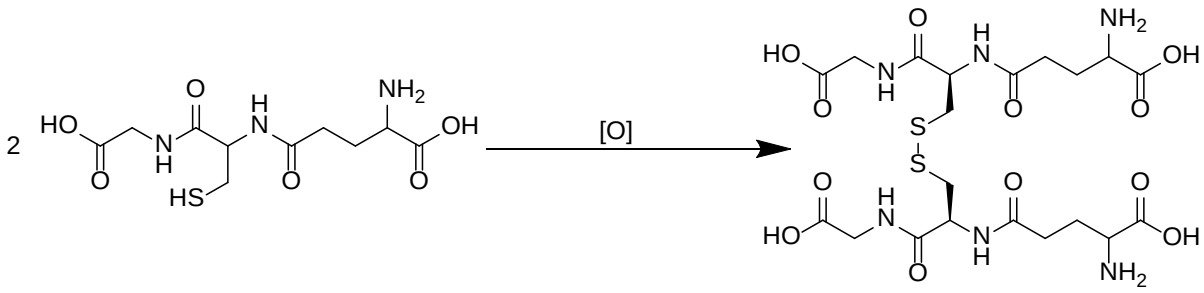

Figure 33: Glutatione dimerisation via oxidation

This dimerization also happens to the lone cysteine amino acid (which makes up the thiol-section of glutathione) in the body to form disulphide bonds in proteins[28]. The sulfur atoms in this dimer form would be far less likely to interact with an inhibitor molecule. Thus, this would result in a loss of the reactive thiol in the inhibitor-test reaction mixture and a shift in the equilibrium (like that seen in Figure 32).

To have this interaction be possible, there would need to be an oxidative environment in the glutathione tests and the solvent (DMSO) provides that. A recent paper[29] studied the interaction of l-cysteine with a slight excess of DMSO at room temperature for 24 hrs. Using infrared spectrometry, the reaction was monitored and substantial changes to the mixture were seen in just a couple of hours (see Figure 34).

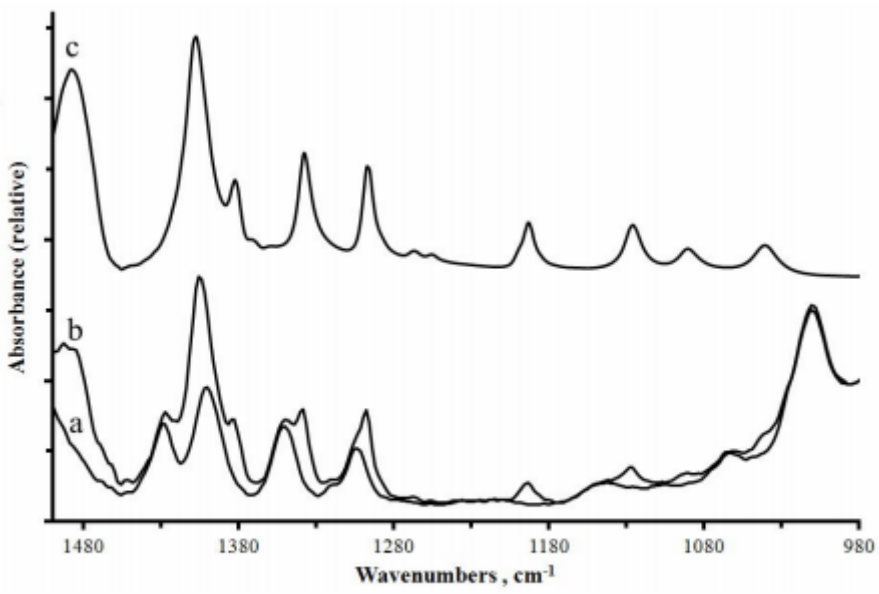

IR spectra recorded in the course of the reaction of L-cysteine with DMSO after (a) 0 *min*; (b) 2 *h*; (c) of the isolated product.

Figure 34: IR spectra data showing the reaction between l-cysteine and glutathione, with the isolated product (c) at the top

The initial mixture (graph a in Figure 34) and much-changed sample after 2 hours (b) can be seen on the bottom side of the Figure, and b was later isolated and found to be l-cystine (c), the dimeric form of l-cysteine. As a result, it is likely that glutathione in the inhibitor tests was being lost to a similar oxidation, with the DMSO being reduced to dimethyl sulphide (DMS) and water also being formed. This would explain the behaviour seen in Figure 32.

3 Conclusions and Further Work

The work detailed in this report highlights the potential of this synthetic route to a diverse range of cyanoacrylamides. The initial aims of the project have been met using this approach, with more than 15 fragment molecules made and the majority of them in appropriate amounts.

However, while in theory fragment synthesis using this method can work with all reactants, in practice it is clearly not a “one size fits all” process. Making the 17 cyanoacrylamides in this project has required variation in purification, method and coupling reagents, and each synthesis requires its own optimisation approach. As a result, not all syntheses worked, and the route faced problems in purification and conversion aspects at times.

Other synthesis options were also considered during this project (partly to counter these problems), such as the conversion of the precursor acids to acyl chlorides to give the carbonyl a more favourable leaving group with a lower pKa (see Figure 35):

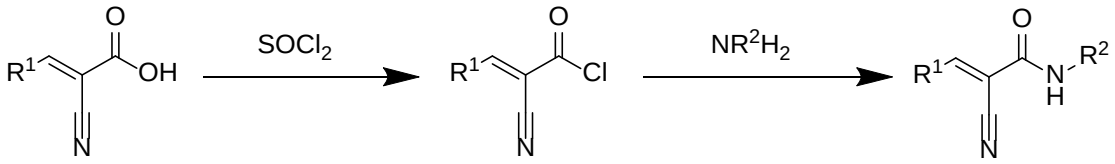

Figure 35:Alternative approach converting our precursor molecules into acyl chlorides

This would eliminate the need for coupling agents and the reagents they require and may also aid reactions with weakly-nucleophilic amines such as the 2-chloroaniline discussed earlier. The reason for not doing this conversion during the project was because of the requirement of an extra step in the scheme, as well as the fact that the aim of getting at least 15 fragment molecules took priority. This is a point to consider for future work as a result. In addition, looking into more precursor molecules such as the isopropyl variant (Figure 36) would also be worth doing to further show the potential of this synthetic plan:

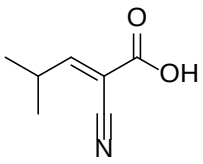

Figure 36: Isopropyl precursor molecule

The tests involving glutathione in this project were adequate for comparisons of relative binding affinities, and good comparisons were made for the fragment. However, a more quantitative investigation would be useful in future and the method could be modified for this. For instance, using an internal standard for the NMR would allow for direct conversion of integral size to concentration, and access to additional data such as equilibrium constants.

Conditions in the body could be simulated with a pH buffer solution (pH 7.4) and heating of the sample to 37 degrees, while glutathione could be reacted in excess (like in the original paper) as this would likely be the case in the body. Following the interaction for longer would also help the quality of the data and allow for better understanding of equilibria but the method in this project was done out of convenience and the need to get relative data. The potential for this method can easily be seen however.

In addition, DMSO should not be used in future tests due to the potential oxidative environment it provides which was thought to interfere with our testing. Finding a solvent that would dissolve both the fragments and glutathione while not interfering with the equilibrium would be challenging and take time. Hence this would be another point to consider if any future work were to be carried out.

4 Experimental

4.1 General Experimental Practice

Starting reagents were obtained from commercial suppliers and were used without further purification, except for the majority of amines used in cyanoacrylamide syntheses which were supplied by KeyOrganics, the industrial collaborator for this project. All water used in the reactions was deionised and organic extracts were dried over anhydrous sodium sulfate before solvent removal using a Büchi rotary evaporator. 'Petrol' refers to the fraction bp 40-60°C, “DCM” refers to Dichloromethane and “EtOAc” refers to ethyl acetate. NMR spectra were retrieved at 298 K, at 400 MHz using a Bruker AV400 or AVIII 400 and were typically run in a solution of CD_3OD (deuterated methanol) (or $(CD_3)_2SO$ (deuterated DMSO) in some cases).

NMR shifts are given in ppm downfield and the residual solvent peak (CD_3OD δ_H 3.31, δ_C 49.00, $(CD_3)_2SO$ δ_H 2.50, δ_C 39.52) was used as an internal standard. All coupling constants are given in Hertz (Hz) and peaks are labelled s (singlet), d (doublet), t (triplet), q (quartet), dd (doublet of doublets) or m (multiplet). Relevant atoms on molecular structures are labelled with numbers to better identify them for analysis. When required, a distinction is made between protons attached to the same carbon that have different chemical shifts. Also, where there is more than 1 carbon or hydrogen environment on a peak, this is noted and the number of protons from each environment is shown (e.g. 2x H-3/7 means 2 of the protons on carbons 3 and 7, but not all)

In some cases, carbons and protons are referred to by their functional group (e.g. C=O refers to the carbon peak for the carbonyl group, and ArC refers to a carbon in an aromatic environment) or by their adjacent numbered carbons (e.g. C-1=**C** refers to the carbon connected to carbon 1 via an alkene bond, with the carbon in question in bold/underlined text) Mass spectra were recorded using a Bruker MicroTOF which used electrospray (ES) ionisation techniques with the positive ion detection method in methanol.

4.2 Precursor molecules syntheses

2-cyano-3-cyclopropylacrylic acid (1):

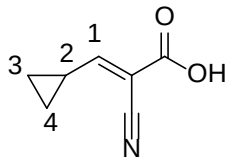

A solution of 2-cyanoacetic acid (1.2759 g, 15 mmol) and cyclopropanecarbaldehyde (1.1208 mL, 15 mmol) in absolute ethanol (150 mL) was treated portion-wise with piperidine (0.1482 mL, 1.5 mmol) and stirred at 60 degrees for 3 hrs. The resulting mixture was cooled to room temperature and dried under vacuum to give a wet white solid. The crude product was purified by flash chromatography (98:2 DCM: Methanol) to give a white powdery solid (2.0565 g, 46%). TOFMS *m/z* (ESI^+): 138.0546 ($M+H^+$, $C_7H_8NO_2$ requires 138.0550), 160.0371 ($M+Na^+$, $C_7H_7NNaO_2$ requires 160.0369); ^1H NMR (400 MHz, CD_3OD): 7.12 (d, 1H, H-1, J 11.4), 2.06 (m, 1H, H-2), 1.34 (m, 2H, H-4), 1.03 (m, 2H, H-3); ^{13}C NMR (400 MHz, CD_3OD): 169.0 (C-1), 163.0 (C=O), 114.4 (CN), 105.5 (C-1=**C**), 15.4 (C-2), 10.2 (C-3 and C-4)

2-cyano-3-cyclohexylacrylic acid (2):

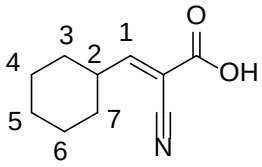

A solution of 2-cyanoacetic acid (1.2759 g, 15 mmol) and cyclohexanecarbaldehyde (1.8175 mL, 15 mmol) in absolute ethanol (150 mL) was treated portion-wise with piperidine (0.1482 mL, 1.5 mmol) and stirred at 60 degrees for 3 hrs. The resulting mixture was cooled to room temperature and dried under vacuum to give a wet white solid. The crude product was purified by flash chromatography (98:2 DCM: Methanol) to give a yellow powdery solid

(0.9619 g, 36%). TOFMS *m/z* (ESI^+): 202.0838 ($M+Na^+$, $C_{10}H_{13}NNaO_2$ requires 202.0838); ^1H NMR (400 MHz, CD_3OD): 7.51 (d, 1H, H-1, J 10.3), 2.68 (m, 1H, H-2), 1.83 (m, 2H, H-4_a and H-6_a), 1.76 (m, 3H, H-3_a, H-7_a, H-5_a), 1.38 (m, 5H, H-4_b, H-5_b, H-6_b, H-3_b, H-7_b); ^{13}C NMR (400 MHz, CD_3OD): 167.1 (C-1), 162.8 (C=O), 113.6 (CN), 108.0 (C-1=**C**), 41.2 (C-3 and C-7), 30.7 (C-2), 25.1 (1x C-4/5/6), 24.7 (2x C-4/5/6)

2-cyano-3-phenylacrylic acid (3):

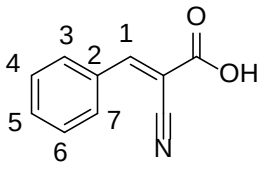

A solution of 2-cyanoacetic acid (1.2759 g, 15 mmol) and benzaldehyde (1.5303 mL, 15 mmol) in absolute ethanol (150 mL) was treated portion-wise with piperidine (0.1482 mL, 1.5 mmol) and stirred at 60 degrees for 3 hrs. The resulting mixture was cooled to room temperature and dried under vacuum to give a wet white solid. The crude product was purified by flash chromatography (98:2 DCM: Methanol) to give a white solid (0.6902 g, 27%). TOFMS *m/z* (ESI^+): 174.0544 ($M+H^+$, $C_{10}H_8NO_2$ requires 174.0550), 196.0361 ($M+Na^+$, $C_{10}H_7NNaO_2$ requires 196.0374); ^1H NMR (400 MHz, CD_3OD): 8.34 (s, 1H, H-1), 8.04, (d, 2H, H-3 and H-7, J 7.6), 7.59, (m, 3H, H-4, H-5, H-6); ^{13}C NMR (400 MHz, CD_3OD): 163.5 (C-1), 154.5 (C=O), 132.8 (C-2), 131.8 (C-3 and C-7), 130.5 (C-4 and C-6), 128.9 (C-5) 115.4 (CN), 103.6 (C-1=**C)**

4.3 Cyanoacrylamide syntheses

N-benzyl-2-cyano-3-phenylacrylamide (4):

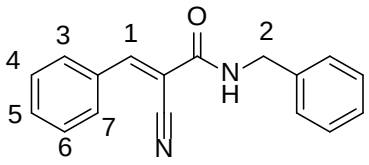

Compound 3 (0.0866 g, 0.5 mmol), HOBt.H_2O (0.0811 g, 0.6 mmol) and EDC.HCl (0.1150 g, 0.6 mmol) were dissolved in DCM:DMF (2 mL, 10:1 v/v) at 0^{o}C and stirred for 10 minutes under inert atmosphere. Then, benzylamine (0.0601 mL, 0.55 mmol) and DIPEA (0.2298 mL, 1.32 mmol) were added and the reaction continued at 0^{o}C for 30 minutes. The mixture was stirred at room temperature for a further 24 hrs. The solution was then dried under vacuum to give a yellow oil, which was purified by flash chromatography (10:4 Petrol: EtOAc) to give pure product as a white solid. TOFMS *m/z* (ESI^+): 263.1173 ($M+H^+$, $C_{17}H_{15}N_2O$ requires 263.1179), 285.1006 ($M+Na^+$, $C_{17}H_{14}N_2NaO$ requires 285.0998); ^{1}H NMR (400 MHz, CD_3OD): 8.23 (s, 1H, H-1), 8.00 (d, 2H, H-3 and H-7, J 7.5), 7.56 (m, 3H, H-4, H-5, H-6), 7.36 (m, 4H, Ar-H), 7.28 (m, 1H, Ar-H), 4.55 (s, 2H, H-2); ^{13}C NMR (400 MHz, CD_3OD): 151.6 (C=O), 132.3 (C-1), 130.1 (ArC), 128.9 (ArC) 128.1 (ArC), 127.2 (ArC), 127.0 (CN), 94.9 (C-1=**C**), 43.5 (C-2)

N-benzyl-2-cyano-3-cyclopropylacrylamide (5):

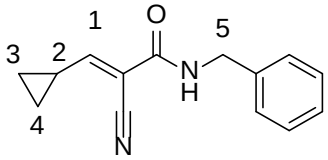

Compound 1 (0.0686 g, 0.5 mmol), HOBt.H_2O (0.0811 g, 0.6 mmol) and EDC.HCl (0.1150 g, 0.6 mmol) were dissolved in DCM:DMF (2 mL, 10:1 v/v) at 0^{o}C and stirred for 10 minutes under inert atmosphere. Then, benzylamine (0.0601 mL, 0.55 mmol) and DIPEA (0.2298 mL, 1.32 mmol) were added and the reaction continued at 0^{o}C for 30 minutes. The mixture

was stirred at room temperature for a further 24 hrs. The solution was then dried under vacuum to give a yellow oil, which was purified by flash chromatography (10:4 Petrol: EtOAc) to give pure product as a white flaky solid (17.3 mg, 15%). TOFMS *m/z* (ESI^+): 227.1172 ($M+H^+$, $C_{14}H_{15}N_2O$ requires 227.1179), 249.1007 ($M+Na^+$, $C_{14}H_{14}N_2NaO$ requires 249.0998); ^1H NMR (400 MHz, CD_3OD): 7.31 (m, 5H, Ar-H), 6.95 (d, 1H, H-1, J 11.2), 4.47 (s, 2H, H-5), 2.05 (m, 1H, H-2), 1.30 (m, 2H, H-4), 0.97 (m, 2H, H-3); ^{13}C NMR (400MHz, CD_3OD): 163.4 (C-1), 160.1 (C=O), 136.8 (ArC), 126.6 (ArC), 125.6 (ArC), 125.3 (ArC), 113.1 (CN), 105.6 (C-1=**C**), 41.6 (C-5), 13.6 (C-2), 8.1 (C-3 and C-4)

tert-butyl-4-(2-cyano-3-cyclopropylacryloyl) piperazine-1-carboxylate (6):

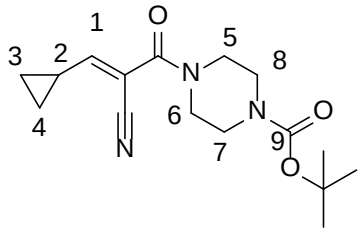

Compound 1 (0.0686 g, 0.5 mmol), $HOBt.H_2O$ (0.0811 g, 0.6 mmol) and EDC.HCl (0.1150 g, 0.6 mmol) were dissolved in DCM:DMF (2 mL, 10:1 v/v) at 0^oC and stirred for 10 minutes under inert atmosphere. Then, 1-boc-piperazine (0.1025 g, 0.55 mmol) and DIPEA (0.2298 mL, 1.32 mmol) were added and the reaction continued at 0^oC for 30 minutes. The mixture was stirred at room temperature for a further 24 hrs. The solution was then dried under vacuum to give a yellow oil, which was purified by flash chromatography (10:4 Petrol: EtOAc) to give pure product as a white solid (27.1 mg, 18%). TOFMS *m/z* (ESI^+): 328.1641 ($M+Na^+$, $C_{16}H_{23}N_3NaO_3$ requires 328.1632), 323.2078 ($M+NH_4^+$, $C_{16}H_{27}N_4O_3$ requires 323.2078); ^1H NMR (400 MHz, CD_3OD): 6.59 (d, 1H, H-1, J 11.1), 3.63 (m, 4H, 4x H-5/6/7/8), 3.51 (m, 4H, 4x H-5/6/7/8), 2.05 (m, 1H, H-2), 1.49 (s, 9H, t-Bu), 1.35 (m, 2H, H-4), 0.95 (m, 2H, H-3) ^{13}C NMR (400MHz, CD_3OD): 163.3 (**C**=O), 161.7 (C-1), 158.8 (C-9), 113.2 (CN), 104.8 (C-1=**C**), 78.9 (**C**-$(CH_3)_3$), 78.8 (C-5, C-6, C-7, C-8), 25.7 (C-(**C**$H_3)_3$) 13.5 (C-2), 7.7 (C-4), 7.5 (C-3)

2-cyano-3-cyclopropyl-N-(3-(trifluoromethyl)phenyl)acrylamide (7):

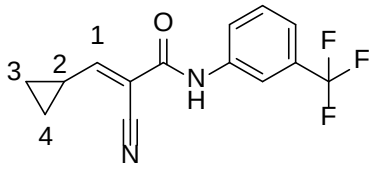

Compound 1 (0.0686 g, 0.5 mmol), EDC.HCl (0.1150 g, 0.6 mmol) and HOBt.H_2O (0.0811 g, 0.6 mmol) were dissolved in DCM:DMF (2 mL, 10:1 v/v) at 0^{o}C and stirred for 10 minutes under inert atmosphere. Then, 3-(trifluoromethyl)aniline (0.0687 mL, 0.55 mmol) and DIPEA (0.2298 mL, 1.32 mmol) were added and the reaction continued at 0^{o}C for 30 minutes. The mixture was stirred at room temperature for a further 24 hrs. The solution was then dried under vacuum to give a yellow oil, which was purified by flash chromatography (1:2 Petrol: EtOAc) to give pure product as a yellow solid (34 mg, 24%). TOFMS *m/z* (ESI^+): 303.0715 ($M+Na^+$, $C_{14}H_{11}N_2F_3NaO$ requires 303.0721); ^{1}H NMR (400 MHz, CD_3OD): 8.04 (s, 1H, Ar-H), 7.85 (m, 1H, Ar-H), 7.55 (t, 1H, Ar-H, J 8.1), 7.45 (m, 1H, Ar-H), 7.08 (d, 1H, H-1, J 11.1), 2.11 (m, 1H, H-2), 1.36 (m, 2H, H-4), 1.05 (m, 2H, H-3); ^{13}C NMR (400 MHz, CD_3OD): 166.7 (C=O), 160.5 (C-1), 138.7 (ArC), 129.3 (ArC), 129.2 (ArC), 123.9 (ArC), 120.7 (ArC), 117.2 (ArC), 114.4 (CN), 108.0 (C-1=**C**), 15.4 (C-2), 9.9 (C-3 and C-4)

2-cyano-3-cyclohexyl-N-(2-morpholinoethyl) acrylamide (8):

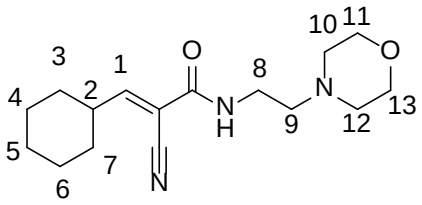

Compound 2 (0.0896 g, 0.5 mmol), HOBt.H_2O (0.0811 g, 0.6 mmol) and EDC.HCl (0.1150 g, 0.6 mmol) were dissolved in DCM:DMF (2 mL, 10:1 v/v) at 0^{o}C and stirred for 10 minutes under inert atmosphere. Then, 2-morpholino ethan-1-amine (0.0722 mL, 0.55 mmol) and DIPEA (0.2298 mL, 1.32 mmol) were added and the reaction continued at 0^{o}C for 30 minutes. The mixture was stirred at room temperature for a further 24 hrs. The solution was then dried under vacuum to give an orange oil, which was purified by flash chromatography

(1:2 Petrol: EtOAc) to give pure product as a yellow oil (20.1 mg, 14%). TOFMS *m/z* (ESI^+): 292.2025 ($M+H^+$, $C_{16}H_{26}N_3O_2$ requires 292.2020), 314.1846 ($M+Na^+$, $C_{16}H_{25}N_3NaO_2$ requires 314.1839); ^1H NMR (400 MHz, CD_3OD): 7.35 (d, 1H, H-1, J 10.2), 3.72 (t, 4H, H-11 and H-13, J 4.7), 3.45 (t, 2H, H-8, J 6.6), 2.66 (m, 1H, H-2), 2.56 (t, 2H, H-9, J 6.6), 2.52 (m, 4H, H-10 and H-12), 1.83 (m, 2H, $H\text{-}4_a$ and $H\text{-}6_a$), 1.76 (m, 3H, $H\text{-}3_a$, $H\text{-}7_a$, $H\text{-}5_a$), 1.38 (m, 5H, $H\text{-}4_b$, $H\text{-}5_b$, $H\text{-}6_b$, $H\text{-}3_b$, $H\text{-}7_b$); ^{13}C NMR (400 MHz, CD_3OD): 161.4 (C-1), 159.9 (C=O), 112.4 (CN), 108.1 (C-1=**C**), 64.9 (C-11 and C-13), 55.3 (C-10 and C-12), 51.7 (C-9), 39.6 (C-8), 34.8 (C-3 and C-7), 29.4 (C-2), 23.6 (1x C-4/5/6), 23.2 (2x C-4/5/6)

N-benzyl-2-cyano-3-cyclohexylacrylamide (9):

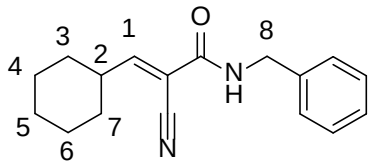

Compound 2 (0.0896 g, 0.5 mmol), EDC.HCl (0.1150 g, 0.6 mmol) and $HOBt.H_2O$ (0.0811 g, 0.6 mmol) were dissolved in DCM:DMF (2 mL, 10:1 v/v) at 0°C and stirred for 10 minutes under inert atmosphere. Then, benzylamine (0.0601 mL, 0.55 mmol) and DIPEA (0.2298 mL, 1.32 mmol) were added and the reaction continued at 0°C for 30 minutes. The mixture was stirred at room temperature for a further 24 hrs. The solution was then dried under vacuum to give a yellow oil, which was purified by flash chromatography (10:4 Petrol: EtOAc) to give pure product as a yellow oil (45 mg, 34%). TOFMS *m/z* (ESI^+): 269.1637 ($M+H^+$, $C_{17}H_{21}N_2O$ requires 269.1648), 291.1473 ($M+Na^+$, $C_{17}H_{20}N_2NaO$ requires 291.1468); ^1H NMR (400 MHz, CD_3OD): 7.33 (m, 6H, Ar-H + H-1), 3.37 (s, 2H, H-8), 2.67 (m, 1H, H-2), 1.75 (m, 5H, $H\text{-}3_a$, $H\text{-}4_a$, $H\text{-}7_a$, $H\text{-}5_a$, $H\text{-}6_a$), 1.32 (m, 5H, $H\text{-}3_b$, $H\text{-}4_b$, $H\text{-}5_b$, $H\text{-}6_b$, $H\text{-}7_b$); ^{13}C NMR (400 MHz, CD_3OD): 163.0 (C-1), 153.7 (C=O) 138.2 (ArC), 128.6 (ArC), 128.4 (ArC), 128.2 (ArC), 127.2 (ArC), 126.9 (CN), 110.2 (C-1=**C**) 43.3 (C-8), 41.2 (1x C-3/7), 30.1 (C-2 and 1x C-3/7), 25.1 (C-5), 24.8 (C-4 and C-6)

2-cyano-3-phenyl-N-(3-(trifluoromethyl)phenyl)acrylamide (10):

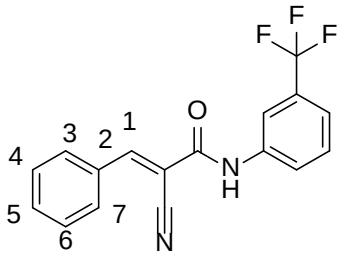

Compound 3 (0.0866 g, 0.5 mmol) and HATU (0.2281 g, 0.6 mmol) were dissolved in DCM:DMF (2 mL, 10:1 v/v) at 0^{o}C and stirred for 10 minutes under inert atmosphere. Then, 3-(trifluoromethyl) aniline (0.0687 mL, 0.55 mmol) and DIPEA (0.2298 mL, 1.32 mmol) were added and the reaction continued at 0^{o}C for 30 minutes. The mixture was stirred at room temperature for a further 24 hrs, before being diluted with water and washed with EtOAc. The organic layer was dried using anhydrous sodium sulphate and the solvent was evaporated under vacuum to give an orange/brown wet solid, which was purified by flash chromatography (1:5 Petrol: EtOAc) to give pure product as a yellow wet solid (75 mg, 47%). TOFMS *m/z* (ESI^{+}): 339.0714 (M+Na^{+}, $C_{17}H_{11}F_3N_2NaO$ requires 339.0716); ^{1}H NMR (400 MHz, CD_3OD): 8.32 (s, 1H, Ar-H), 8.12 (s, 1H, H-1), 8.06 (d, 2H, H-3 and H-7, J 7.5), 7.58 (m, 4H (Under impurities), H-4, H-5, H-6 and 1x Ar-H), 7.23 (t, 1H, Ar-H, J 7.9), 6.88 (d, 1H, Ar-H, J 7.9); ^{13}C NMR (400 MHz, CD_3OD): 157.2 (C=O), 156.4 (C-1), 130.3 (ArC), 129.4 (ArC), 128.9 (ArC), 123.5 (ArC), 116.4 (CN), 100.0 (C-1=**C**)

2-cyano-N-cyclohexyl-3-cyclopropylacrylamide (11):

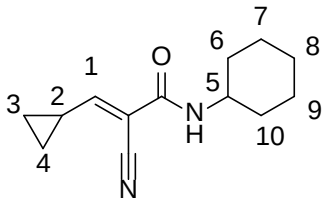

Compound 1 (0.0696 g, 0.5 mmol) and HATU (0.2281 g, 0.6 mmol) were dissolved in DCM:DMF (2 mL, 10:1 v/v) at 0^{o}C and stirred for 10 minutes under inert atmosphere. Then, cyclohexylamine (0.0631 mL, 0.55 mmol) and DIPEA (0.2298 mL, 1.32 mmol) were added and the reaction continued at 0^{o}C for 30 minutes. The mixture was stirred at room temperature for a further 24 hrs, before being diluted with water and washed with EtOAc.

The organic layer was dried using anhydrous sodium sulphate and the solvent was evaporated under vacuum to give a yellow oil, which was purified by flash chromatography (1:5 Petrol: EtOAc) to give pure product as a yellow solid (46 mg, 42%). TOFMS *m/z* (ESI^+): 219.1489 ($M+H^+$, $C_{13}H_{19}N_2O$ requires 219.1492), 241.1314 ($M+Na^+$, $C_{13}H_{18}N_2NaO$ requires 241.1317); ^1H NMR (400 MHz, CD_3OD): 6.87 (d, 1H, H-1, J 11.1), 3.48 (m, 1H, H-5), 2.05 (m, 1H, H-2), 1.91 (m, 5H, H-6, H-10 and 1x H-8), 1.79 (m, 5H, H-7, H-8, H-9), 1.34 (m, 2H, H-4), 0.97 (m, 2H, H-3); ^{13}C NMR (400 MHz, CD_3OD): 164.0 (C-1), 161.0 (C=O), 114.8 (CN), 107.8 (C-1=**C**), 49.4 (C-5), 32.0 (C-6 and C-10), 31.7 (C-8), 29.4 (C-7 and C-9), 15.1 (C-2), 9.5 (C-3 and C-4)

2-cyano-3-cyclopropyl-N-(4-fluorophenyl) acrylamide (12):

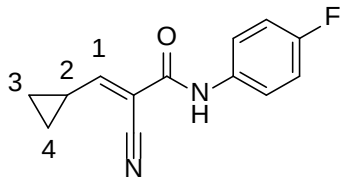

Compound 1 (0.0686 g, 0.5 mmol) and HATU (0.2281 g, 0.6 mmol) were dissolved in DCM:DMF (2 mL, 10:1 v/v) at 0°C and stirred for 10 minutes under inert atmosphere. Then, 4-fluoroaniline (0.0521 mL, 0.55 mmol) and DIPEA (0.2298 mL, 1.32 mmol) were added and the reaction continued at 0°C for 30 minutes. The mixture was stirred at room temperature for a further 24 hrs, before being diluted with water and washed with EtOAc. The organic layer was dried using anhydrous sodium sulphate and the solvent was evaporated under vacuum to give an orange oil, which was purified by flash chromatography (1:4 Petrol: EtOAc) to give pure product as a yellow solid (18 mg, 16%). TOFMS *m/z* (ESI^+): 253.0752 ($M+Na^+$, $C_{13}H_{11}FN_2O$ requires 253.0748); ^1H NMR (400 MHz, CD_3OD): 7.58 (m, 2H, Ar-H), 7.07 (m, 3H, 2x Ar-H and H-1), 2.11 (m, 1H, H-2), 1.34 (m, 2H, H-4), 1.03 (m, 2H, H-3); ^{13}C NMR (400 MHz, CD_3OD): 165.2 (C=O), 145.1 (C-1), 123.1 (ArC), 123.0 (ArC), 115.0 (C-1=**C**), 114.8 (CN), 15.3 (C-2), 9.8 (C-3 and C-4); ^{19}F NMR (400 MHz, CD_3OD): -117.82 (ArF), -117.93 (ArF), -119.34 (ArF), -119.58 (ArF), -119.87 (ArF)

3-cyclopropyl-2-(4-methylpiperidine-1-carbonyl) acrylonitrile (13):

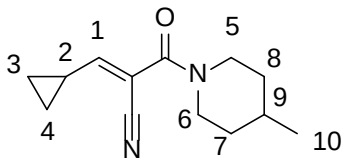

Compound 1 (0.0686 g, 0.5 mmol) and HATU (0.2281 g, 0.6 mmol) were dissolved in DCM:DMF (2 mL, 10:1 v/v) at 0^{o}C and stirred for 10 minutes under inert atmosphere. Then, 4-methyl piperidine (0.0702 g, 0.55 mmol) and DIPEA (0.2298 mL, 1.32 mmol) were added and the reaction continued at 0^{o}C for 30 minutes. The mixture was stirred at room temperature for a further 24 hrs, before being diluted with water and washed with EtOAc. The organic layer was dried using anhydrous sodium sulphate and the solvent was evaporated under vacuum to give an orange oil, which was purified by flash chromatography (1:4 Petrol: EtOAc) to give pure product as a yellow oil (20 mg, 18%). TOFMS *m/z* (ESI^{+}): 219.1484 (M+H^{+}, $C_{13}H_{19}N_2O$ requires 219.1492), 241.1321 (M+Na^{+}, $C_{13}H_{18}N_2NaO$ requires 241.1311); ^{1}H NMR (400 MHz, CD_3OD): 6.51 (d, 1H, H-1, J 11.0), 4.49 (m, 1H, 1x H-5/6), 3.91 (m, 1H, 1x H-5/6), 3.20 (m, 1H, 1x H-5/6), 2.77 (m, 1H, 1x H-5/6), 2.03 (m, 1H under ethyl acetate, H-2), 1.78 (m, 1H, 1x H-7/8), 1.74 (m, 1H, 1x H-7/8), 1.70 (m, 1H, 1x H-7/8), 1.15 (m, 3H, 1x H-7/8 and 2x H-3), 1.00 (m, 3H, H-10), 0.93 (m, 2H, H-3), 0.86 (m, 1H, H-9); ^{13}C NMR (400 MHz, CD_3OD): 171.6 (C=O), 163.7 (C-1), 114.8 (CN), 106.9 (C-1=**C**), 42.2 (C-5 and C-6), 34.4 (1x C7/8), 33.4 (1x C-7/8), 30.7 (C-9), 19.5 (C-10), 14.9 (C-2), 13.1 (C-4), 9.0 (C-3)

2-(4-(5-bromo-1H-indol-3-yl)-1,2,3,6-tetrahydropyridine-1-carbonyl)-3-cyclopropylacrylonitrile (14):

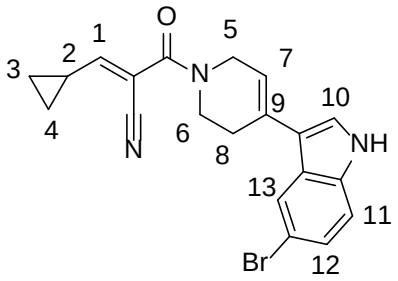

Compound 1 (0.0686 g, 0.5 mmol) and HATU (0.2281 g, 0.6 mmol) were dissolved in DCM:DMF (2 mL, 10:1 v/v) at 0^{o}C and stirred for 10 minutes under inert atmosphere. Then, 5-bromo-3-(1,2,3,6-tetrahydropyridin-4-yl)-indole (0.1525 g, 0.55 mmol) and DIPEA (0.2298 mL, 1.32 mmol) were added and the reaction continued at 0^{o}C for 30 minutes. The mixture was stirred at room temperature for a further 24 hrs, before being diluted with water and washed with EtOAc. The organic layer was dried using anhydrous sodium sulphate and the solvent was evaporated under vacuum to give an orange crude oil, which was purified by flash chromatography (1:4 Petrol: EtOAc) to give pure product as a pale-yellow solid (60 mg, 30%). TOFMS *m/z* (ESI^{+}): 396.0699 (M+H^{+}, $C_{20}H_{19}BrN_3O$ requires 396.0706), 418.0528 (M+Na^{+}, $C_{20}H_{18}BrN_3NaO$ requires 418.0525); ^{1}H NMR (400 MHz, $(CD_3)_2SO$): 7.98 (s, 1H, H-10), 7.51 (s, 1H, H-13), 7.37 (d, 1H, H-12, J 8.6), 7.24 (dd, 1H, H-11, J 8.6, 1.8), 6.67 (d, 1H, H-1, J 11.0), 6.15 (m, 1H, H-7), 4.24 (m, 2H, H-6), 4.03 (m, 2H, H-5), 3.74 (t, 2H, H-8, J 5.8), 1.94 (m, 1H, H-2), 1.19 (m, 2H, H-4), 0.94 (m, 2H, H-3); ^{13}C NMR (400 MHz, $(CD_3)_2SO$): 164.2 (C=O), 162.2 (C-1), 135.9 (C-10), 130.0 (ArC), 126.6 (C-9), 125.0 (ArC), 124.4 (ArC), 122.5 (ArC), 117.0 (C-7), 116.1 (CN), 115.5 (ArC), 114.1 (C-10=**C**), 112.7 (C-1=**C**), 48.0 (C-5 and C-6), 44.0 (C-8), 15.8 (C-2), 10.3 (1x C-3/4), 10.0 (1x C-3/4)

2-cyano-3-cyclopropyl-N-(4-chlorophenyl) acrylamide (15):

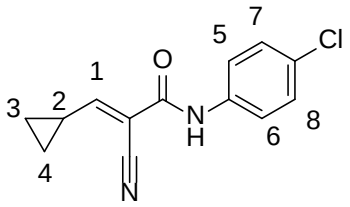

Compound 1 (0.0686 g, 0.5 mmol) and HATU (0.2281 g, 0.6 mmol) were dissolved in DCM:DMF (2 mL, 10:1 v/v) at 0^{o}C and stirred for 10 minutes under inert atmosphere. Then, 4-methyl piperidine (0.0651 mL, 0.55 mmol) and DIPEA (0.2298 mL, 1.32 mmol) were added and the reaction continued at 0^{o}C for 30 minutes. The mixture was stirred at room temperature for a further 24 hrs, before being diluted with water and washed with EtOAc. The organic layer was dried using anhydrous sodium sulphate and the solvent was evaporated under vacuum to give a yellow crude oil, which was purified by flash chromatography (1:4 Petrol: EtOAc) to give pure product as a yellow oil (68 mg, 55%). TOFMS *m/z* (ESI^{+}): 247.0634 (M+H^{+}, $C_{13}H_{12}ClN_2O$ requires 247.0633), 269.0453 (M+Na^{+}, $C_{13}H_{11}ClN_2NaO$ requires 269.0452); ^{1}H NMR (400 MHz, $(CD_3)_2SO$): 10.16 (s, 1H, NH), 7.64 (m, 2H, H-5 and H-6), 7.41 (m, 2H, H-7 and H-8), 7.09 (d, 1H, H-1, J 11.0), 1.95 (m, 1H, H-2), 1.30 (m, 2H, H-4), 1.02 (m, 2H, H-3); ^{13}C NMR (400 MHz, $(CD_3)_2SO$): 165.4 (C=O), 162.4 (C-1) 129.1 (ArC), 122.5 (ArC), 102.5 (CN), 99.4 (C-1=**C**), 16.3, (C-2), 11.2 (C-3 and C-4)

2-cyano-3-cyclohexyl-N-(3-(trifluoromethyl)benzyl)acrylamide (16):

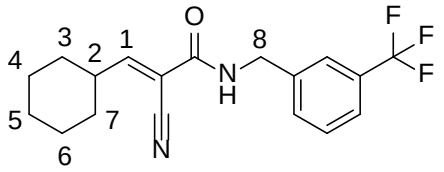

Compound 2 (0.0896 g, 0.5 mmol) and HATU (0.2281 g, 0.6 mmol) were dissolved in DCM:DMF (2 mL, 10:1 v/v) at 0^{o}C and stirred for 10 minutes under inert atmosphere. Then, 3-(trifluoromethyl)phenylmethanamine (0.0789 mL, 0.55 mmol) and DIPEA (0.2298 mL, 1.32 mmol) were added and the reaction continued at 0^{o}C for 30 minutes. The mixture was stirred at room temperature for a further 24 hrs. The solution was then dried under vacuum to

give an orange oil, which was purified by flash chromatography (1:2 Petrol: EtOAc) to give pure product as a yellow oil (105 mg, 62%). TOFMS *m/z* (ESI^+): 359.1344 ($M+Na^+$, $C_{18}H_{19}F_3N_2ONa$ requires 359.1347); ^1H NMR (400 MHz, CD_3OD): 7.61 (m, 4H, Ar-H), 7.37 (d, 1H, H-1, J 10.2), 4.54 (s, 2H, H-8), 2.68 (m, 1H, H-2), 1.78 (m, 5H, H-3_a, H-4_a, H-7_a, H-5_a, H-6_a), 1.41 (m, 2H, H-5_b, 1x H-4/6_b), 1.35 (m, 1H, 1x H-4/6_b), 1.31 (m, 2H, H-3_b and H-7_b); ^{13}C NMR (400 MHz, CD_3OD): 163.5 (C-1), 163.3 (C=O), 139.7 (ArC), 137.0 (ArC), 131.1 (ArC), 129.6 (ArC), 129.1 (CF_3), 124.0 (ArC), 123.7 (ArC), 113.9 (CN), 109.6 (C-1=**C**), 42.8 (C-8), 41.2 (C-2), 30.8 (C-3 and C-7), 25.1 (C-5), 24.8 (C-4 and C-6)

N-(4-chlorophenyl)-2-cyano-3-cyclohexylacrylamide (17):

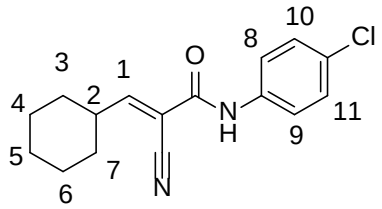

Compound 2 (0.0896 g, 0.5 mmol) and HATU (0.2281 g, 0.6 mmol) were dissolved in DCM:DMF (2 mL, 10:1 v/v) at 0°C and stirred for 10 minutes under inert atmosphere. Then, 4-chloroaniline (0.0702 g, 0.55 mmol) and DIPEA (0.2298 mL, 1.32 mmol) were added and the reaction continued at 0°C for 30 minutes. The mixture was stirred at room temperature for a further 24 hrs. The solution was then dried under vacuum to give a viscous orange oil, which was purified by flash chromatography (1:2 Petrol: EtOAc) to give pure product as an orange oil (47 mg, 33%). TOFMS *m/z* (ESI^+): 311.0920 ($M+Na^+$, $C_{16}H_{17}ClN_2NaO$ requires 311.0922); ^1H NMR (400 MHz, CD_3OD): 7.62 (m, 2H, H-8 and H-9), 7.42 (m, 1H, H-1), 7.36 (m, 2H, H-10 and H-11), 2.72 (m, 1H, H-2), 1.81 (m, 5H, H-3_a, H-4_a, H-7_a, H-5_a, H-6_a), 1.41 (m, 1H, H-5_b), 1.34 (m, 2H, H-4_b and H-6_b), 1.31 (m, 1H, H-3/7_b), 1.28 (t, 1H, H-3/7_b, J 3.2); ^{13}C NMR (400 MHz, CD_3OD): 163.2 (C=O), 160.3 (C-1), 136.5 (ArC), 129.1 (ArC), 128.5 (ArC), 128.4 (ArC), 122.3 (ArC), 116.1 (CN), 110.6 (C-1=**C**), 41.4 (1x C-3/7), 37.5 (1x C-3/7), 30.9 (C-2), 25.2 (1x C-4/5/6), 24.8 (2x C-4/5/6)

3-cyclohexyl-2-(4-methylpiperidine-1-carbonyl)acrylonitrile (18):

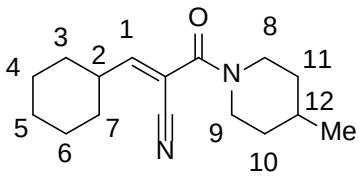

Compound 2 (0.0896 g, 0.5 mmol) and HATU (0.2281 g, 0.6 mmol) were dissolved in DCM:DMF (2 mL, 10:1 v/v) at 0°C and stirred for 10 minutes under inert atmosphere. Then, 4-methyl piperidine (0.0651 mL, 0.55 mmol) and DIPEA (0.2298 mL, 1.32 mmol) were added and the reaction continued at 0°C for 30 minutes. The mixture was stirred at room temperature for a further 24 hrs. The solution was then dried under vacuum to give an orange oil, which was purified by flash chromatography (1:2 Petrol: EtOAc) to give pure product as a yellow oil (35 mg, 27%). TOFMS *m/z* (ESI^+): 261.1961 ($M+H^+$, $C_{16}H_{25}N_2O$ requires 261.1961), 283.1793 ($M+Na^+$, $C_{16}H_{24}N_2NaO$ requires 283.1781) ^1H NMR (400 MHz, CD_3OD): 6.82 (d, 1H, H-1, J 10.0), 4.44 (m, 1H, 1x H-8/9), 3.93 (m, 1H, 1x H-8/9), 3.19 (m, 1H, 1x H-8/9), 2.81 (m, 1H, 1x H-8/9), 2.63 (m, 1H, H-2), 1.77 (m, 8H, H-10, H-11, H-12, H-4_a, H-6_a and 1x H-$3/7_a$), 1.37 (m, 5H, H-4_b, H-6_b, H-5 and 1x H-$3/7_a$), 1.17 (m, 2H, H-3_b and H-7_b), 1.00 (d, 3H, Me, J 6.1); ^{13}C NMR (400 MHz, CD_3OD): 162.5 (C=O), 161.2 (C-1), 113.8 (CN), 109.1 (C-1=**C**), 42.1 (1x C-8/9), 41.2 (1x C-8/9), 39.9 (1x C-10/11), 34.3 (1x C-10/11), 30.9 (C-3 and C-7), 30.7 (C-2), 30.6 (C-12), 25.1 (C-5), 24.8 (C-4 and C-6), 20.5 (Me)

N-(1-benzylpiperidin-4-yl)-2-cyano-3-cyclohexylacrylamide (19):

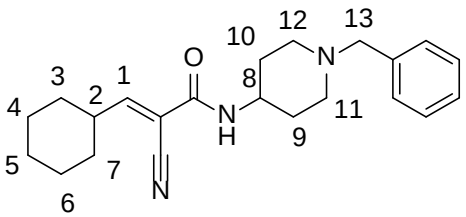

Compound 2 (0.0896 g, 0.5 mmol) and HATU (0.2281 g, 0.6 mmol) were dissolved in DCM:DMF (2 mL, 10:1 v/v) at 0°C and stirred for 10 minutes under inert atmosphere. Then, 4-amino-1-benzylpiperidine (0.1122 mL, 0.55 mmol) and DIPEA (0.2298 mL, 1.32 mmol)

were added and the reaction continued at 0°C for 30 minutes. The mixture was then stirred at room temperature for a further 24 hrs. The solution was then dried under vacuum to give a viscous yellow oil, which was purified by flash chromatography (1:2 Petrol: EtOAc) to give pure product as an orange oil (52 mg, 29%). TOFMS *m/z* (ESI^+): 352.2400 ($M+H^+$, $C_{22}H_{30}N_3O$ requires 352.2383), 374.2185 ($M+Na^+$, $C_{22}H_{29}N_3NaO$ requires 374.2203); ^1H NMR (400 MHz, CD_3OD): 7.31 (m, 6H, 5x Ar-H and H-1), 3.77 (m, 1H, H-8), 3.53 (m, 2H, 2x H-11/12), 2.93 (m, 2H, 2x H-11/12), 2.83 (s, 2H, H-13), 2.64 (m, 1H, H-2), 2.10 (m, 1H, 1x H-9/10), 1.91 (m, 1H, 1x H-9/10), 1.83 (m, 3H, 3x $H\text{-}4_a$, $H\text{-}6_a$ and 1x $H\text{-}3/7_a$), 1.75 (m, 2H, 1x $H\text{-}3/7_a$ and $H\text{-}5_a$), 1.65 (m, 2H, 2x H-9/10), 1.36 (m, 5H, $H\text{-}3_b$, $H\text{-}4_b$, $H\text{-}5_b$, $H\text{-}6_b$, $H\text{-}7_b$); ^{13}C NMR (400 MHz, CD_3OD): 160.8 (C-1), 159.7 (C=O), 135.6 (ArC), 127.9 (ArC), 126.5 (ArC), 125.6 (ArC), 112.4 (CN), 108.7 (C-1=**C**), 60.9 (C-13), 59.1 (1x C-11/12), 58.6 (1x C-11/12), 50.6 (C-8), 39.7 (1x C-3/7), 36.0 (1x C-3/7), 29.4 (1x C-2 and 1x C-9/10), 29.1 (1x C-9/10), 23.7 (C-5), 23.3 (C-4 and C-6)

2-cyano-3-cyclohexyl-N-(pyridin-3-ylmethyl)acrylamide (20):

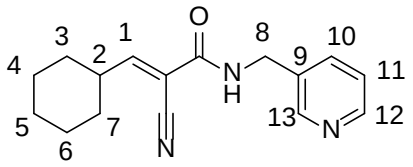

Compound 2 (0.0896 g, 0.5 mmol) and HATU (0.2281 g, 0.6 mmol) were dissolved in DCM:DMF (2 mL, 10:1 v/v) at 0°C and stirred for 10 minutes under inert atmosphere. Then, pyridin-3-yl methanamine (0.0560 mL, 0.55 mmol) and DIPEA (0.2298 mL, 1.32 mmol) were added and the reaction continued at 0°C for 30 minutes. The mixture was stirred at room temperature for a further 24 hrs, before being diluted with water and washed with EtOAc. The organic layer was dried using anhydrous sodium sulphate and the solvent was evaporated under vacuum to give a yellow crude oil, which was purified by flash chromatography (1:4 Petrol: EtOAc) to give pure product as a white solid (7.1 mg, 5%). TOFMS *m/z* (ESI^+): 270.1615 ($M+H^+$, $C_{16}H_{20}N_3O$ requires 270.1601), 292.1441 ($M+Na^+$, $C_{16}H_{19}N_3NaO$ requires 292.1426); ^1H NMR (400 MHz, CD_3OD): 8.54 (m, 1H, H-13), 8.46 (dd, 1H, H-12, J 4.9, 1.6), 7.84 (m, 1H, H-10), 7.43 (dd, 1H, H-11, J 7.9, 4.9), 7.36 (d, 1H, H-1, J 10.2), 4.51 (s, 2H, H-8), 2.67 (m, 1H, H-2), 1.83 (m, 1H, 1x $H\text{-}4/6_a$), 1.75 (m, 4H, 1x $H\text{-}4/6_a$, $H\text{-}3_a$, $H\text{-}7_a$, $H\text{-}5_a$), 1.38 (m, 5H, $H\text{-}3_b$, $H\text{-}4_b$, $H\text{-}5_b$, $H\text{-}6_b$, $H\text{-}7_b$); ^{13}C NMR (400 MHz, CD_3OD): 171.6 (C-1),

163.4 (C=O), 148.2 (C-13), 147.6 (C-12), 136.8 (1x C-9/10), 136.4 (1x C-9/10), 123.9 (C-11), 113.7 (CN), 109.4 (C-1=**C**), 41.2 (C-8), 40.8 (C-2), 30.8 (C-3 and C-7) , 25.1 (C-5), 24.7 (C-4 and C-6)

4.4 Glutathione NMR tests

Inhibitor in excess:

L-glutathione reduced (4.6 μmol, 1.41 mg) and a cyanoacrylamide (50 mmol) were made into separate solutions in deuterated DMSO-d^6. These were then mixed together and a ^{1}H NMR was taken every hour for 3-4 hrs. The size of the β-hydrogen integral was calculated by setting one of the known peaks on the inhibitor to its known value and comparing to the original pure inhibitor spectrum.

1:1 reaction:

L-glutathione reduced (0.02 mmol, 6.15 mg) and one of the fragment compounds above (0.02 mmol) were made into separate solutions in deuterated DMSO-d^6. These were then mixed together and a ^{1}H NMR was taken every hour for 3-4 hrs. The size of the β-hydrogen integral was calculated by setting one of the known peaks on its inhibitor to its known value and comparing to the original pure inhibitor spectrum.

5 References

[1] Murray, C., Rees, D., “The rise of fragment-based drug discovery”, Nature, 2009

[2] Barker, J., Hesterkamp, T., Whittaker, M., “Integrating HTS and Fragment-based Drug Discovery”, Drug Discovery World, 2008, https://www.ddw-online.com/screening/p92852-integrating-hts-and-fragment-based-drug-discovery.html [Online]

[3] Wyss DF et al, “Combining NMR and X-ray crystallography in fragment-based drug discovery: discovery of highly potent and selective BACE-1 inhibitors.”, 2012

[4] Davis, B., Roughley, S., “Platform Technologies in Drug Discovery and Validation”, 2017

[5] ThermoFisher Scientific, “Phosphorylation”, https://www.thermofisher.com/uk/en/home/life-science/protein-biology/protein-biology-learning-center/protein-biology-resource-library/pierce-protein-methods/phosphorylation.html [Online]

[6] Shchemelinin, I., Sefc, L., & Necas, E, “Protein kinases, their function and implication in cancer and other diseases”, Folia Biologica, 52(3), 81-100, 2006

[7] Roskoski, Robert, “Enzyme Structure and Function”, 10.1016/B978-0-12-801238-3.05007-8, 2014

[8] John A. Cooper, “Kinase”, Encyclopædia Britannica, https://www.britannica.com/science/kinase, 2018

[9] Roskoski, R, “Classification of small molecule protein kinase inhibitors based upon the structures of their drug-enzyme complexes”, 2016

[10] Zheng Zhao, Philip E. Bourne, “Progress with covalent small-molecule kinase inhibitors”, Drug Discovery Today, 2018

[11] Liu, Quingsong et al., “Developing Irreversible Inhibitors of the Protein Kinase Cysteinome”, Chemistry & Biology, 2013

[12] Macmillan Cancer Support, “Afatinib”, https://www.macmillan.org.uk/information-and-support/treating/targeted-biological-therapies/find-your-therapy/afatinib.html#319055, 2016

[13] Iana M Serafimova et al., “Reversible targeting of noncatalytic cysteines with chemically tuned electrophiles”, Nature, 2012

[14] Rand M. Miller et al., “Electrophilic Fragment-Based Design of Reversible Covalent Kinase Inhibitors”, J. Am. Chem. Soc, 2013

[15] Krishnan, S. et al., “Design of Reversible, Cysteine-Targeted Michael Acceptors Guided by Kinetic and Computational Analysis”, 2014

[16] Richard A. Ward et al., “Structure- and Reactivity-Based Development of Covalent Inhibitors of the Activating and Gatekeeper Mutant Forms of the Epidermal Growth Factor Receptor (EGFR)”, J. Med.Chem., 2013

[17] Zhang, L. et al. “Bioactivity Focus of α-Cyano-4-hydroxycinnamic acid (CHCA) Leads to Effective Multifunctional Aldose Reductase Inhibitors.” Sci. Rep. 6, 24942; doi: 10.1038/srep24942 (2016).

[18] Singh, A. et al., “Tuning Solid-State Fluorescence to the Near-Infrared: A Combinatorial Approach to Discovering Molecular Nanoprobes for Biomedical Imaging”, 2013

[19] BACHEM, “Coupling Reagents”, http://documents.bachem.com/coupling_reagents.pdf, 2016

[20] Brooks, W H et al. “The significance of chirality in drug design and development.” Current topics in medicinal chemistry vol. 11,7 (2011): 760-70.

[21] UC Davis, “Nuclear Magnetic Resonance (NMR) of Alkenes”, https://chem.libretexts.org/Bookshelves/Organic_Chemistry/Supplemental_Modules_(Organic_Chemistry)/Alkenes/Properties_of_Alkenes/Nuclear_Magnetic_Resonance_(NMR)_of_Alkenes, 2019

[22] Decatur, J., “NOESY and ROESY”, Columbia University, http://www.columbia.edu/cu/chemistry/groups/nmr/noesy.pdf, 2018

[23] Gemmecker, G., “The NOE Effect”, SpectroscopyNOW, https://www.spectroscopynow.com/userfiles/sepspec/file/specNOW/Tutorials/chem843-6.pdf, 1999

[24] Basu, D., et al., “Structure-based design and synthesis of covalent reversible inhibitors to overcome drug resitance in EGFR”, 2015

[25] Qian, H.-F., Huang, W. & Yao, C., “2-Cyano-3-(4-hydroxy-phenyl)-propenoic acid” (2005). Acta Cryst. E61, o370-o372.

[26] Pompella, A. et al., "The changing faces of glutathione, a cellular protagonist", Biochemical Pharmacology, (2003)

[27] Kettle, A. et al., “Oxidation contributes to low glutathione in the airways of children with cystic fibrosis”, 2014 DOI: 10.1183/09031936.00170213

[28] Jakubowski, H., “Chemistry of Cystine”, Biochemistry Online, https://employees.csbsju.edu/hjakubowski/classes/ch331/protstructure/PS_2A7_Cystine_Chem.html, 2016

[29] Z. Kh. Papanyan, “INTERACTION OF L-CYSTEINE WITH DIMETHYL SULFOXIDE IN MILD CONDITIONS”, 2013

Appendices

NMR and Mass spectrometry data

Characteristic spectroscopic data for each molecule made in this project is listed in this section. Full spectra files can be accessed in the research database, with the files corresponding to the experiment titles in my lab book. The data has been made available in this report as well for ease of access and to show the purest form of each compound because each sample has a variety of NMR's associated with it.

Appendix 1: ^{1}H NMR, ^{13}C NMR and MS of compound 1 (CD_3OD)

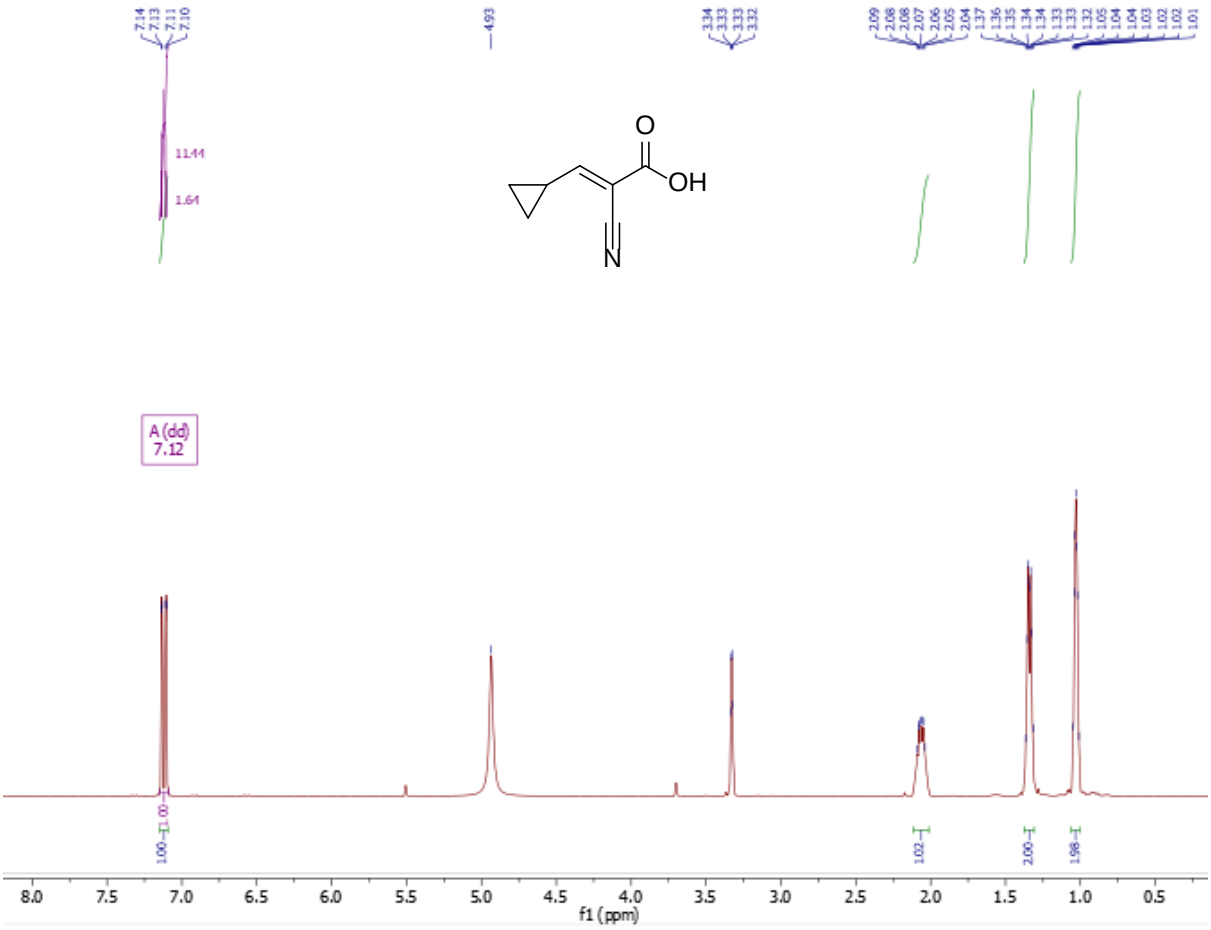

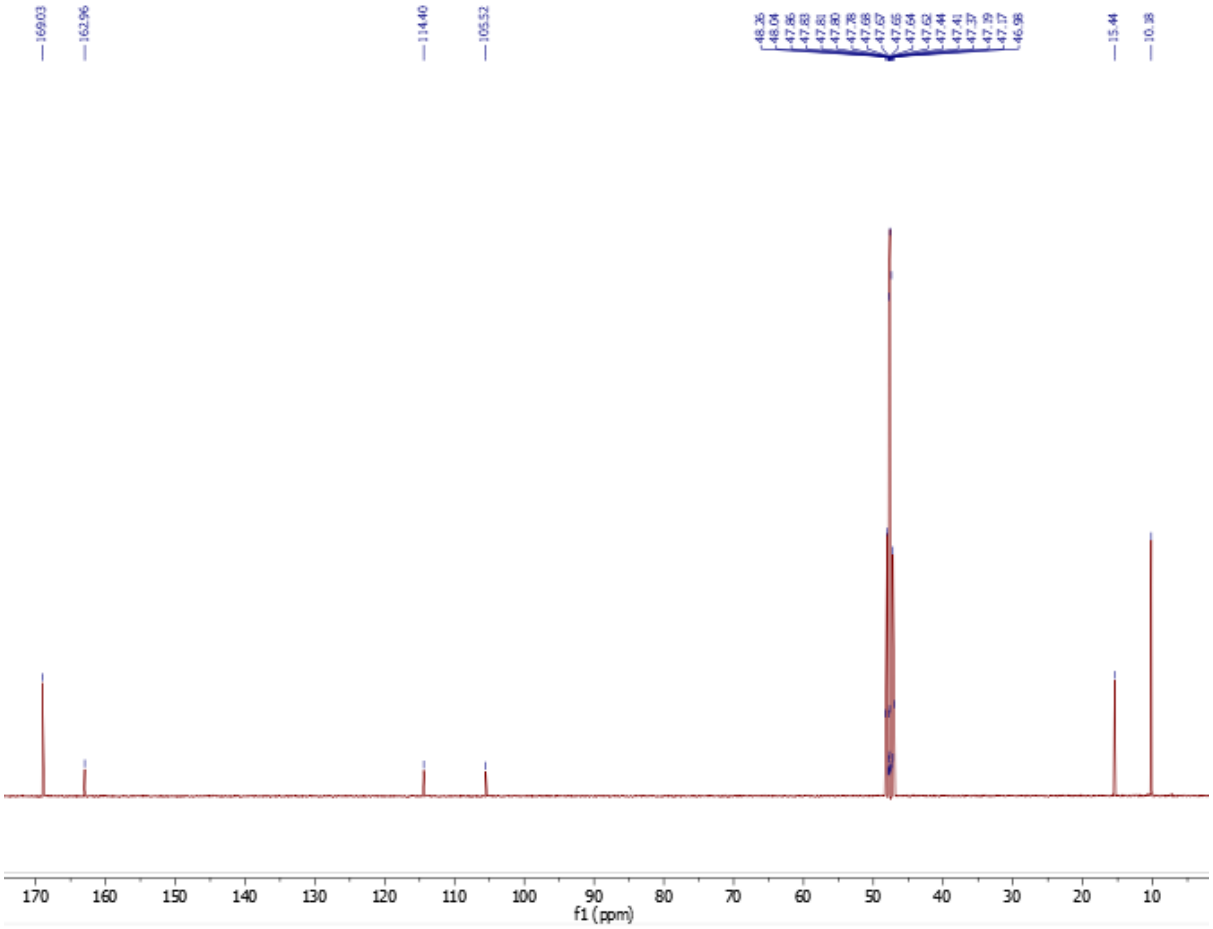

+MS, 0.6-0.8min #51-67

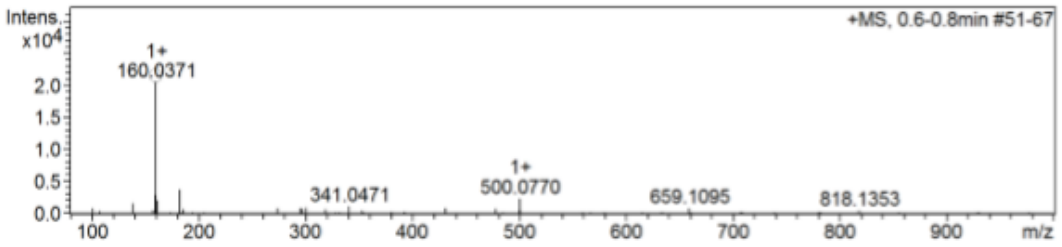

Appendix 2: ^{1}H NMR, ^{13}C NMR and MS of compound 2 (CD_3OD)

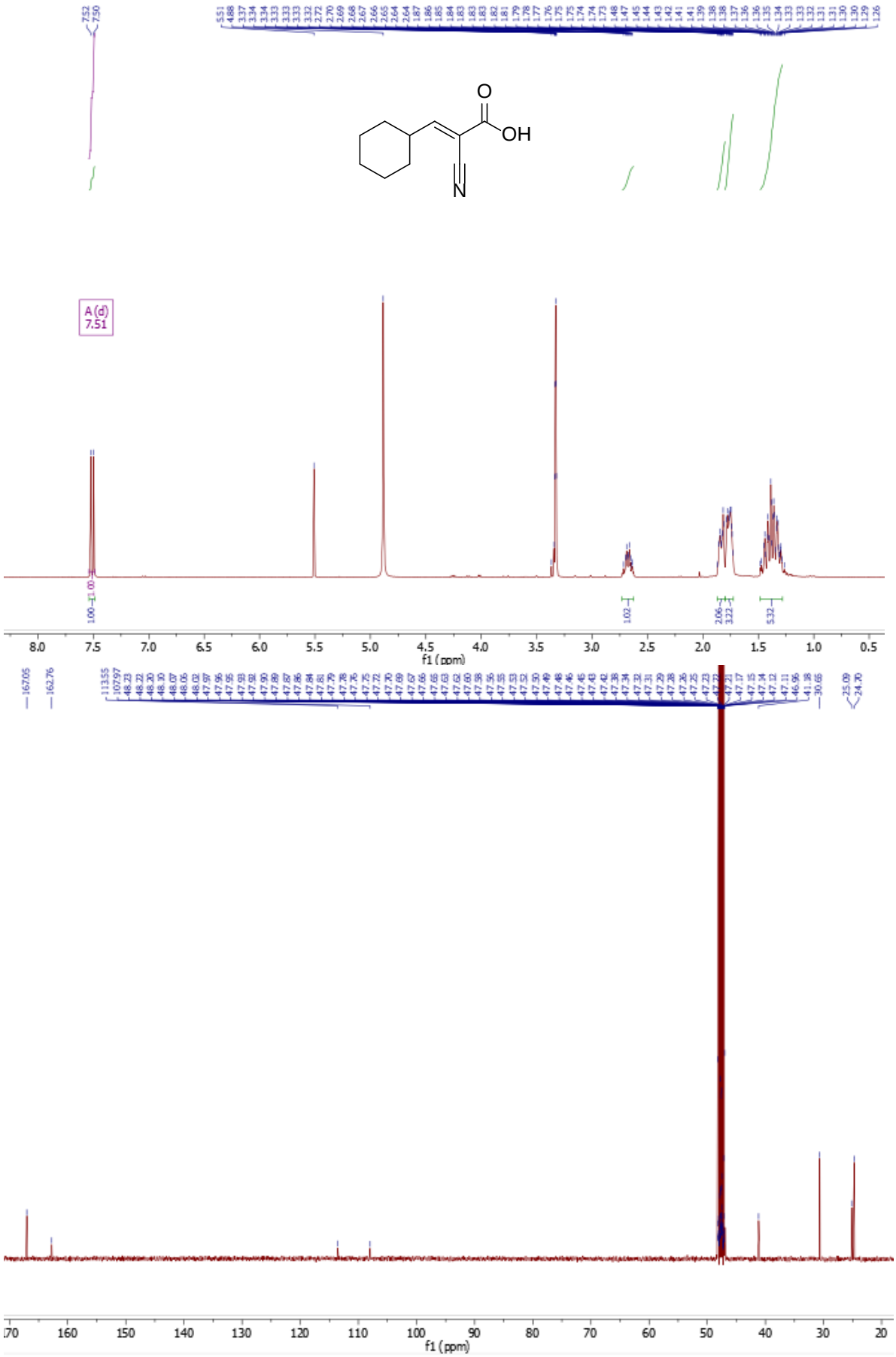

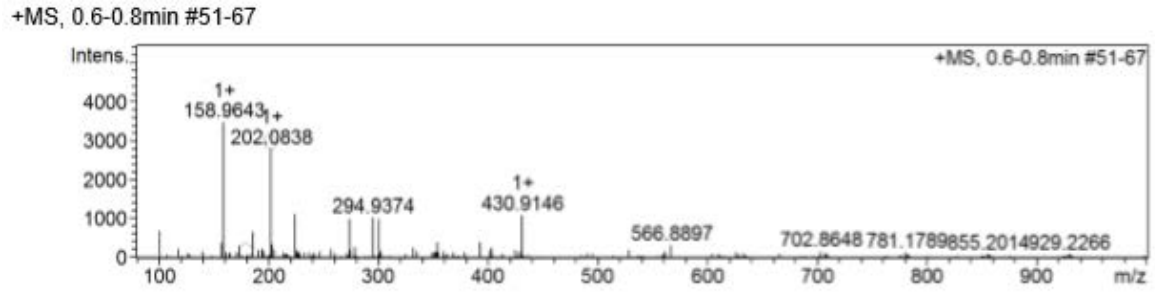

Appendix 3: ^{1}H NMR, ^{13}C NMR and MS of compound 3 (CD_3OD)

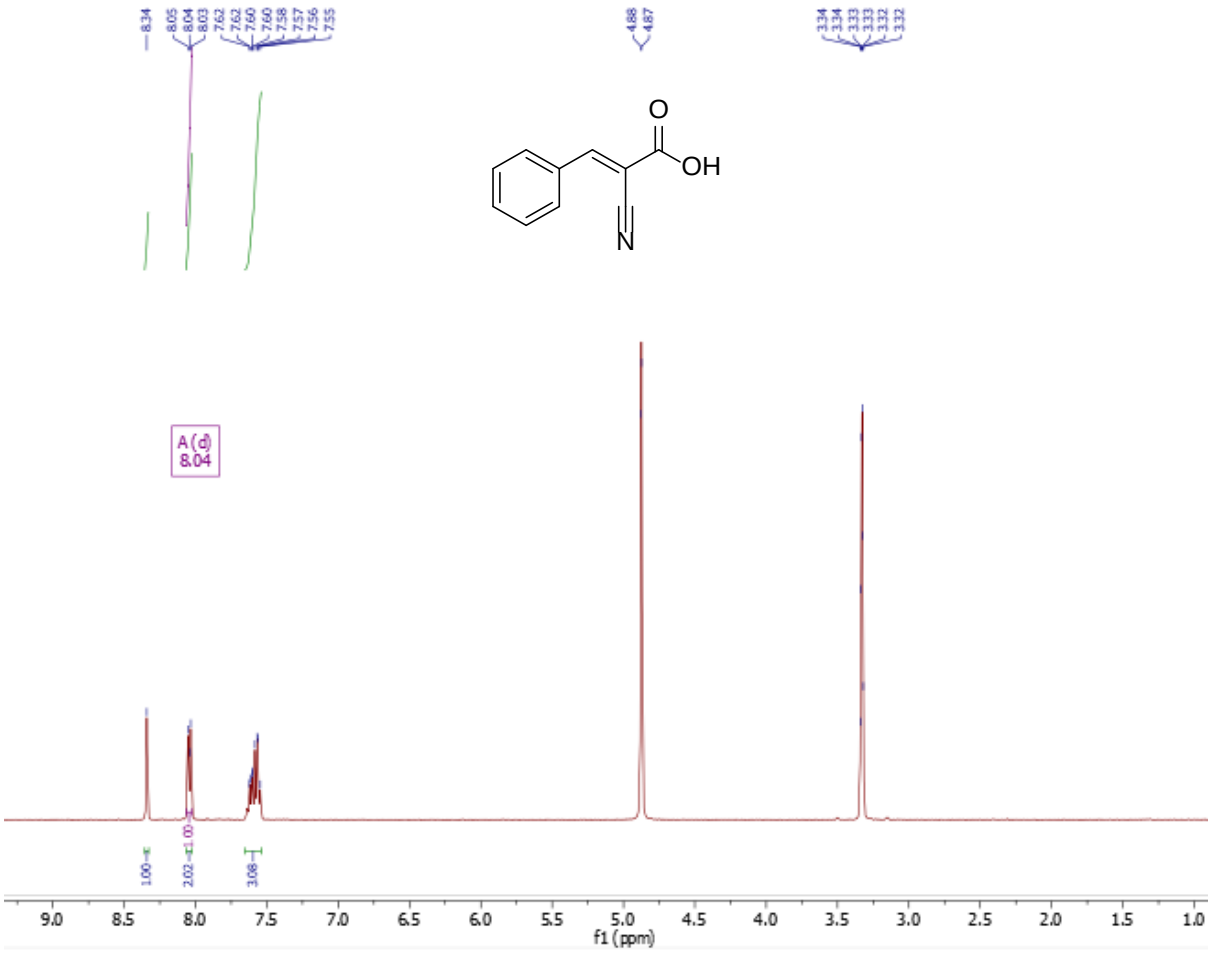

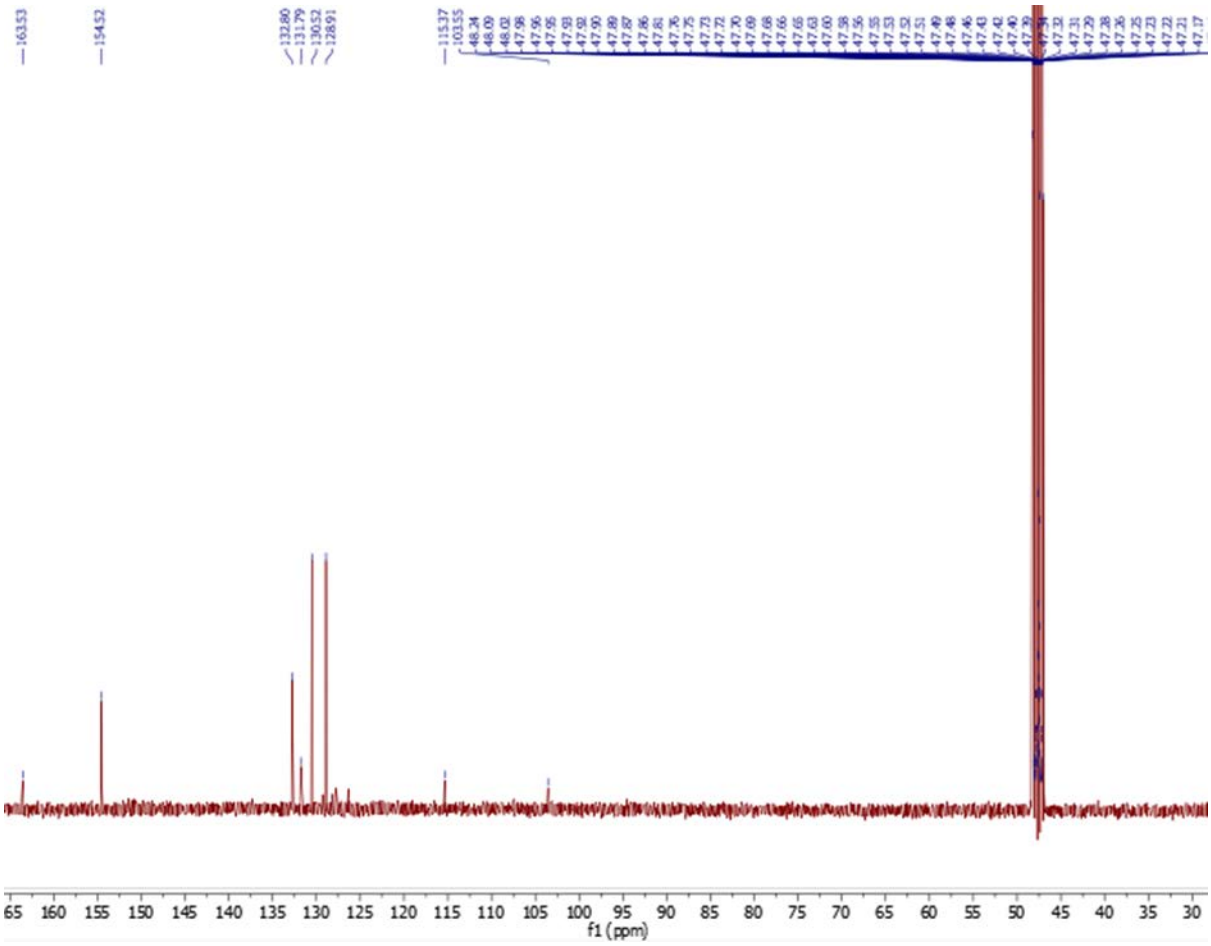

+MS, 0.6-0.8min #51-67

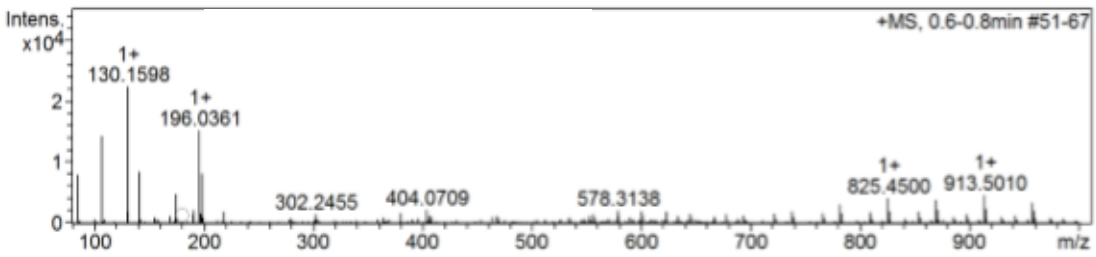

Appendix 4: ^{1}H NMR, ^{13}C NMR and MS of compound 4 (CD_3OD)

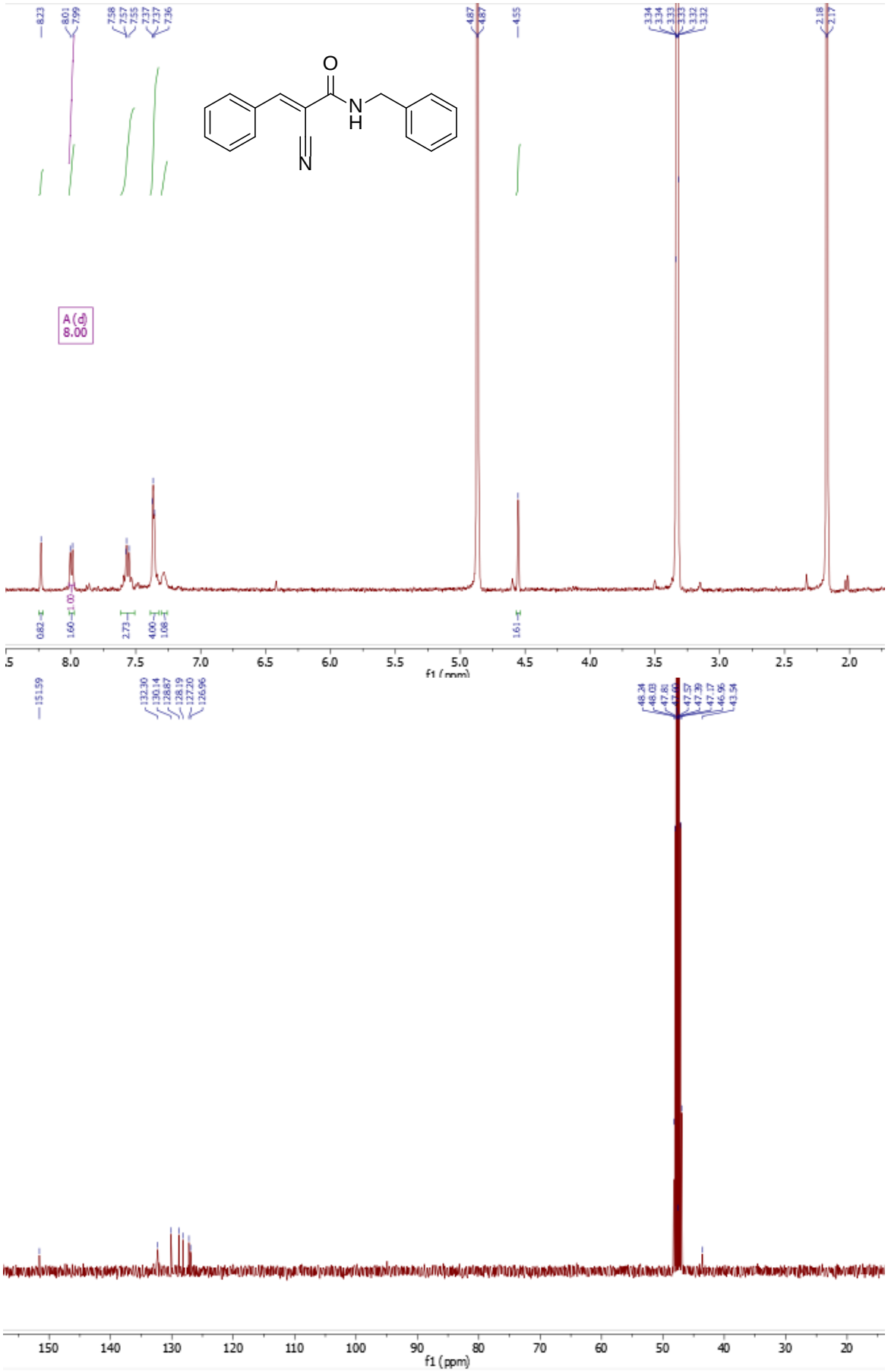

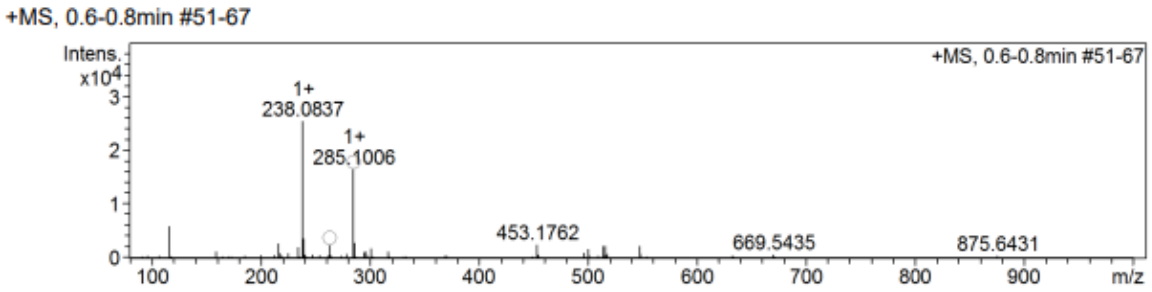

Appendix 5: ^{1}H NMR, ^{13}C NMR and MS of compound 5 (CD_3OD)

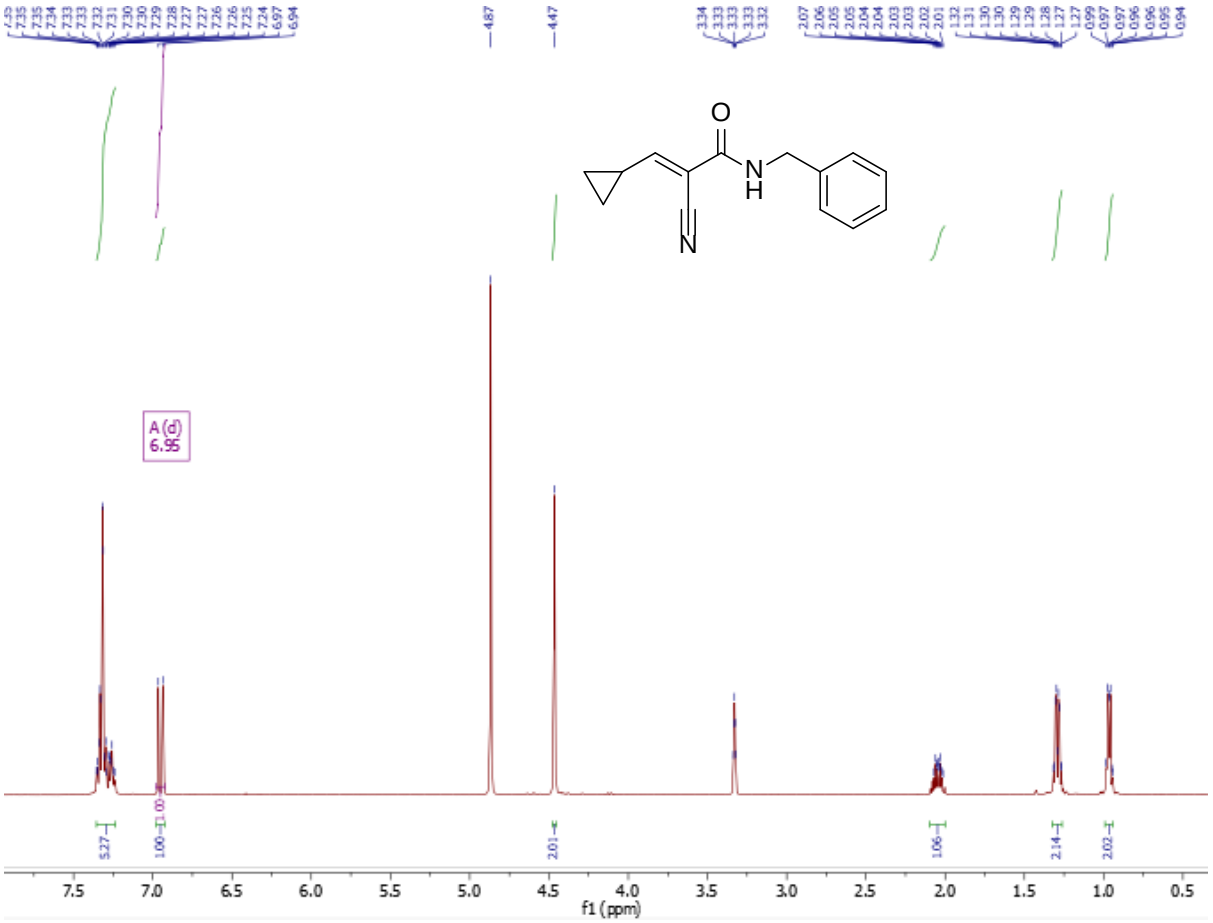

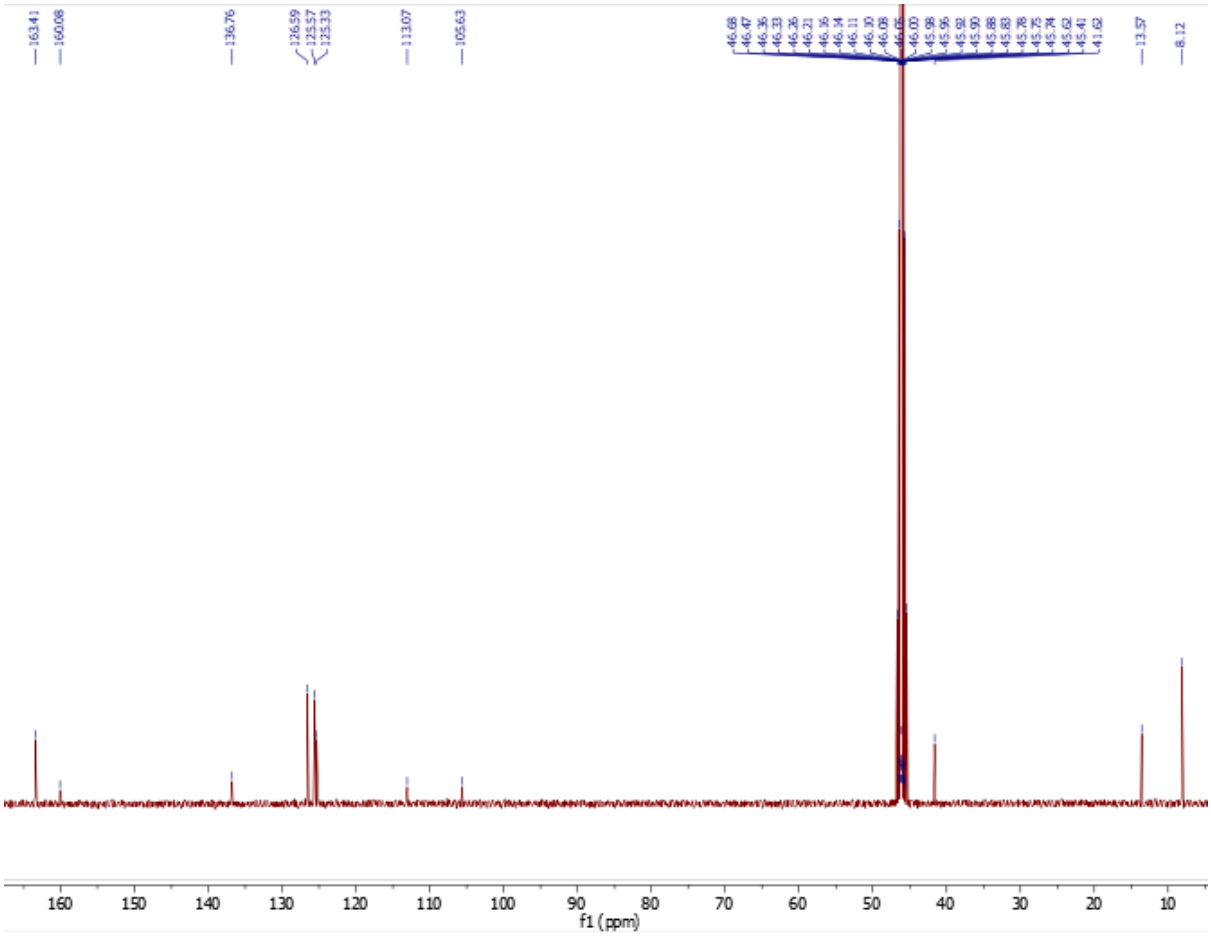

+MS, 0.6-0.8min #51-67

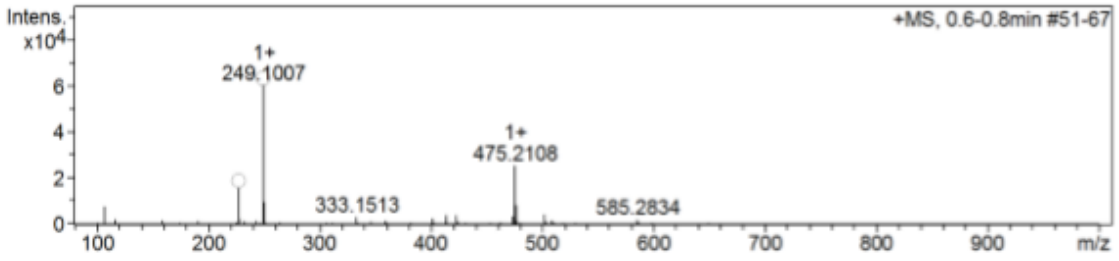

Appendix 6: ^{1}H NMR, ^{13}C NMR and MS of compound 6 (CD_3OD)

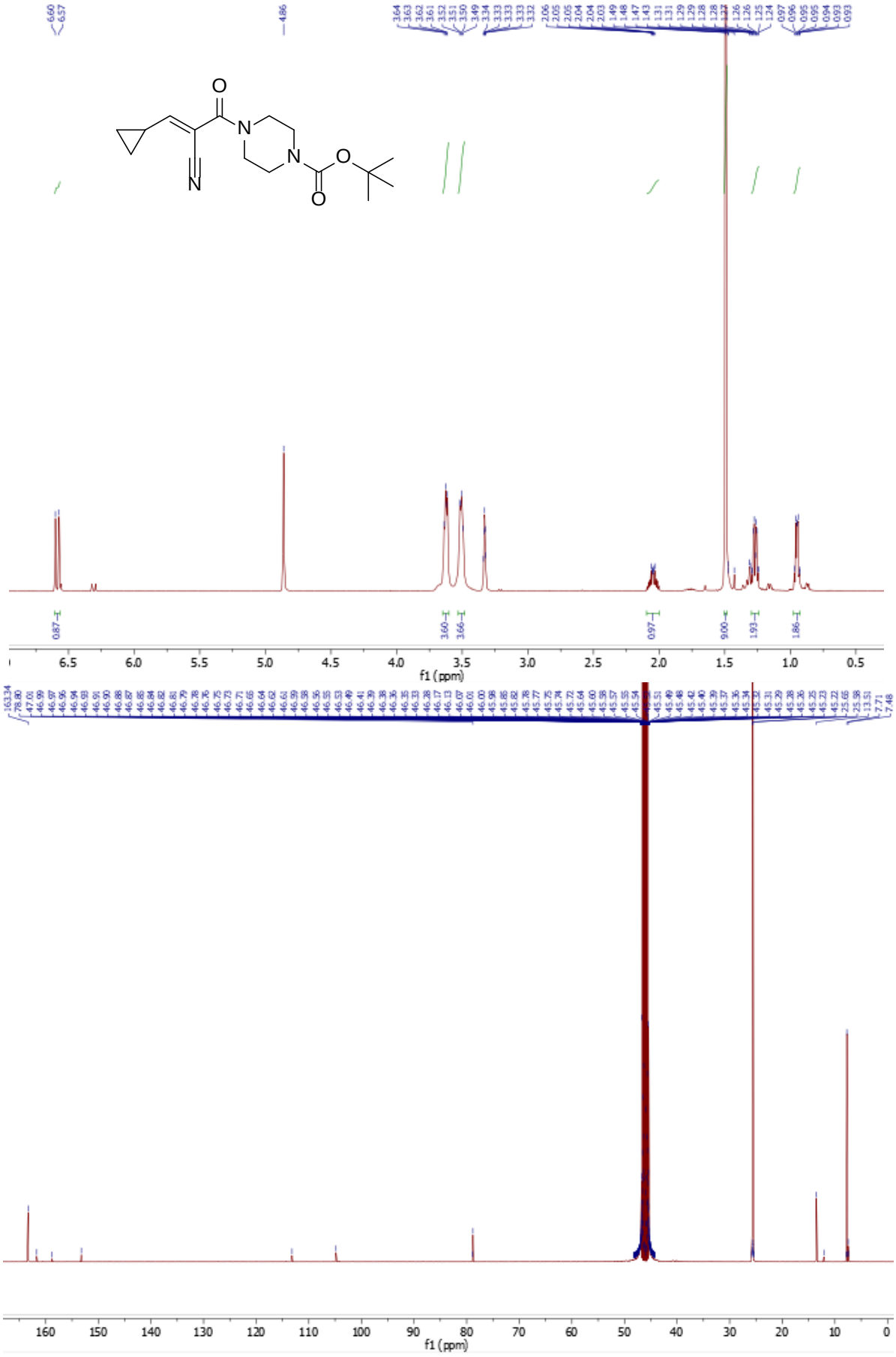

+MS, 0.6-0.8min #50-66

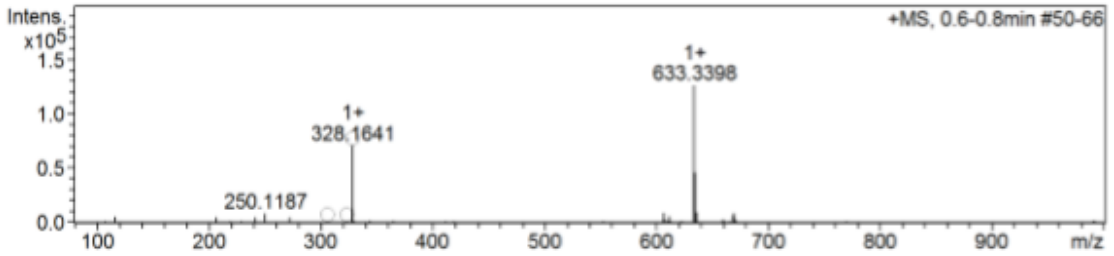

Appendix 7: ^{1}H NMR, ^{13}C NMR and MS of compound 7 (CD_3OD)

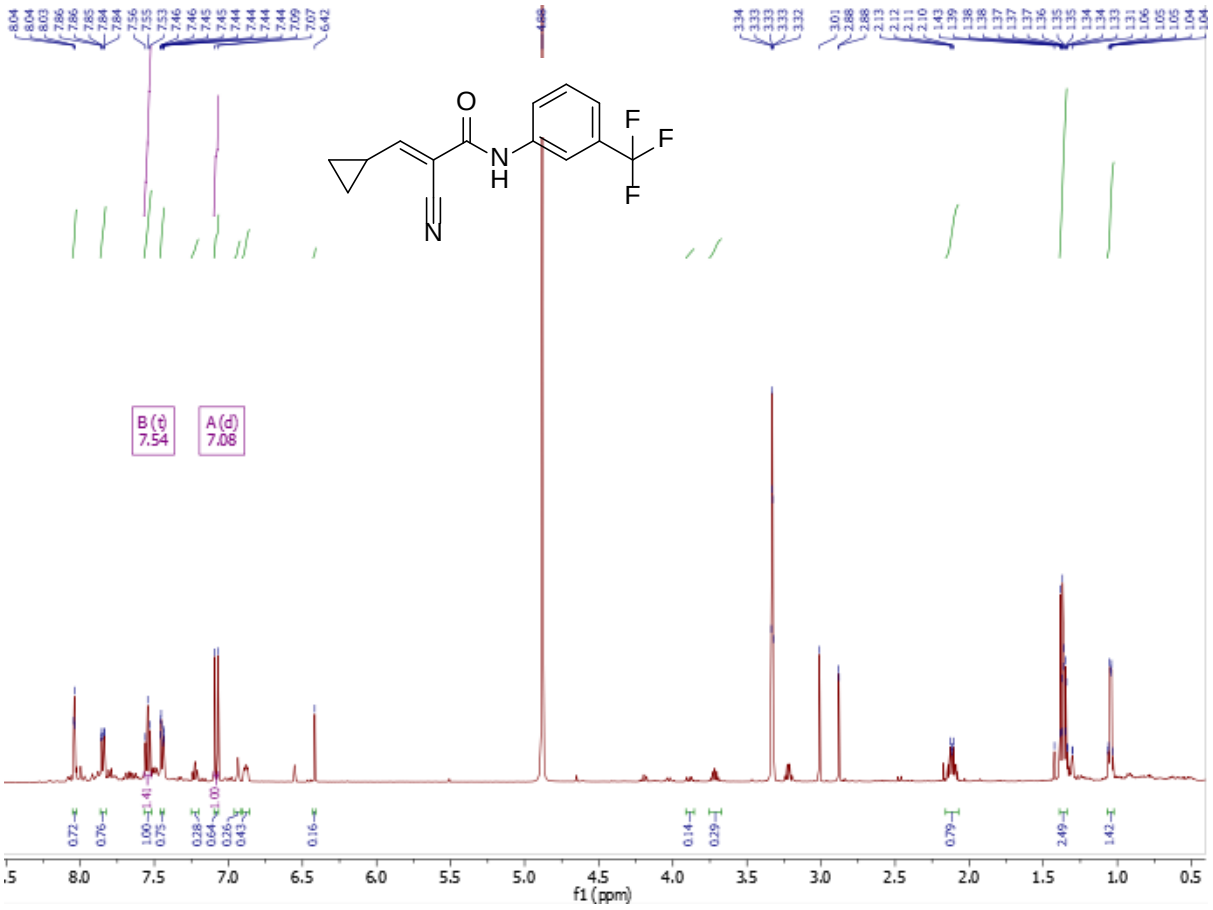

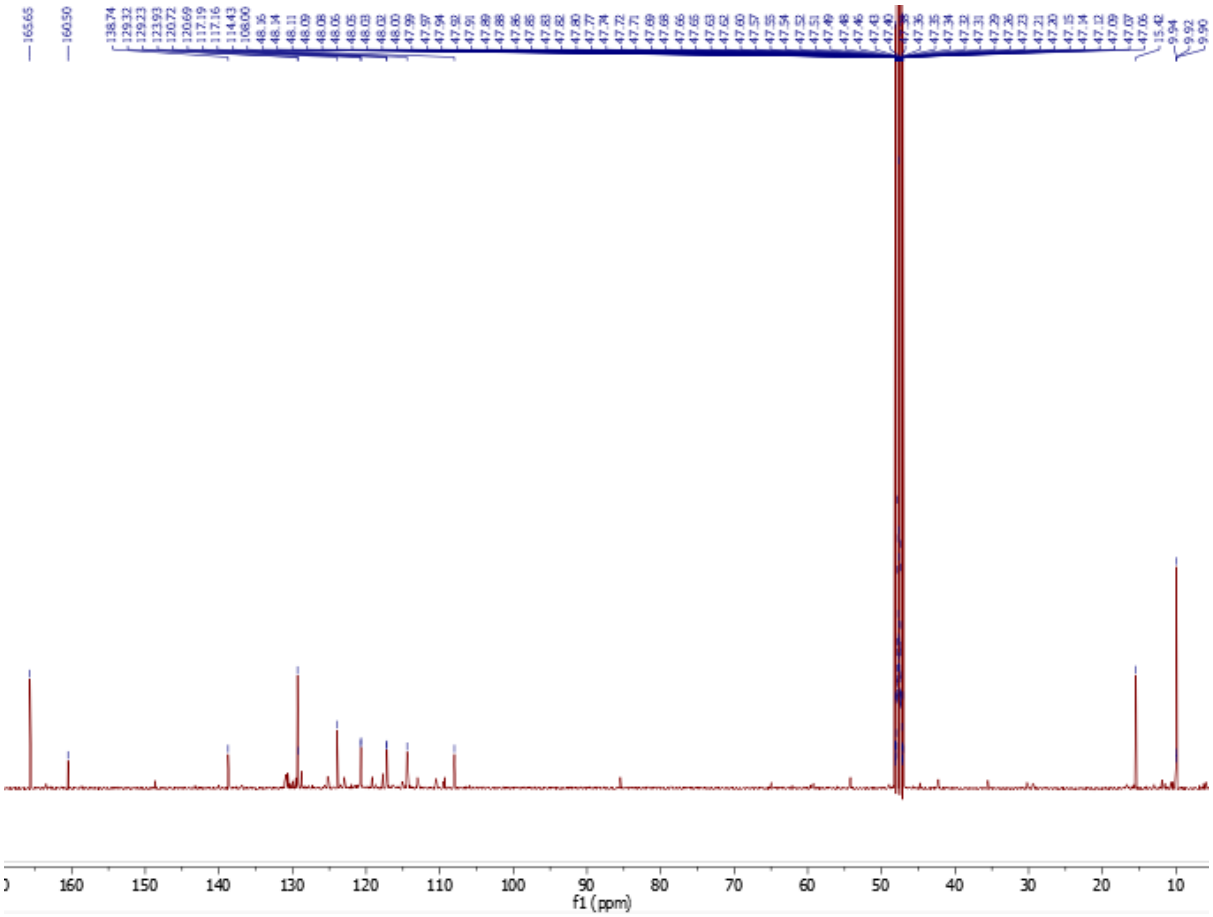

+MS, 0.6-0.8min #51-67

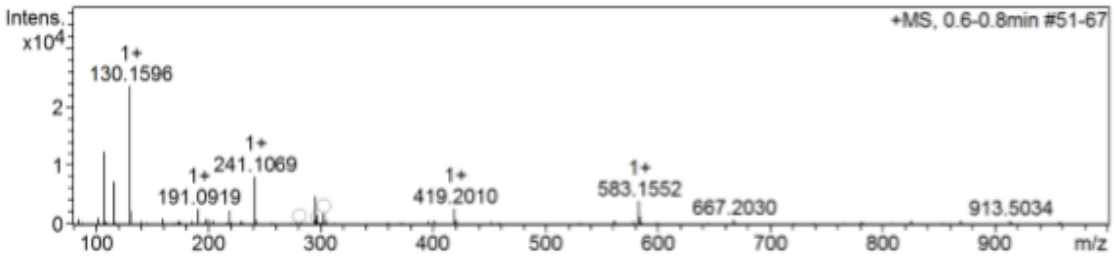

Appendix 8: ^{1}H NMR, ^{13}C NMR and MS of compound 8 (CD_3OD)

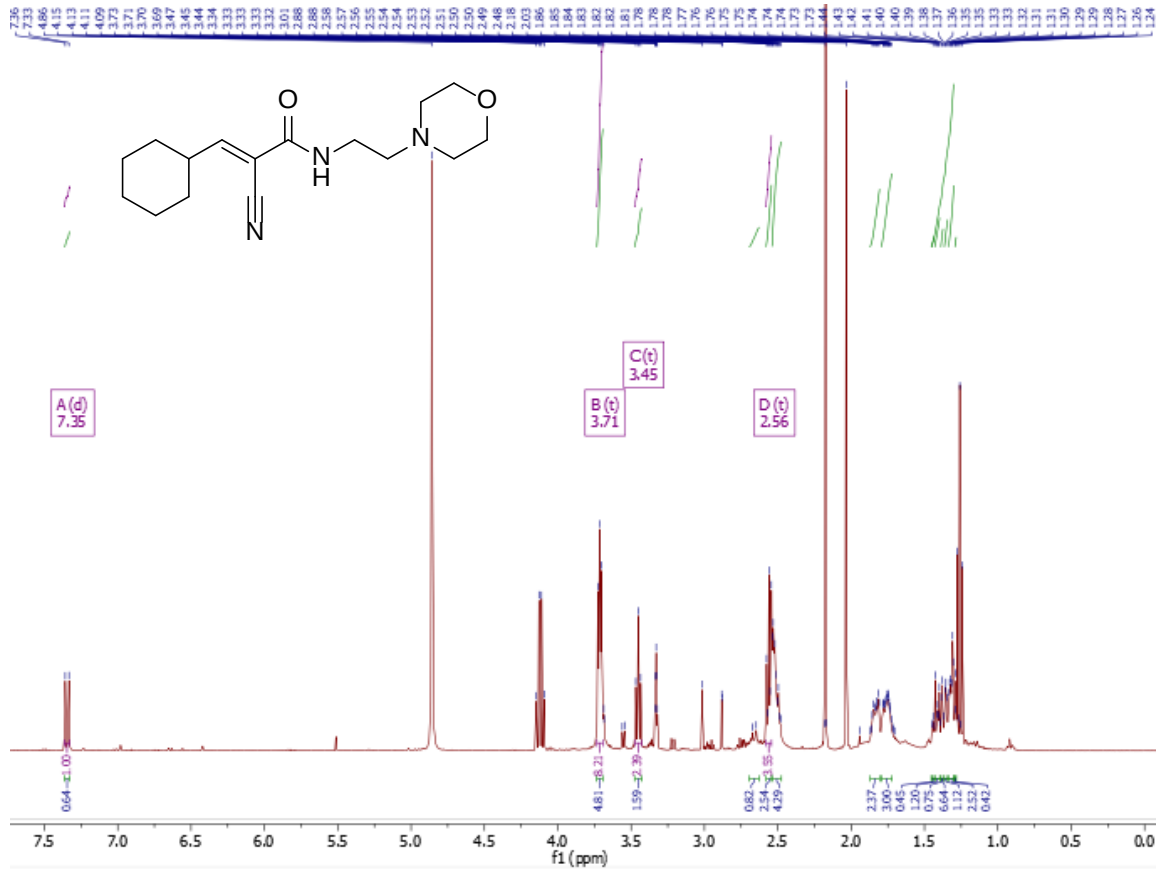

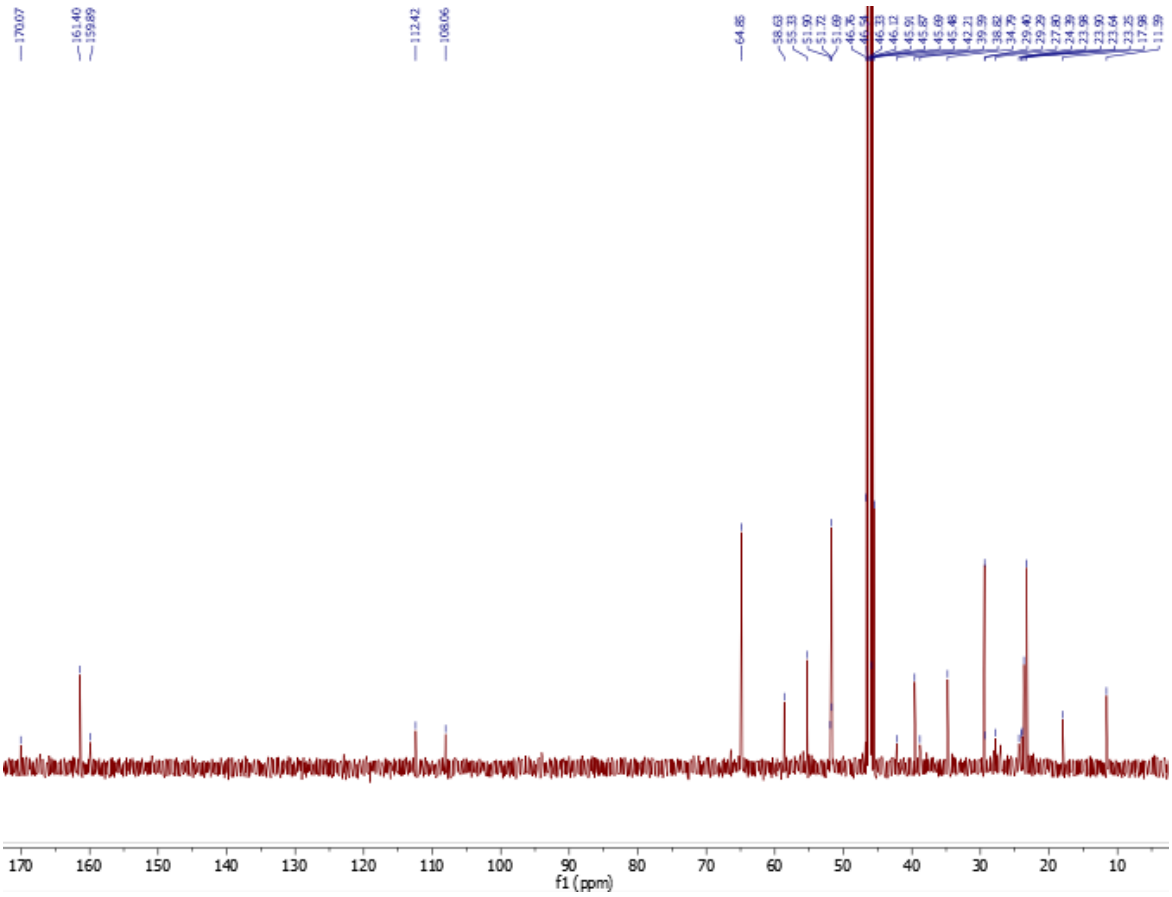

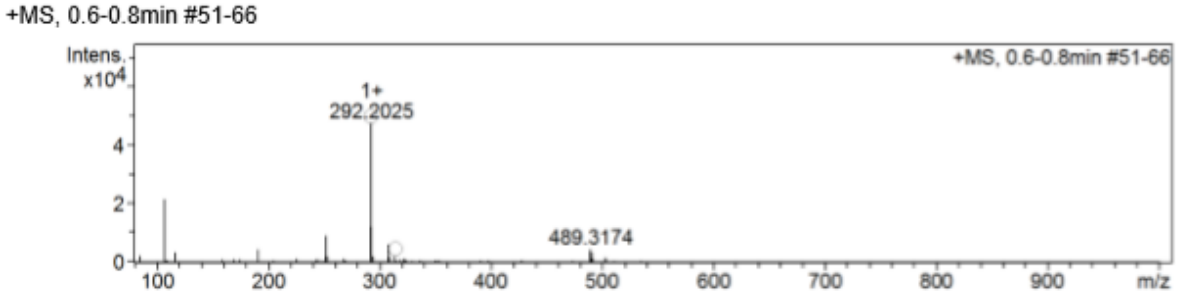

Appendix 9: ^{1}H NMR, ^{13}C NMR and MS of compound 9 (CD_3OD)

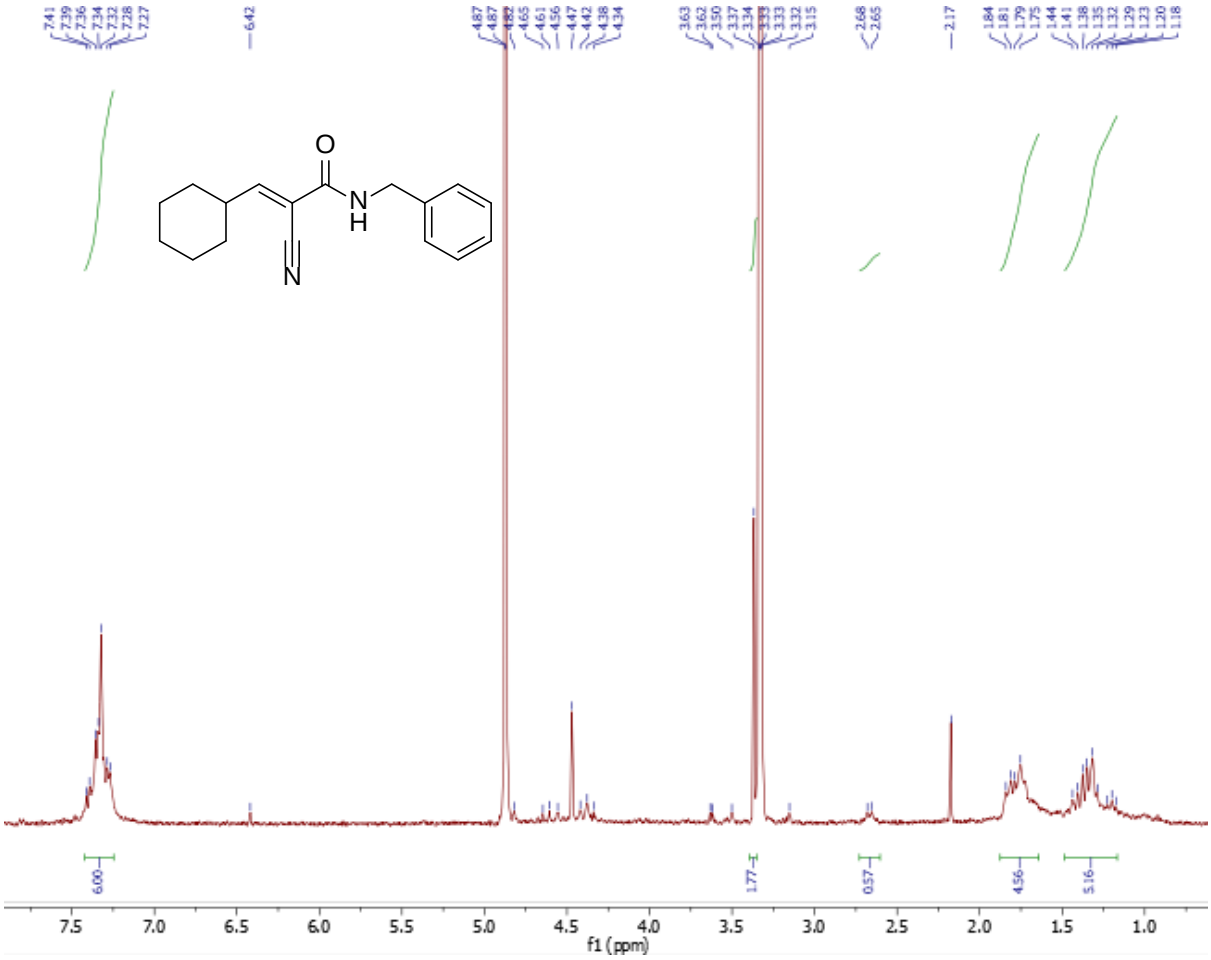

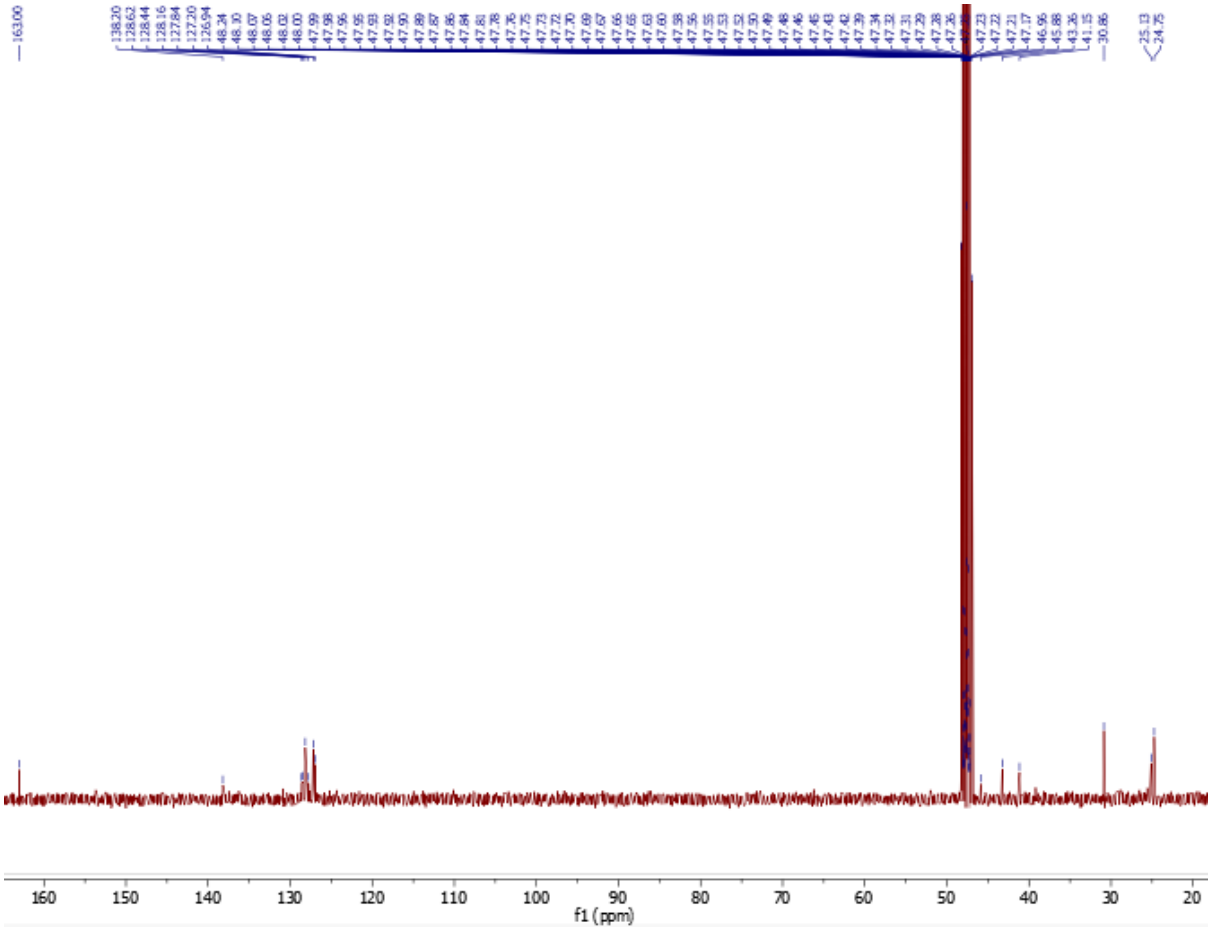

+MS, 0.6-0.8min #50-66

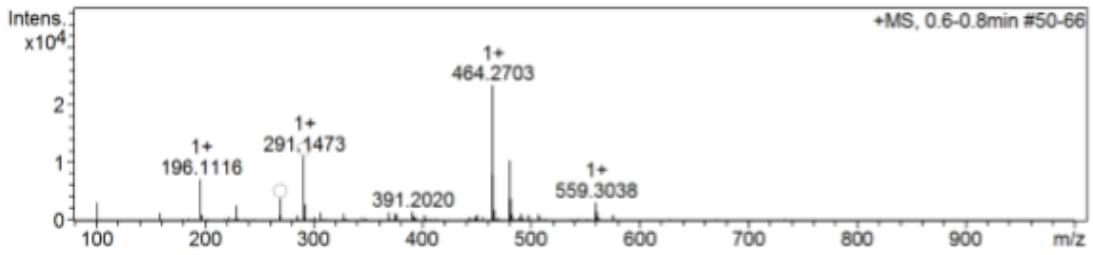

Appendix 10: ^{1}H NMR, ^{13}C NMR and MS of compound 10 (CD_3OD)

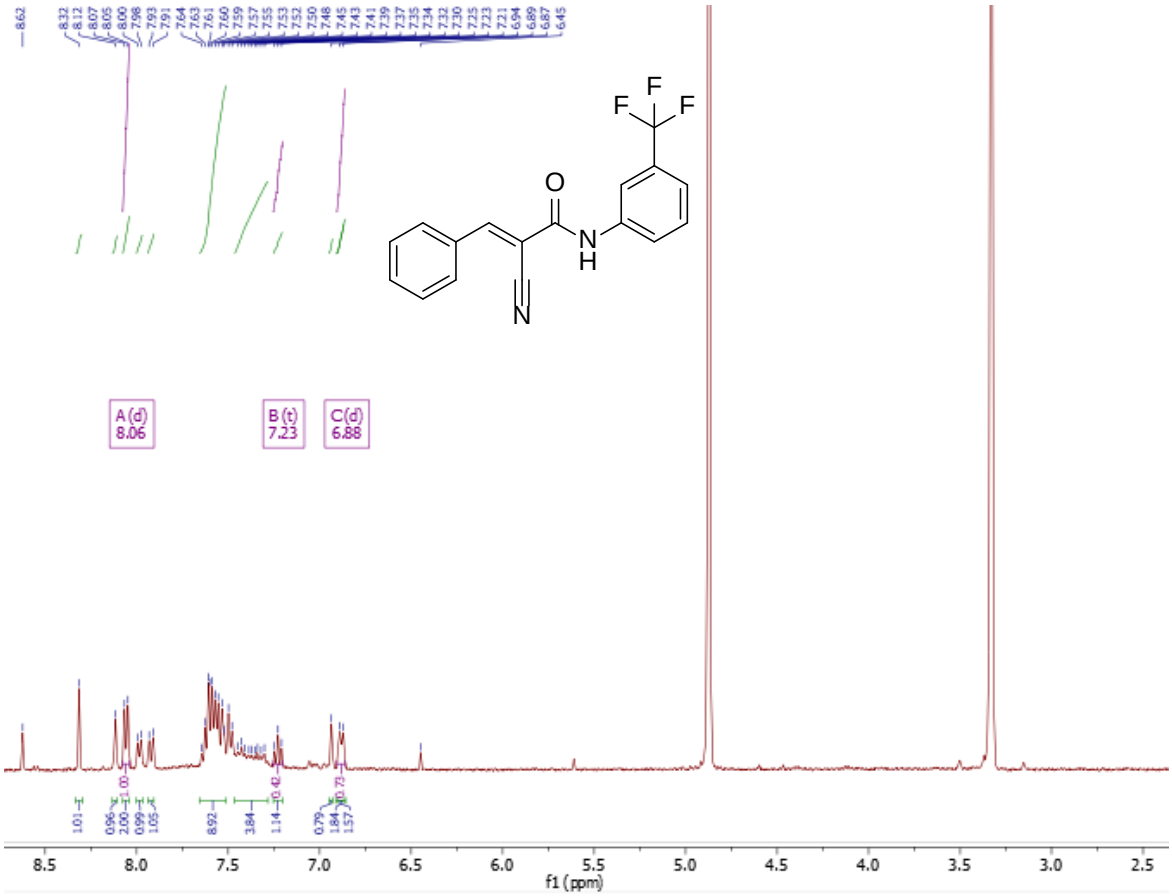

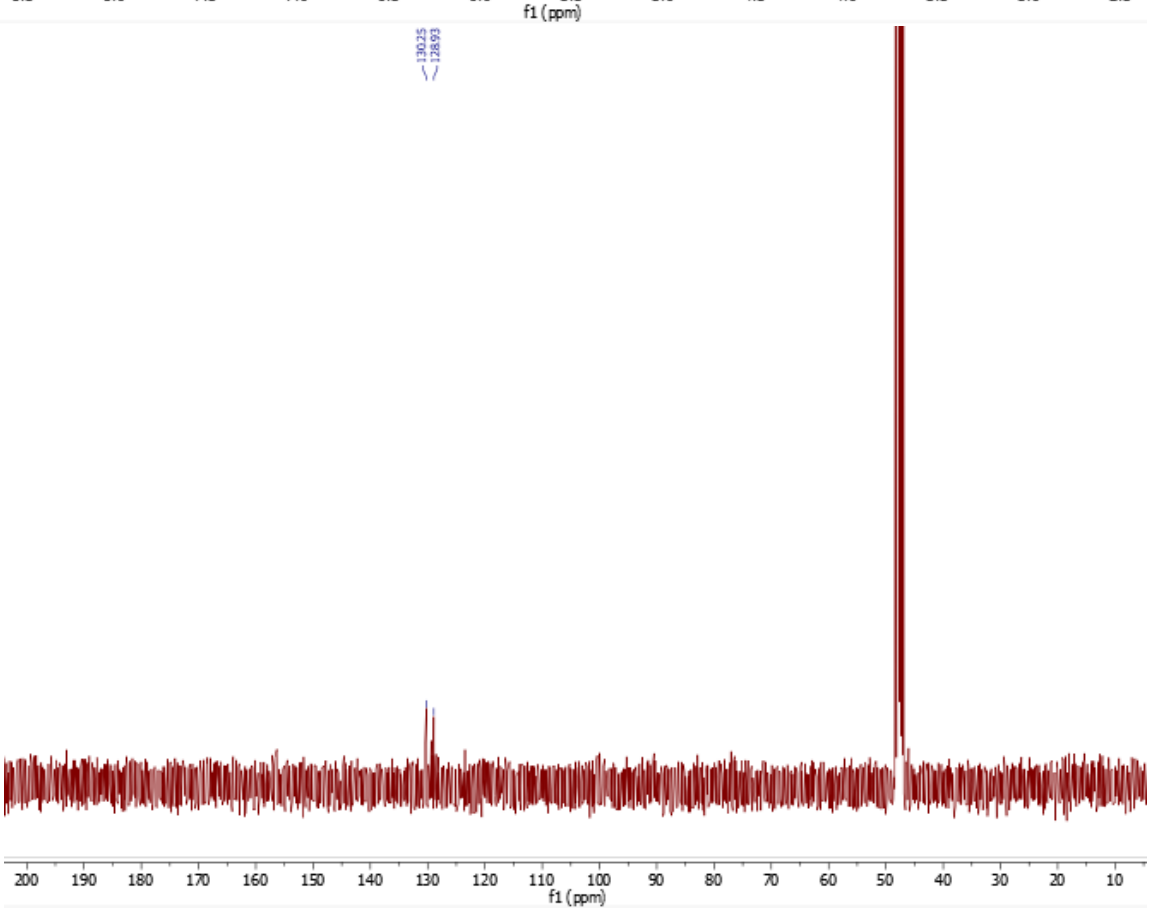

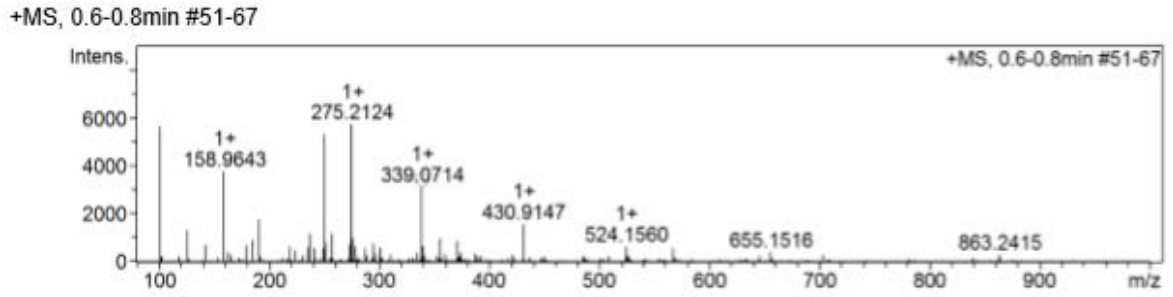

Appendix 11: ^{1}H NMR, ^{13}C NMR and MS of compound 11 (CD_3OD)

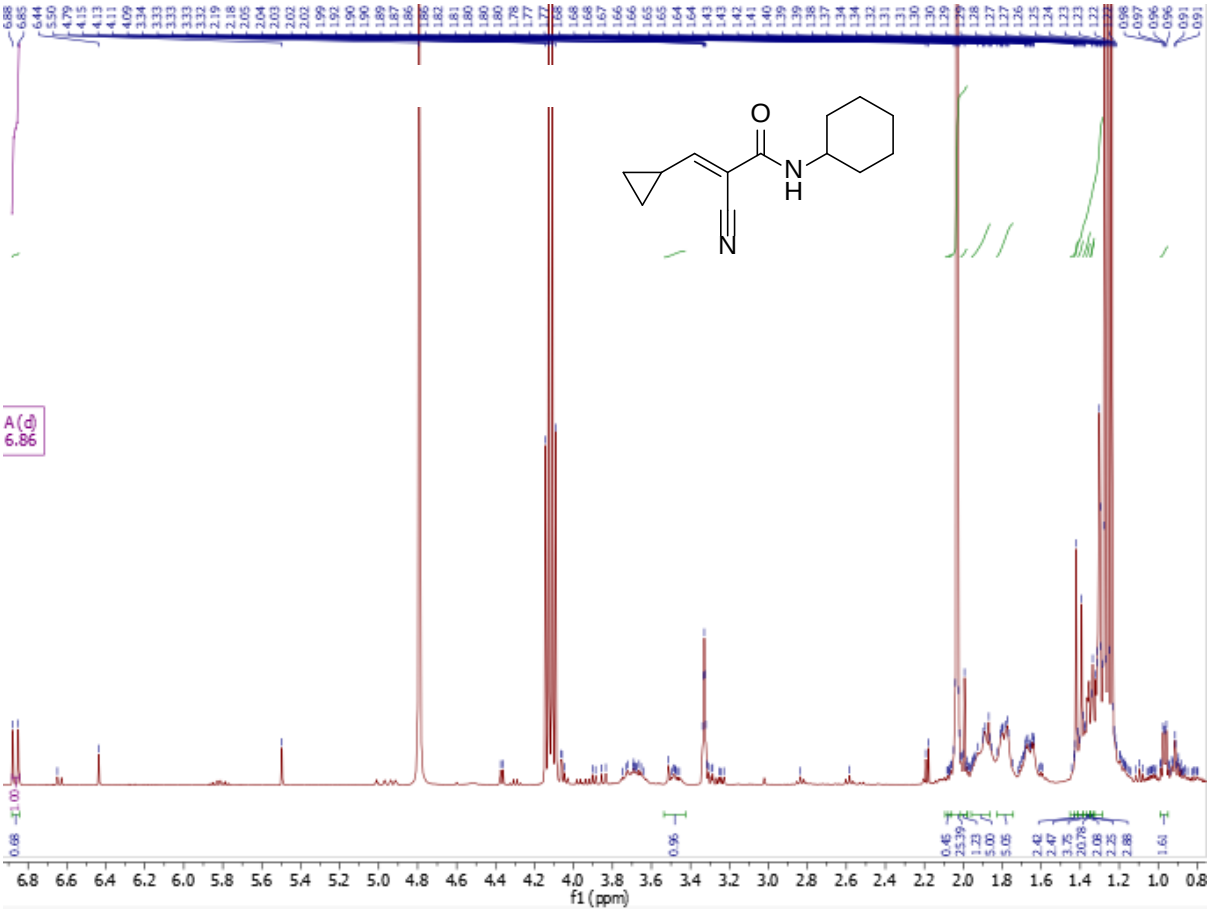

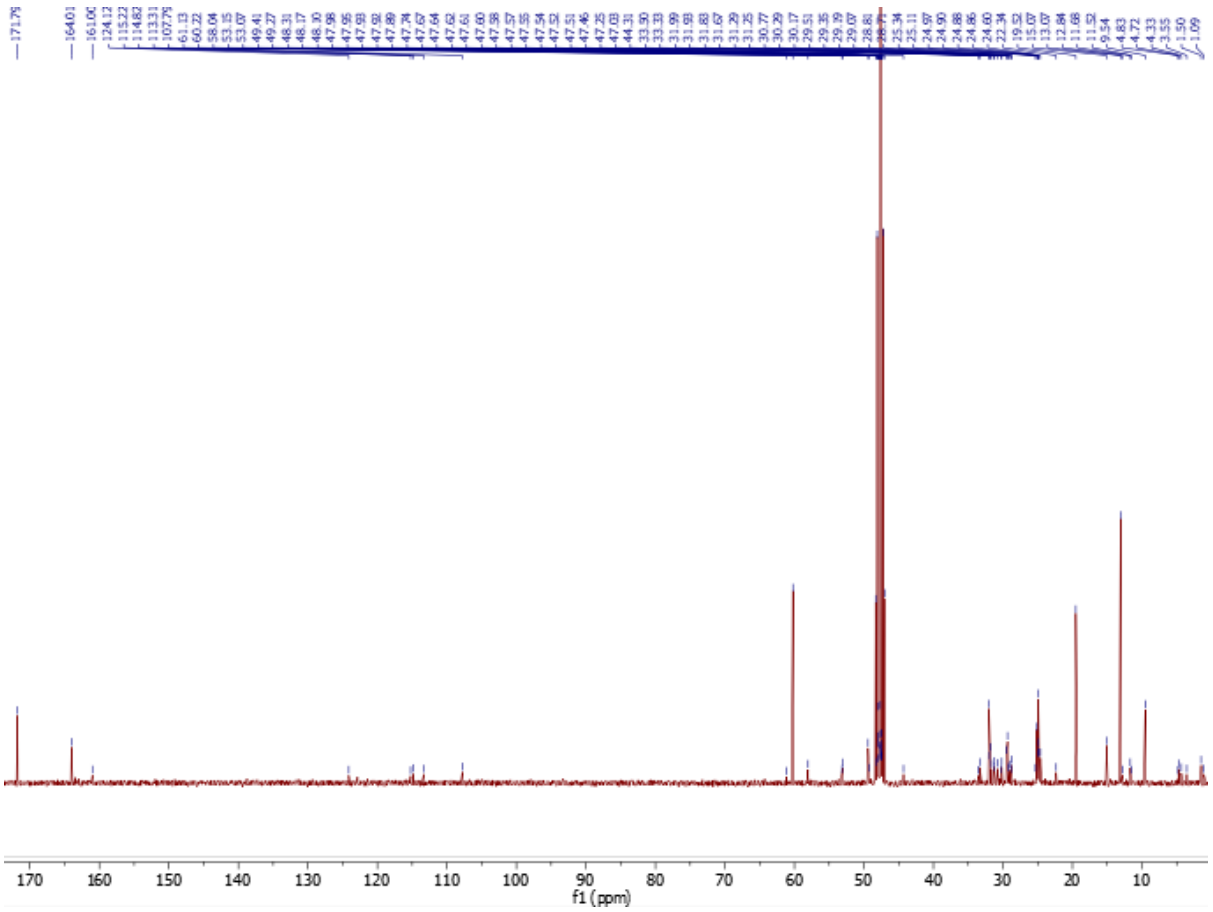

+MS, 0.6-0.8min #50-66

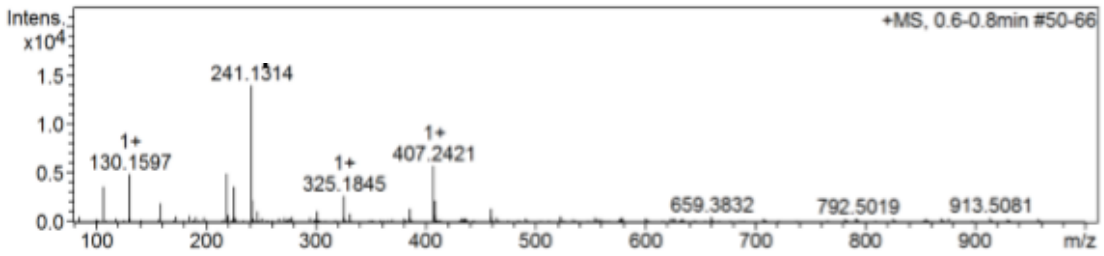

Appendix 12: ^{1}H, ^{13}C, ^{19}F NMRs and MS of compound 12 (CD_3OD)

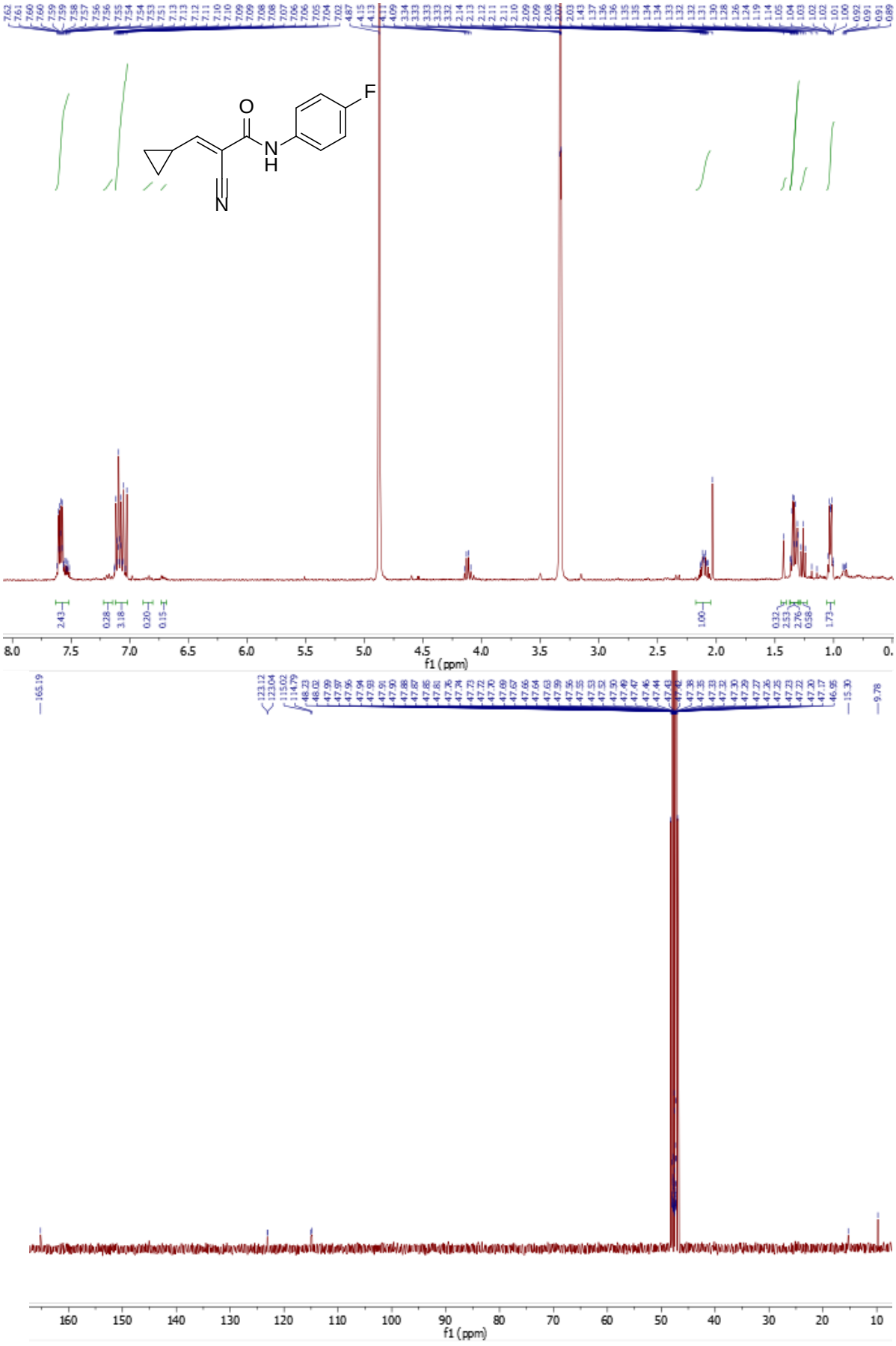

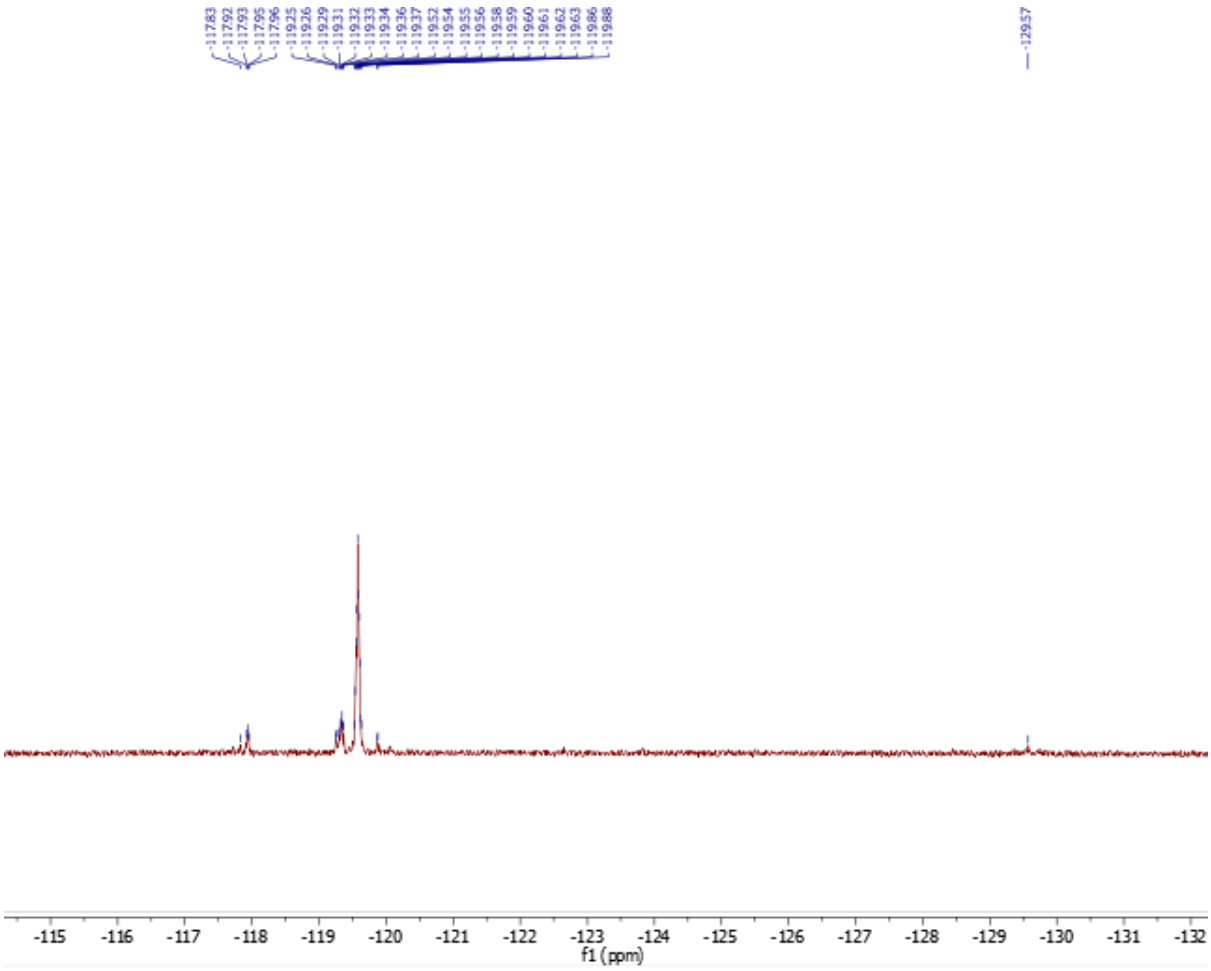

+MS, 0.6-0.8min #51-67

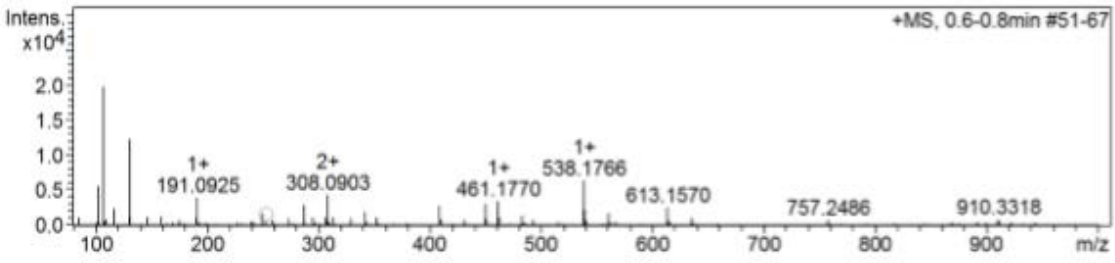

Appendix 13: ^{1}H NMR, ^{13}C NMR and MS of compound 13 (CD_3OD)

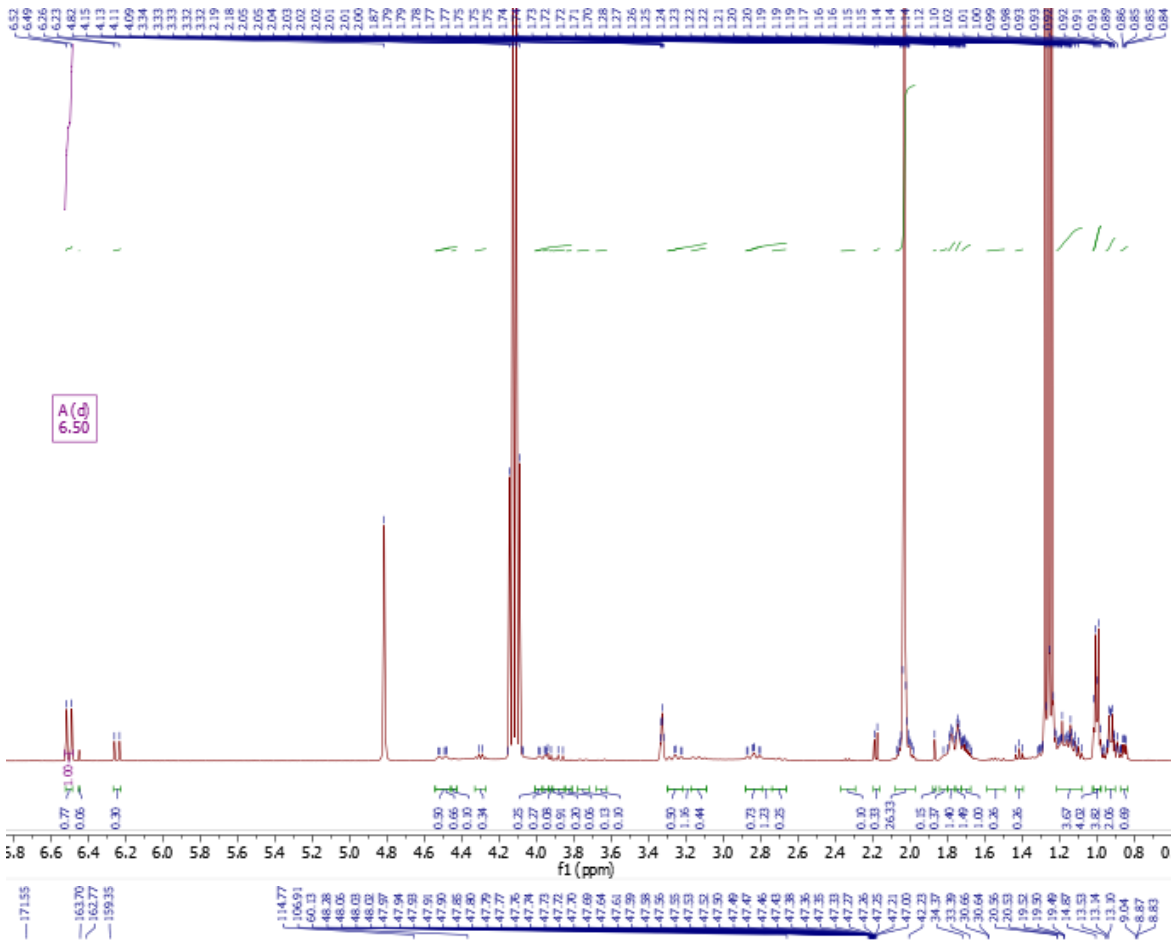

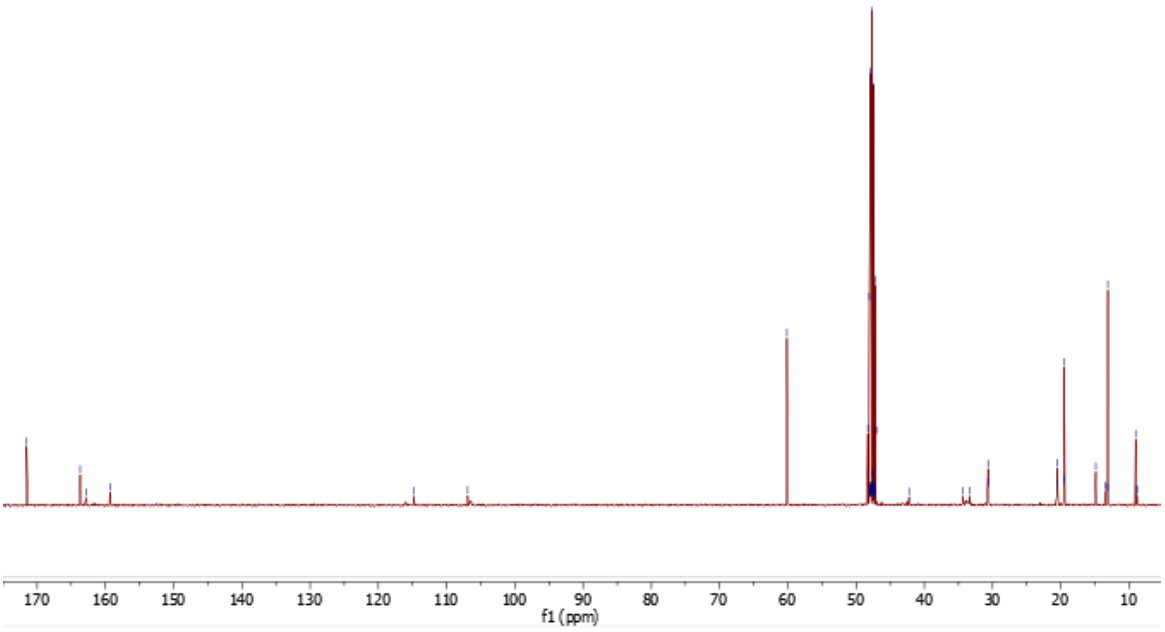

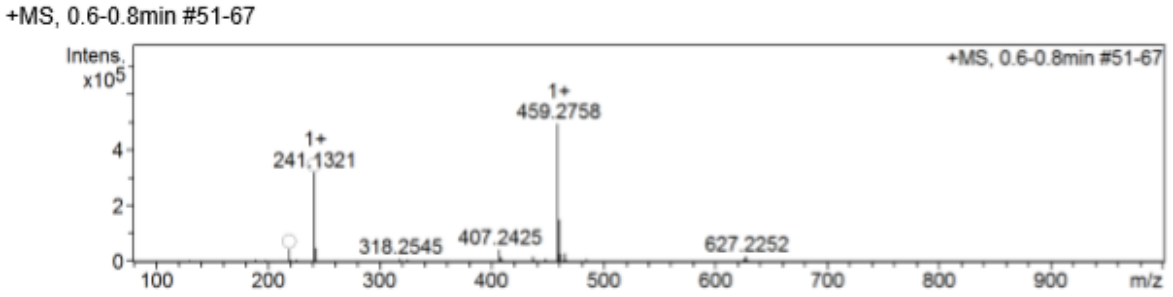

Appendix 14: ^{1}H NMR, ^{13}C NMR and MS of compound 14 ($(CD_3)_2SO$)

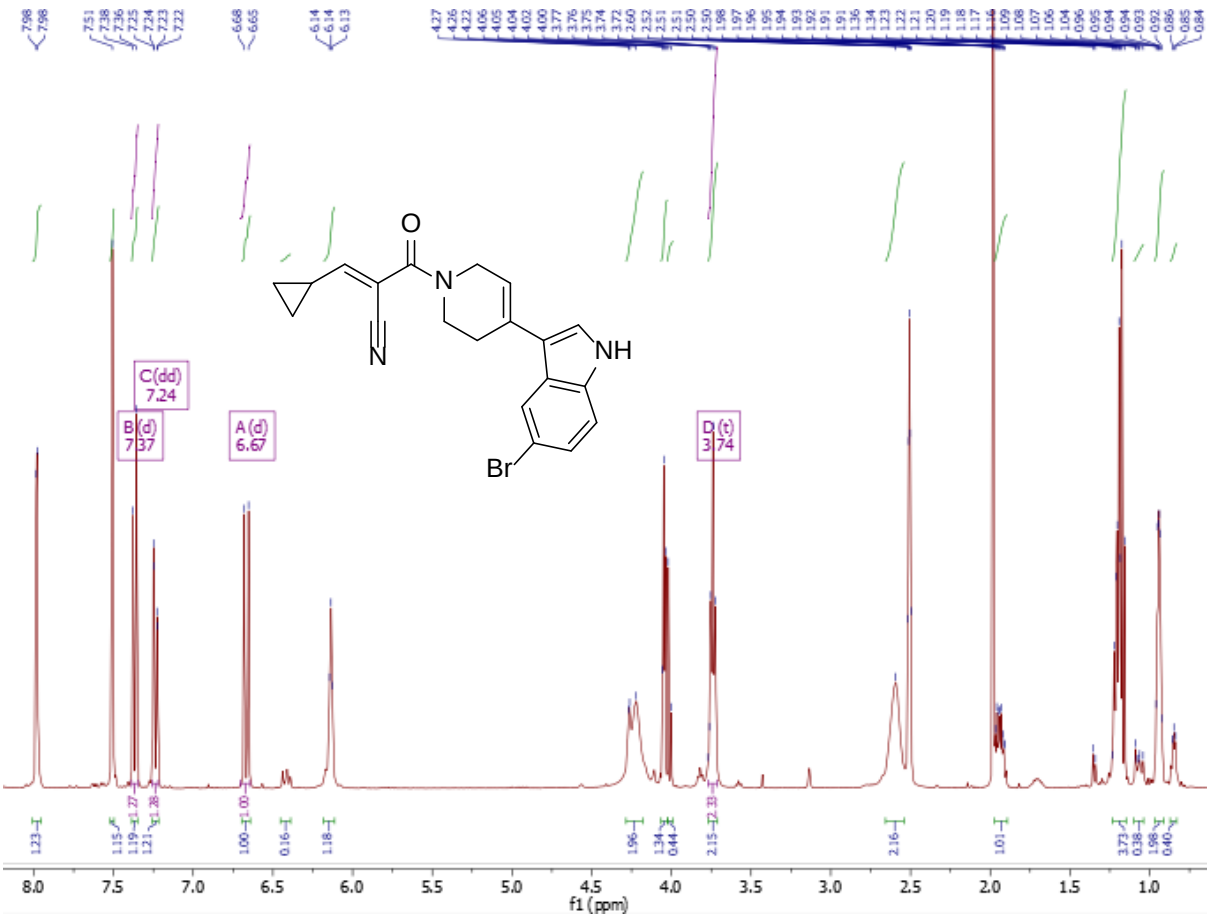

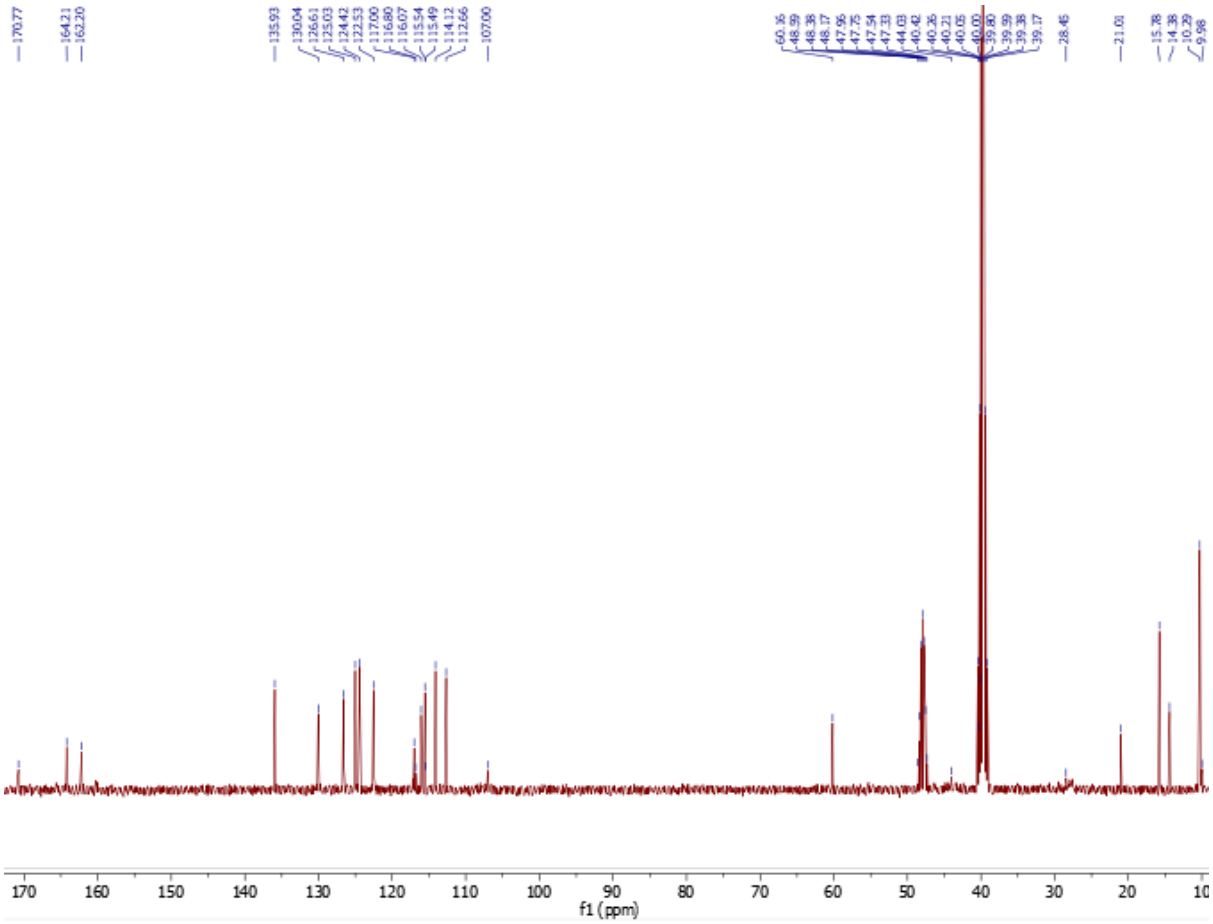

+MS, 0.6-0.8min #50-66

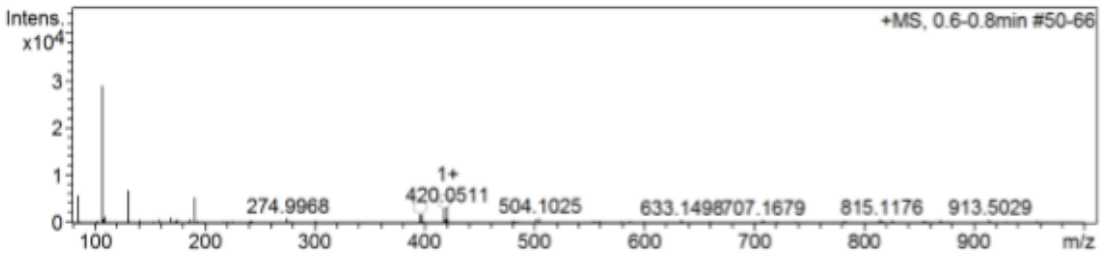

Appendix 15: ^{1}H NMR, ^{13}C NMR and MS of compound 15 ($(CD_3)_2SO$)

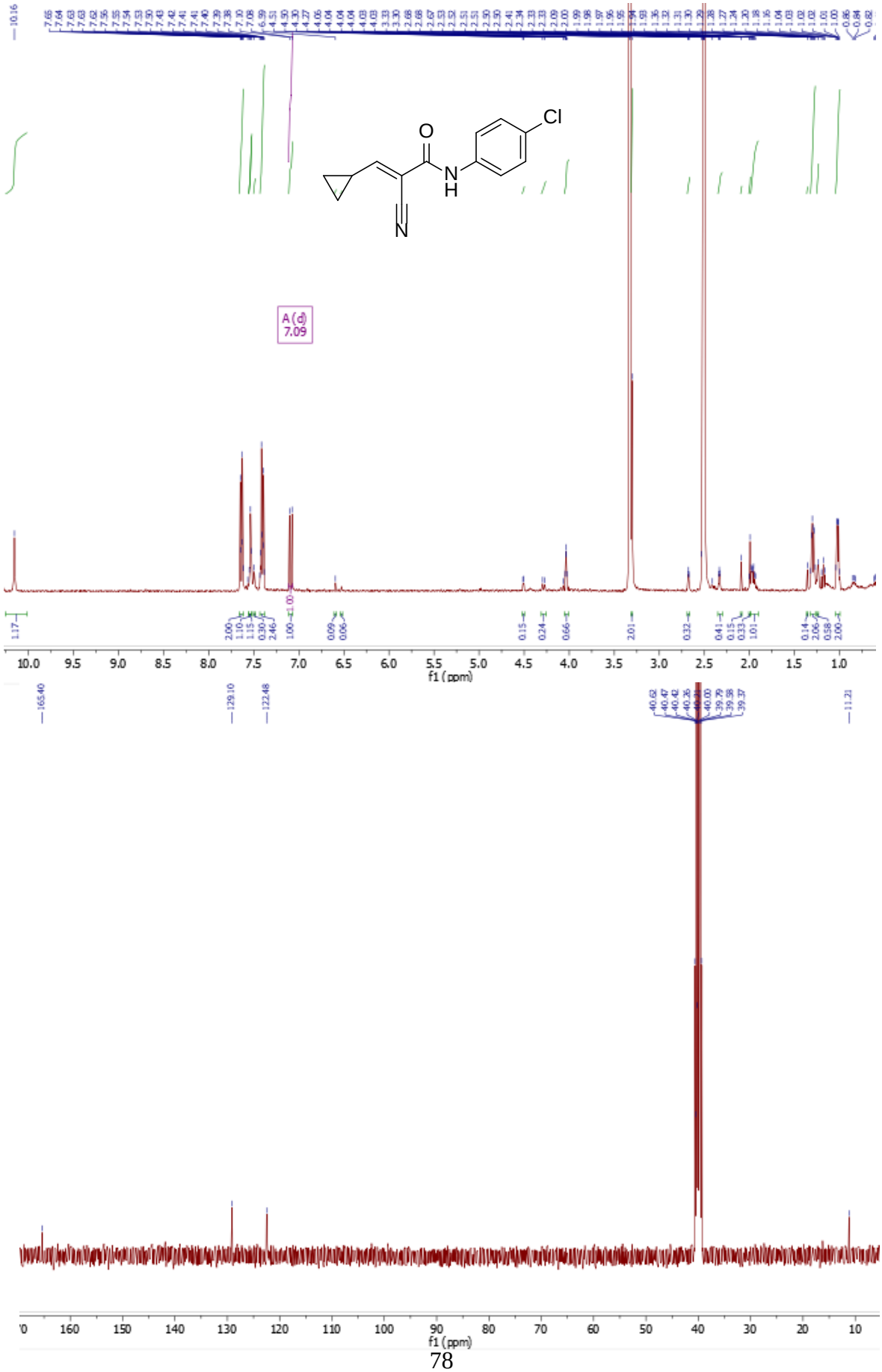

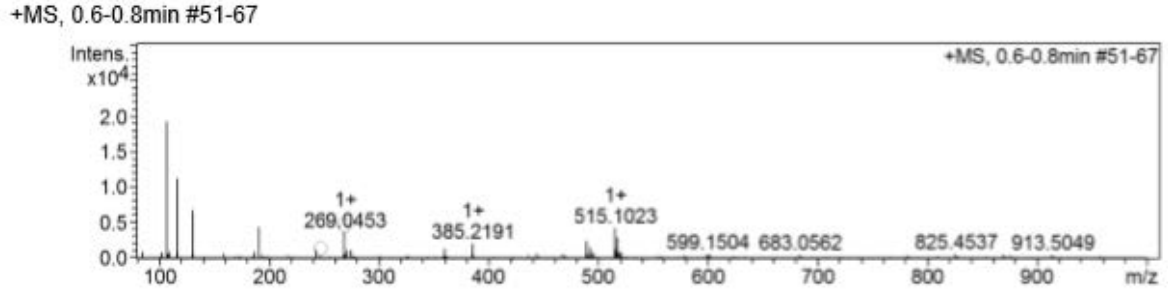

Appendix 16: ^{1}H NMR, ^{13}C NMR and MS of compound 16 (CD_3OD)

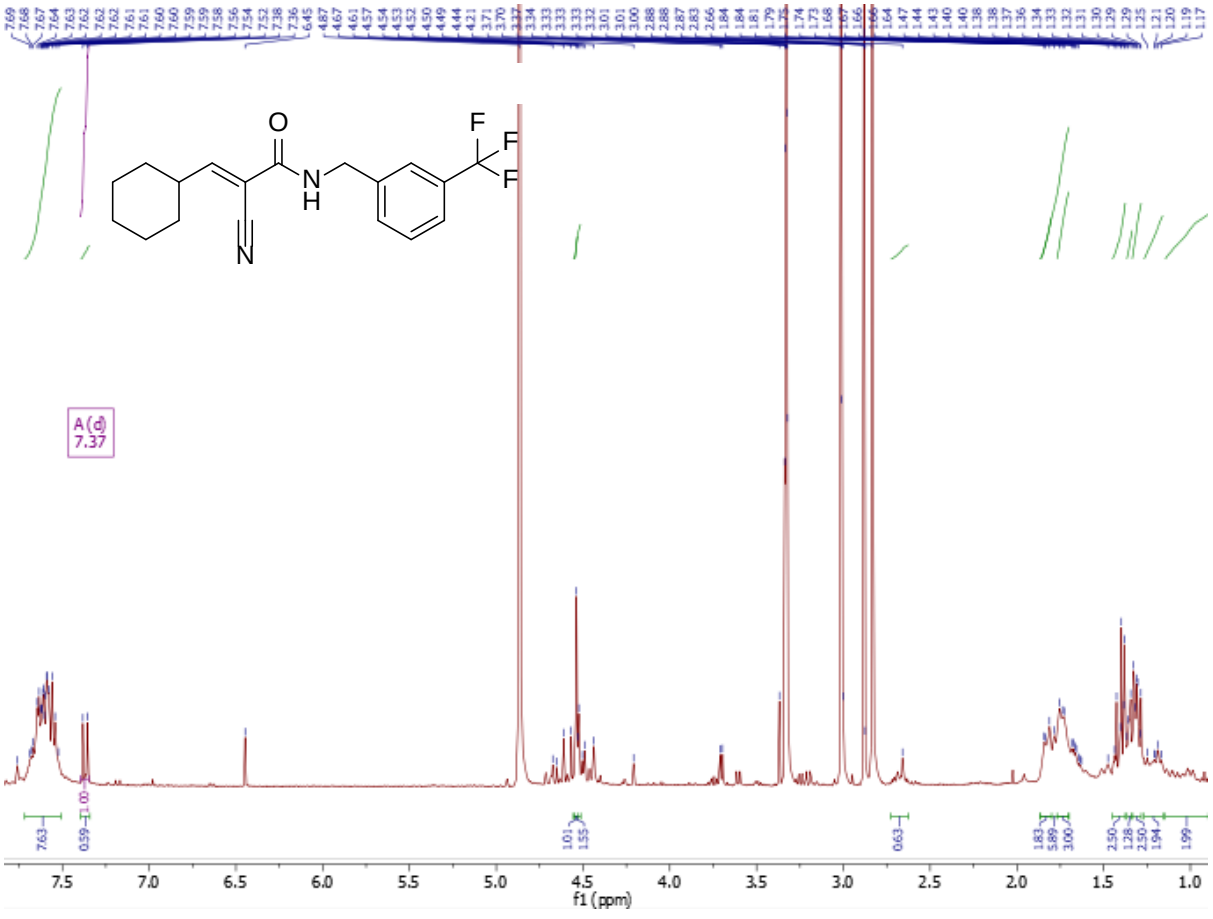

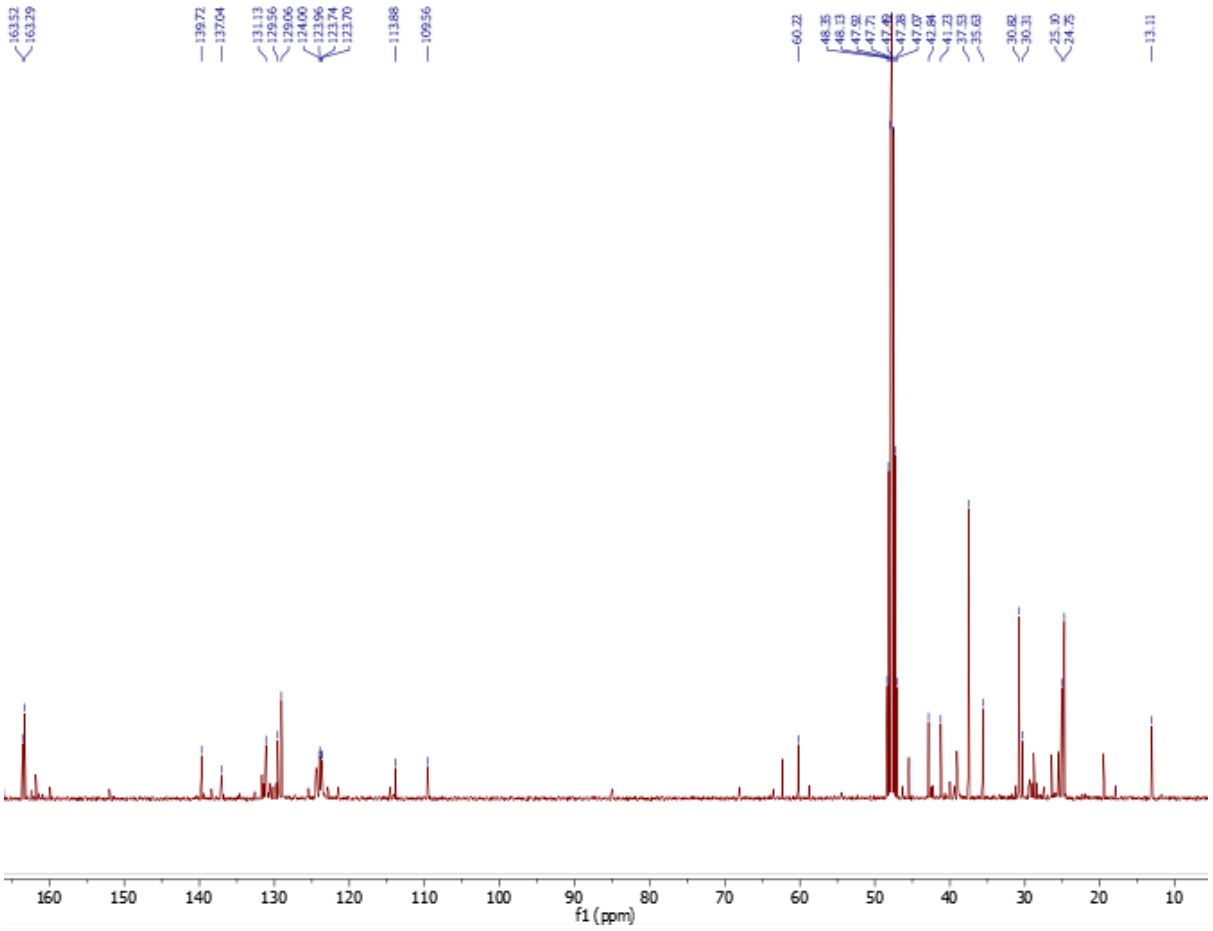

+MS, 0.6-0.8min #51-67

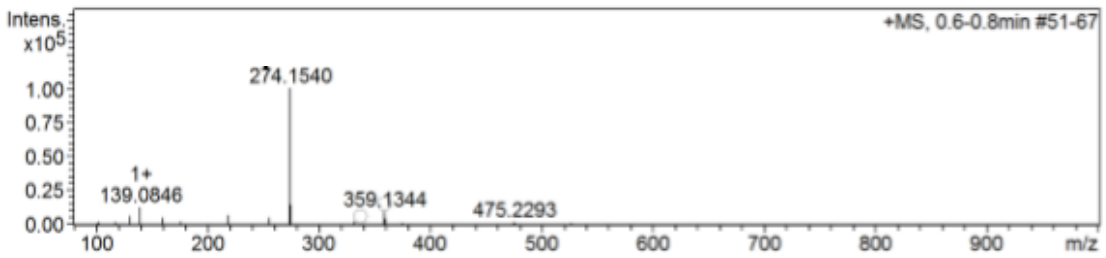

Appendix 17: ^{1}H NMR, ^{13}C NMR and MS of compound 17 (CD_3OD)

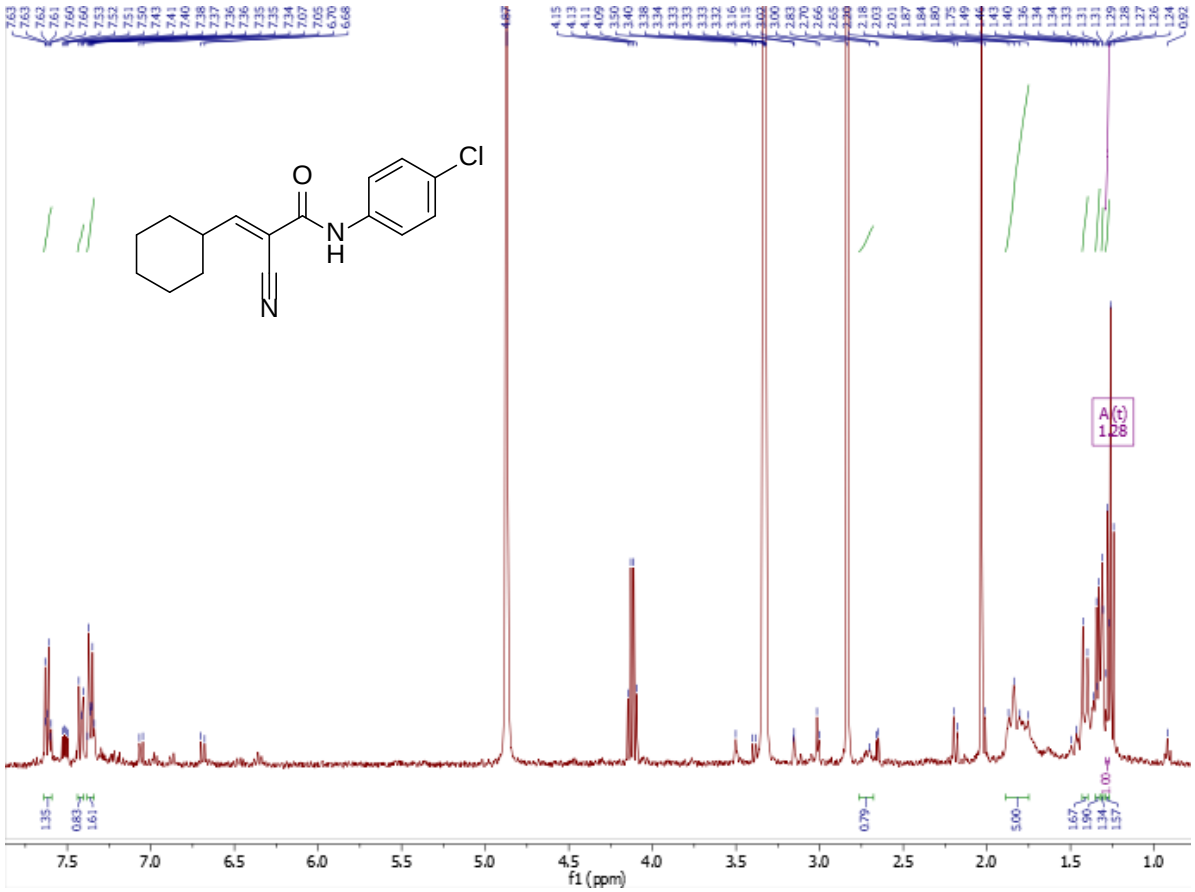

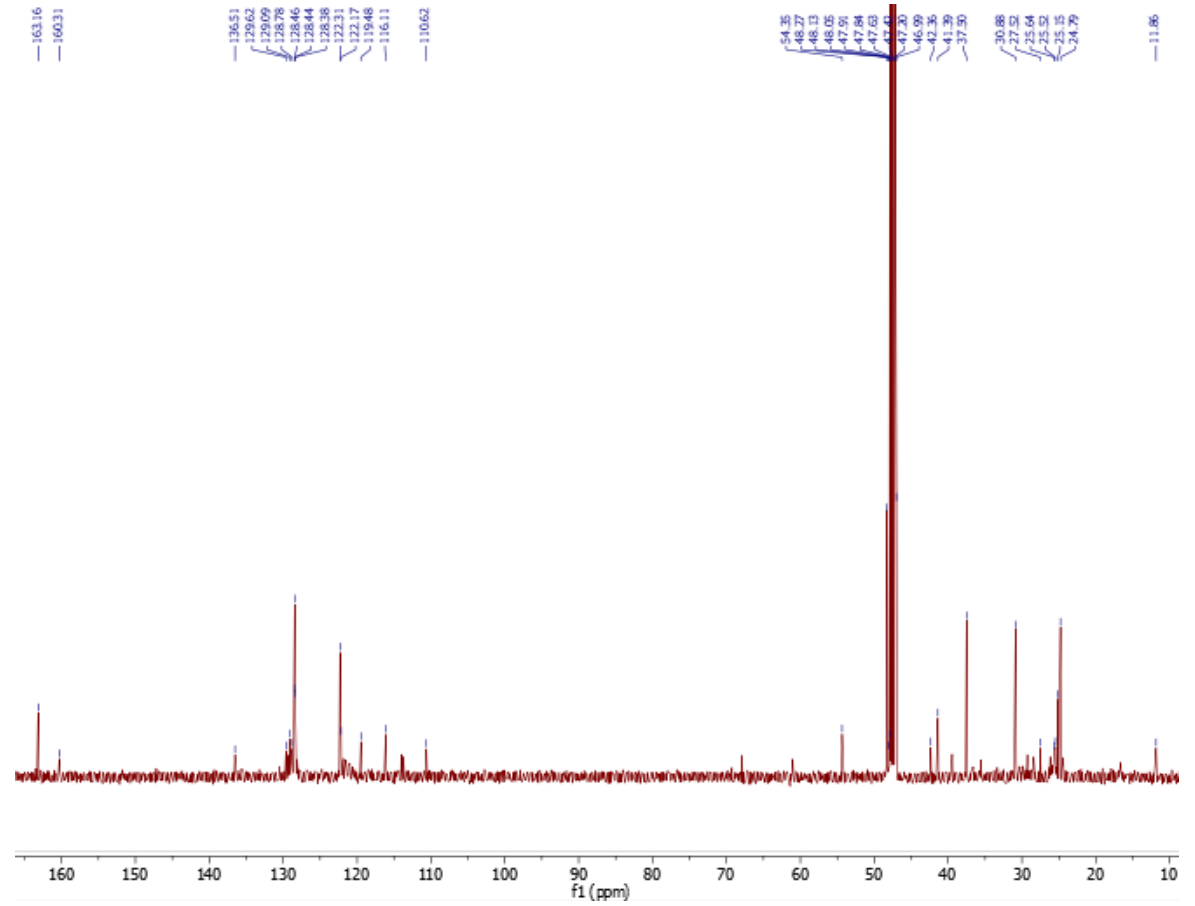

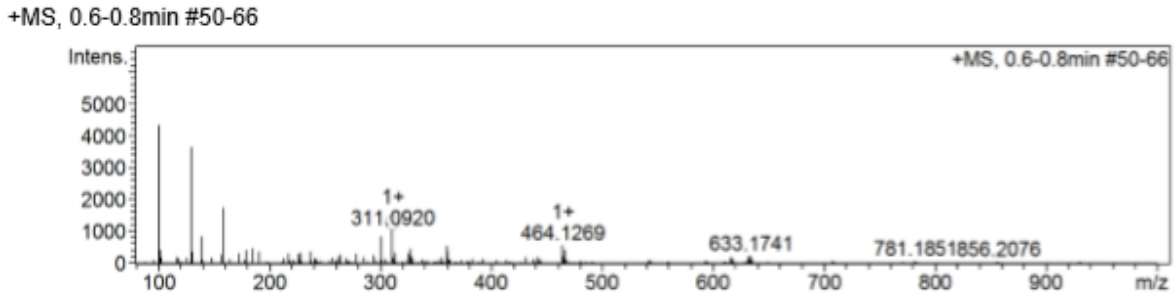

Appendix 18: ^{1}H NMR, ^{13}C NMR and MS of compound 18 (CD_3OD)

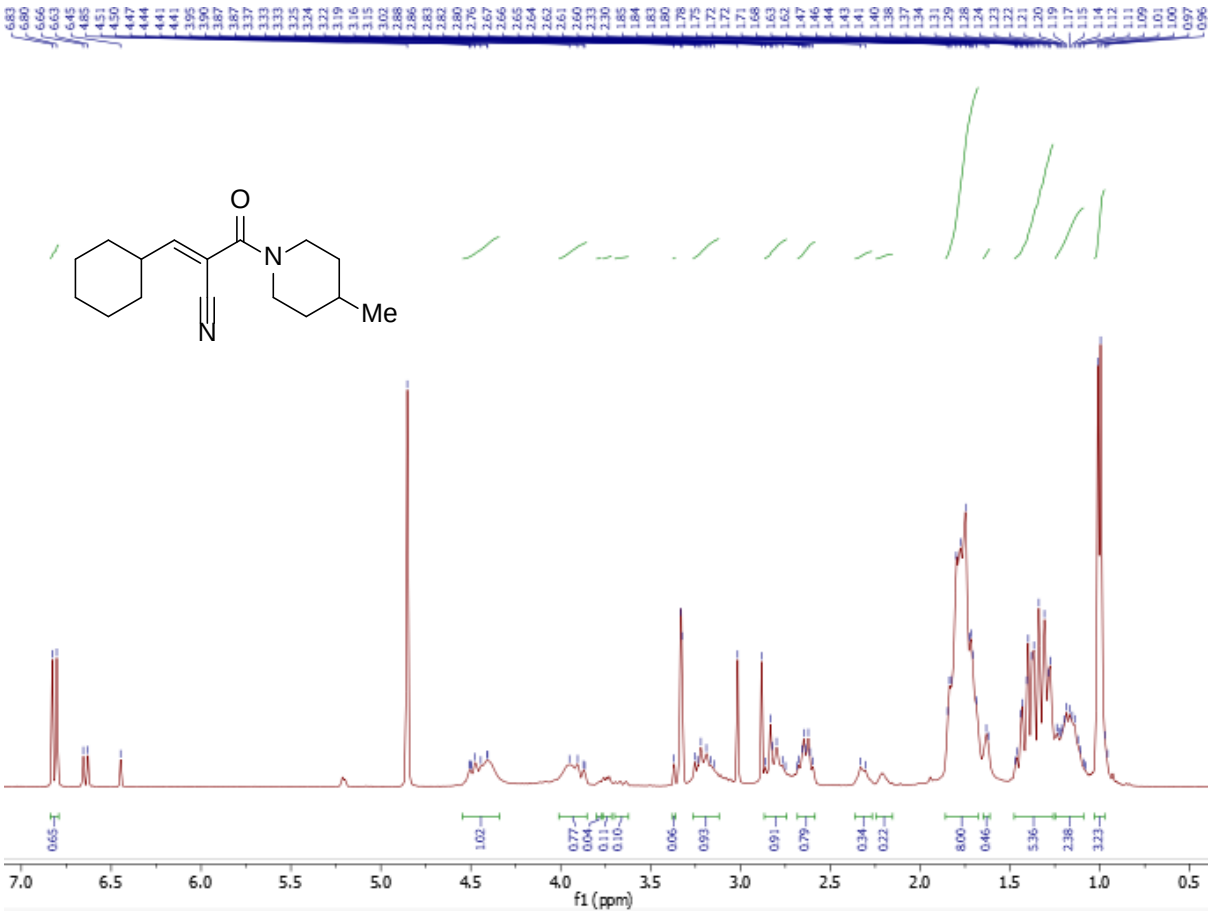

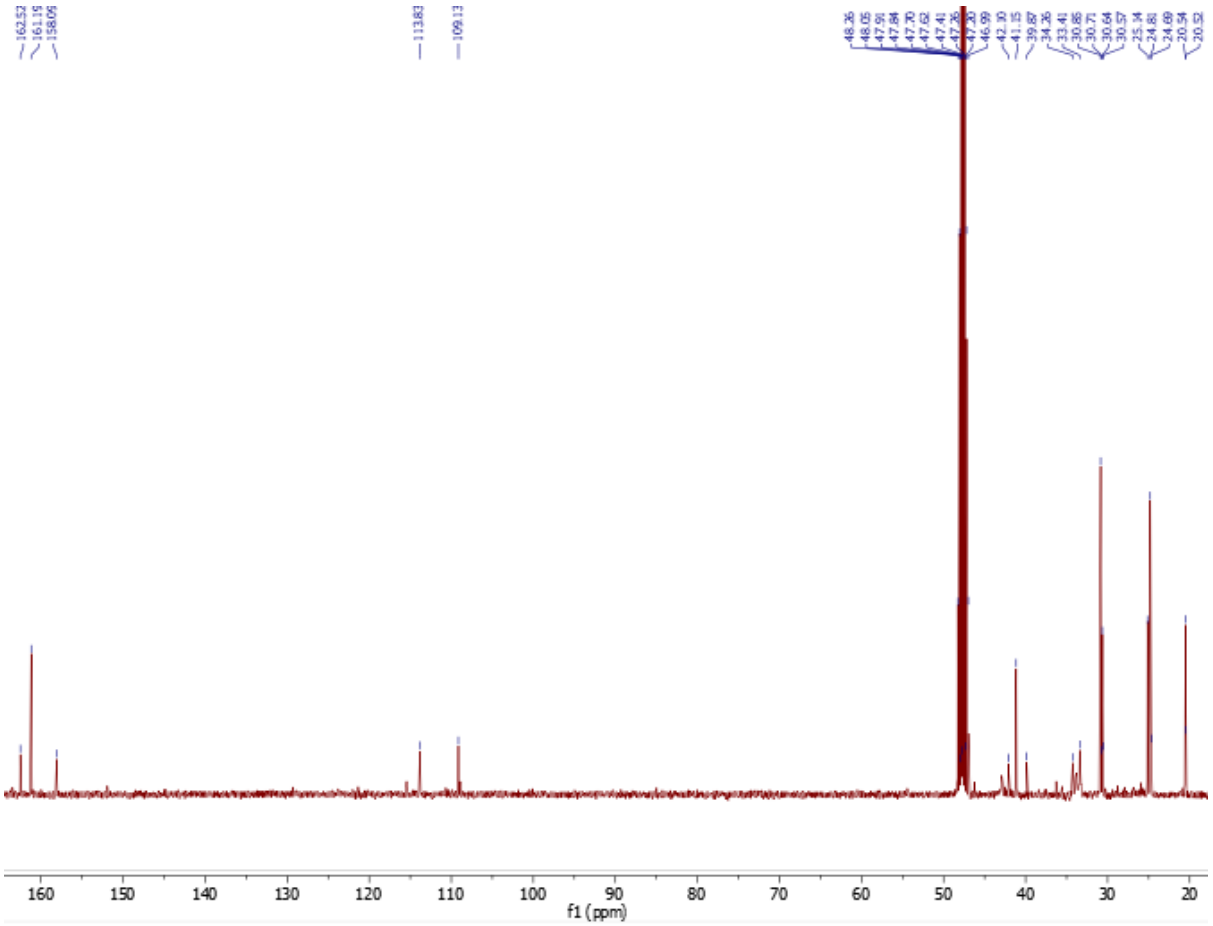

+MS, 0.6-0.8min #51-67

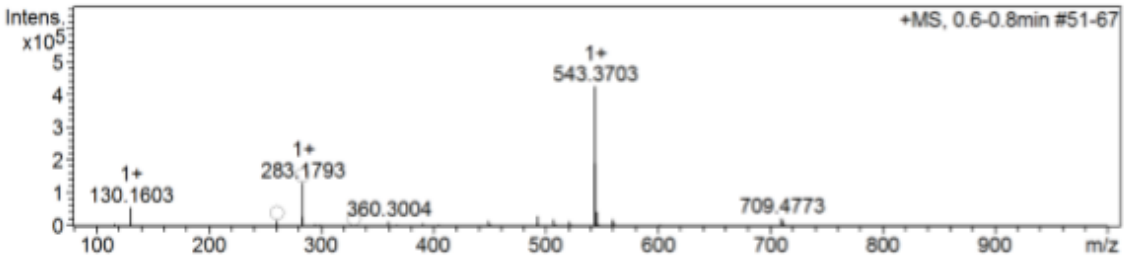

Appendix 19: ^{1}H NMR, ^{13}C NMR and MS of compound 19 (CD_3OD)

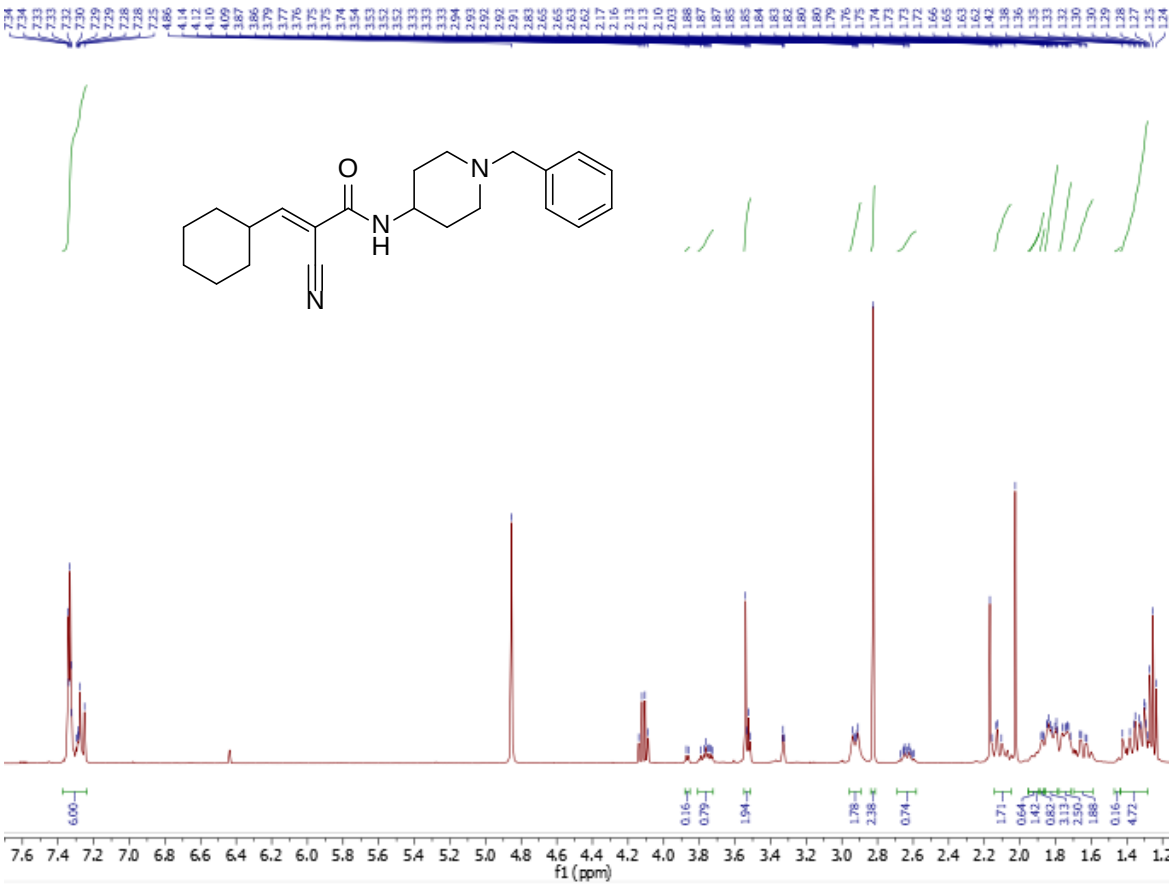

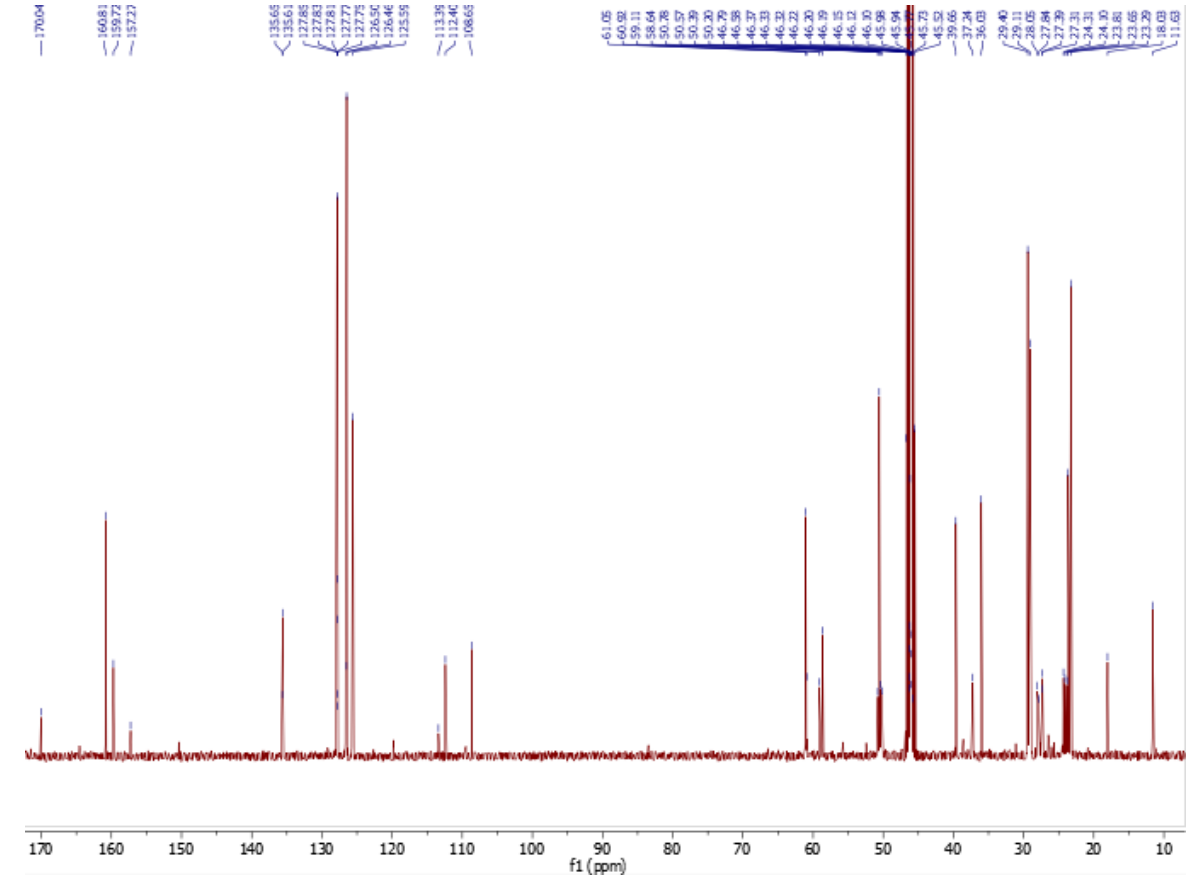

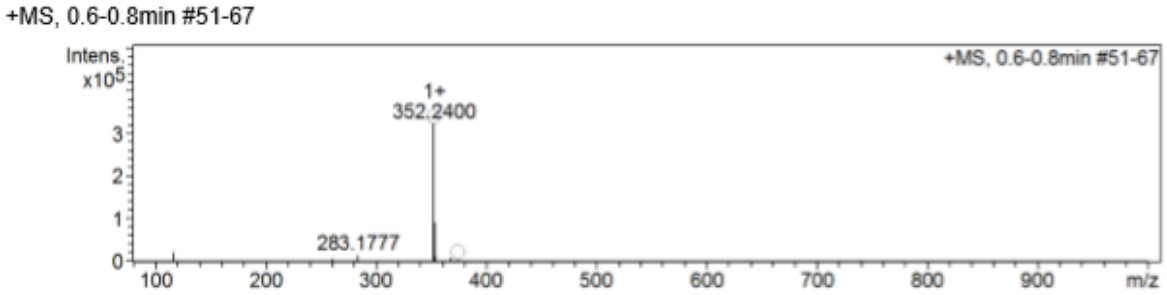

Appendix 20: ^{1}H NMR, ^{13}C NMR and MS of compound 20 (CD_3OD)

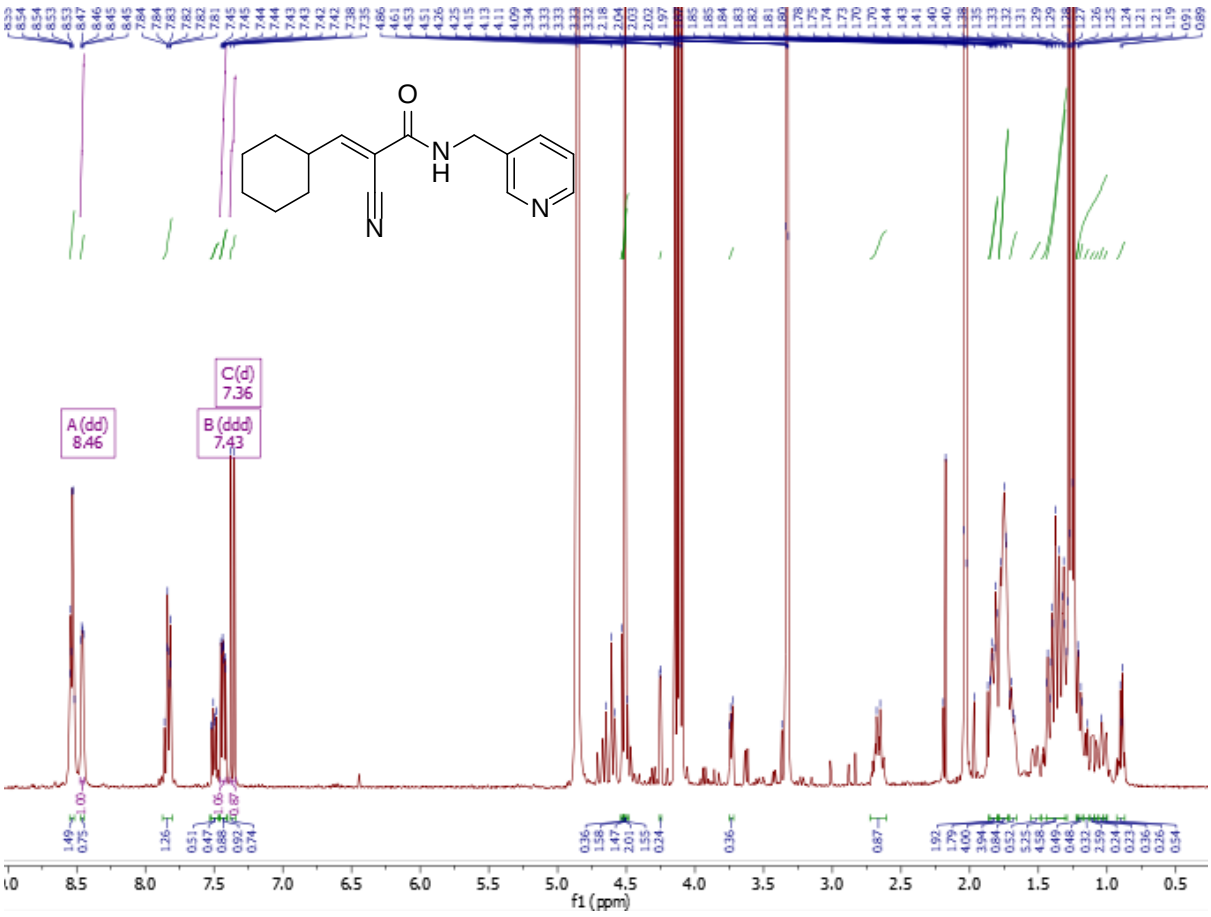

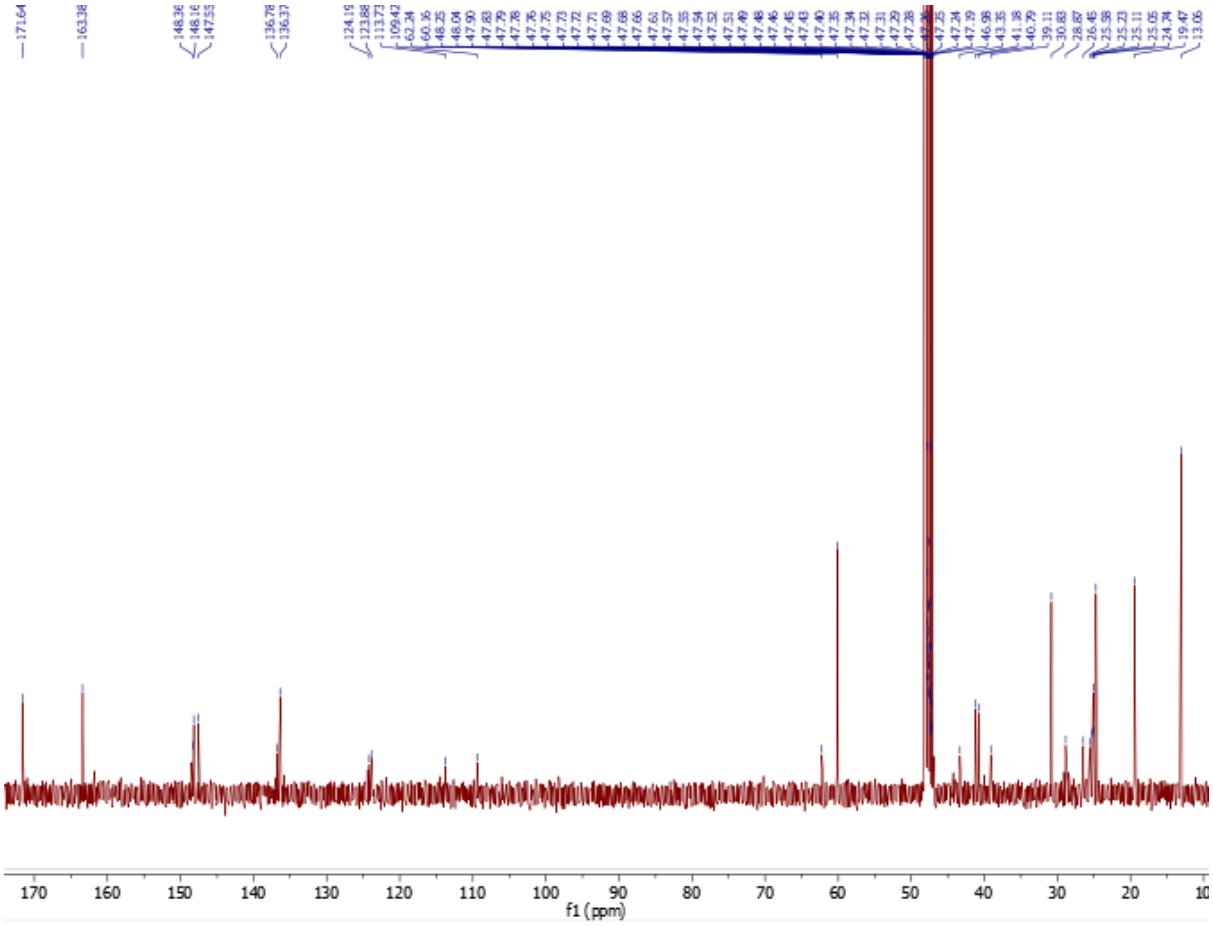

+MS, 0.6-0.8min #51-67

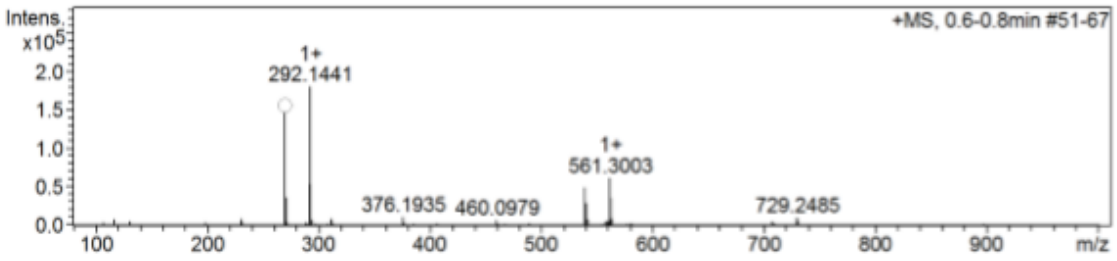

Glutathione test data

The tables below list the integral size data gathered for each numbered compound tested that resulted in any inhibition event. This data was used to gather the graphs (like that in Figure 26) and the rate constants for each reaction by plotting the natural log of the integral against time. The first table shows the data for the first experiment which was ran with excess inhibitor. The rest were done in 1:1 ratios of inhibitor and glutathione:

Appendix 21: Compound 12 (excess)

Hour	Integral size	Ln(integrals)
0	1	0
1	0.79	-0.235722334
2	0.81	-0.210721031
3	0.82	-0.198450939
24	0.79	-0.235722334

Appendix 22: Compound 16 (1:1)

Hour	Integral size	Ln(integrals)
0	1	0
1	0.92	-0.083381609
2	0.89	-0.116533816
3	0.85	-0.162518929
4	0.89	-0.116533816
24	1	0

Appendix 23: Compound 11 (1:1)

Hour	Integral size	Ln(integrals)
0	1	0
1	1.1	0.09531018
2	1.02	0.019802627
3	0.79	-0.235722334
4	0.9	-0.105360516
24	0.9	-0.105360516

Appendix 24: Compound 8 (1:1)

Hour	Integral size	Ln(integrals)
0	1	0
1	0.66	-0.415515444
2	0.54	-0.616186139
3	0.57	-0.562118918
24	0.59	-0.527632742

Appendix 25: Compound 6 (1:1)

Hour	Integral size	Ln(integrals)
0	1	0
1	0.68	-0.385662481
2	0.65	-0.430782916
3	0.65	-0.430782916
24	0.64	-0.446287103